CLOSED LOOP DEVELOPMENT TESTS OF AN EVAPORATING EXPERIMENT FOR THE INTERNATIONAL SPACE STATION FLUID SCIENCE LABORATORY

Stefano Carli

Dissertação para obtenção do Grau de Mestre em

Engenharia Aeroespacial

Júri

Presidente: Prof. Fernando Lau
Orientador: Dr. André C. Marta
Vogais: Prof. Viriato Semião

Orientador externo: Rodrigo Carpy from EADS Astrium

September 2011

Dedicato ai miei genitori

Acknowledgments

This achievement would not have been reached without the support of those people to whom I am deeply grateful.

I thank my supervisor, from IST, Dr. André Marta, who helped me during the entire thesis project. In particular, I show my gratitude for the important advice he gave me when I was looking for a Company with which to develop my thesis. His suggestions were important for influencing the right choice.

I show appreciation also to Prof. Aires dos Santos for helping me in the theoretical part of the thesis and for being willing to reply to all my questions.

I am deeply grateful to Rodrigo Carpy, my supervisor in EADS Astrium, who supported me during all my time in the Company. Thanks to him I understood many working aspects which will surely be important for my professional career. I am also grateful for his confidence in me and for the responsibility that I received. I also thank all the other colleagues of the TO-52 section for their contributions and in particular, Dr. Gerold Picker, project manager, who gave me the possibility to work in his department.

I also thank my friends, Jeremy Hills and Desy Cogo, who helped me in the thesis revision.

I wish to acknowledge my Prof. Gianandrea Bianchini, for the important advice and the support. Nevertheless I thank him for his kind patience during the past years.

I have to mention my friend Fabio Luongo with whom I studied at the IST in Lisbon for more than one and a half year. His support was important for successfully completing my studies. I also thank him for being one of the dearest friends who made my period in Portugal one of the best in my life.

I must thank Pedro Albuquerque, friend and colleague at IST, who gave me important advice and help during the whole master degree.

During the studies in Padua I received important support from my friend Alessandro Tonazzo. Thanks also to his help and to our team work, I managed to reach this important achievement. I am also grateful to Alessandro´s mother, Assunta, for her generous hospitality every time that Alessandro and me decided to study together.

I also thank my sisters Laura and Francesca, my aunts and uncles, my cousins, my grandparents and my friend Michele for their closeness during the whole studies.

The people to whom I am most grateful are in particular my parents, Ester and Giovanni. They supported me for my studies and thank to them I managed to spend the happiest periods of my life in Lisbon and in Germany. All this was possible because of their generosity, since the difficult situation that they had to face daily, was surely not easier without me. I hope that this achievement could partially pay them back for their sacrifices.

Deep thanks.

Ringraziamenti

Il raggiungimento di questo traguardo non sarebbe stato possibile senza l'appoggio, diretto o indiretto, di numerose persone alle quali devo tutta la mia riconoscenza.

Ringrazio il mio relatore, Dr. André Marta, che mi ha aiutato durante il periodo di preparazione della tesi. In particolare, gli rendo grazie per avermi dato preziosi consigli quand'ero alla ricerca di un'azienda presso la quale intraprendere una valida esperienza. I suggerimenti da lui ricevuti hanno certamente contribuito a fare la scelta giusta.

Devo una sentita riconoscenza al Prof. Aires dos Santos per avermi consigliato nella parte teorica della tesi e per essersi sempre mostrato disponibile nel rispondere ai miei quesiti.

Sono profondamente grato a Rodrigo Carpy, mio supervisore in EADS Astrium, che mi ha seguito durante tutto il periodo che ho trascorso nella Compagnia. Grazie a lui ho potuto prendere visione di molti aspetti lavorativi, e questo sarà sicuramente utile per la mia futura carriera professionale. Gli sono grato per la fiducia dimostratami e per avermi dato una generosa responsabilità. Ringrazio, inoltre, tutti gli altri colleghi del dipartimento TO-52 per il loro contributo e, in particolare, ringrazio il Dr.Gerold Picker, Project Manager del dipartimento TO-52, che mi ha dato la possibilità di svolgere la tesi in Astrium Space Transportation.

Ringrazio anche i miei amici, Jeremy Hills e Desy Cogo, che mi hanno aiutato nella revisione della tesi. Sono grato anche al Prof. Bianchini per i suoi preziosi consigli e per il valido supporto, specialmente durante il periodo padovano. Non di meno lo ringrazio per la gentile pazienza che ha avuto nei miei confronti durante gli ultimi anni.

Non posso fare a meno di menzionare il mio amico Fabio Luongo con il quale ho frequentato i corsi all'Instituto Superior Técnico di Lisbona per oltre un anno e mezzo. Il suo supporto è stato importante per il completamento dei miei studi. Gli sono inoltre grato, per essere uno dei miei più cari amici che hanno reso il mio soggiorno a Lisbona uno dei periodi più belli della mia vita.

Una forte riconoscenza va sicuramente a Pedro Albuquerque che, con la sua disponibilità e amicizia, mi ha fornito numerosi consigli durante tutta la laura Magistrale a Lisbona.

Durante il periodo padovano ho ricevuto un forte supporto dal mio amico e collega Alessandro Tonazzo. Grazie anche al suo appoggio e alla nostra capacità di lavorare in gruppo sono riuscito a raggiungere questo importante traguardo. Ringrazio inoltre la mamma di Alessandro, Assunta, per la generosa accoglienza mostratami ogni qualvolta Alessandro ed io decidevamo di studiare assieme.

Un sentito ringraziamento va anche alle mie sorelle Laura e Francesca, ai miei zii, ai miei cugini, ai miei nonni e al mio amico Michele che mi sono sempre stati vicini durante tutto il periodo di studi.

Le persone che più di tutti desidero ringraziare sono in particolare i miei genitori, Ester e Giovanni. E´ grazie a loro, infatti, che ho potuto intraprendere gli studi a Padova, ed è grazie a loro che ho potuto trascorrere a Lisbona e in Germania i momenti più felici della mia vita. Tutto questo è stato possibile grazie alla loro generosità, poiché la difficile situazione che ogni giorno hanno dovuto affrontare non è stata certamente facilitata dalla mia assenza. Mi auguro che il traguardo da me raggiunto li ripaghi dei tanti sacrifici fatti negli ultimi anni.

A tutti un profondo Grazie.

Abstract

CIMEX-1 (Convection and Interfacial Mass Exchange) is a microgravity research project foreseen to be carried out onboard the Columbus Module of the International Space Station. The project is sponsored by the European Space Agency and EADS Astrium is the prime contractor for developing the experiment. The main scientific purpose of the mission is studying mass transfer processes through interfaces and their coupling with the surface tension driven instabilities that affect mass and energy transfer. The experiment takes place in a cell, in which the liquid interface allows evaporation to take place through a flow of inert gas. The system is equipped with a liquid and gas closed loop in order to avoid the limitations caused by the use of consumables. The assignments which were carried out were building, testing and analyzing a breadboard setup which is meant to verify the closed loop and the components operability, as it has the same functional characteristics of the flight model. Due to the decision of changing the evaporating fluid from Ethanol to HFE-7100, the system behavior and operability had to be tested. A test campaign took place in June 2011 to collect experimental data and to verify the operability of the CIMEX-1 foreseen parameters range with the new fluid. Moreover, the test campaign aimed to assess the properties of new essential components like the liquid pump and the anti-wetting micro groove.

This work was carried out in the TO-52 department of Astrium Space Transportation in Friedrichshafen, Germany.

Key words: CIMEX, Anti-Wetting, Breadboard, Closed loop, Columbus, Condenser, Evaporator, Flow meter, Fluid Science Laboratory, Gas concentration, Gas concentration sensor, International Space Station, Pressure controller

Resumo

O CIMEX-1 (do inglês: Convection and Interfacial Mass Exchange) é um projecto de pesquisa em ambiente de micro gravidade que se prevê que seja levado a bordo do Módulo Columbus para a Estação Espacial Internacional. O projecto foi patrocinado pela Agência Espacial Europeia que subcontratou a empresa EADS Astrium para o desenvolvimento do mesmo. O principal objectivo científico desta missão é estudar o processo de transferência de massa através de interfaces e a sua relação com instabilidades geradas pela tensão superficial que afecta a transferência de massa e energia.

A experiência tem lugar numa célula na qual o interface líquido permite a ocorrência de evaporação através de um escoamento de gás inerte. O sistema está equipado com líquido e gás em ciclo fechado para evitar limitações causadas pela utilização de consumíveis. O objectivo desta Dissertação de Mestrado é construir, testar e analisar um dispositivo (Breadboard) concebido para verificar a operabilidade de componentes em ciclo fechado, uma vez que possui as mesmas propriedades funcionais do modelo de voo.

Devido à decisão de mudar o fluido de evaporação de etanol para HFE-7100, a funcionalidade do sistema teve de ser testada, pelo que teve lugar em Junho de 2011 uma bateria de testes para recolher dados experimentais no sentido de verificar a validade dos parâmetros previstos CIMEX-1 com o novo fluido.

Além disso, a bateria de testes desenvolvida teve como objectivo avaliar as propriedades de novos componentes tais como a bomba de líquido e tmbém o "anti-wetting micro groove".

Esta Dissertação de Mestrado foi realizada no Departamento TO-52 da Astrium Space Transportation, em Friedrichshafen, na Alemanha.

Contents

List of Tables

List of Figures

List of Abbreviations

Abbreviation	Description
BB	Breadboard
CEM	Central Experiment Module
CIMEX	Convection and Interfacial Mass Exchange
CSS	Condenser Separator System
CS-V	Degassing Valve
EDR	European Drawer Rack
EADS	European Aeronautic Defense and Space Company
EC	Experimental Container
EPDM	Ethylene Propylene Diene Monomer rubber
EPM	European Physiology Module
ESA	European Space Agency
ETC	European Transport Carrier
FMC	Front Mounted Cameras
FSL	Fluid Science Laboratory
GCS	Gas Concentration Sensor
GL-FC	Gas Loop Flow Controller
GL-FM	Gas Loop Flow Meter
GL-GC	Gas Loop Gas Circulation pump
GL-GCS	Gas Loop Gas Concentration Sensor
GL-GP	Gas loop Gas retraction Pump
GL-PC	Gas Loop Pressure Controller
GL-RES	Gas Loop Reservoir
GL-SV	Gas Loop valve
HFE	HydroFluoroEther
I/F	Interface

Abbreviation	Description
ISS	International Space Station
LL-LP	Liquid Loop Liquid Pump
LL-RES	Liquid Loop Reservoir
LL-SV	Liquid Loop Valve
MCU	Master Control Unit
MFC	Mass Flow Controller
MFM	Mass Flow Meter
NDIR	Non Dispersive Infra Red Sensor
ODM	Optical Diagnostic Module
ORT	Optical Reference Targets
PC	Pressure Controller
PCU	Power Control Unit
PFA	PerFluoroAlkoxy
PID	Proportional Integral Derivative
SR	Sensor Readout
TEC	Thermo Electric Cooler
VMU	Video Management Unit

List of Symbols

Symbol	Description	Unit
C	Concentration	%
C_p	Specific heat at constant pressure	kJ/(kg K)
h	Specific enthalpy	kJ/mol
M	Molecular weight	kg/kmol
$\dot{m}$	Mass flow rate	mg/min
$\dot{n}$	Moles flow rate	mol/min
p	Pressure	bar
R	Gas constant	kJ/ (kg K)
$\overline{R}\cdot$	Universal gas constant	kJ/ (kmol K)
T	Temperature	℃
$\dot{V}$	Volumetric flow rate	ml/min
y	Mole fraction	/
ρ	Density	kg/ m^3
η	Efficiency	/

1 Introduction

In 2002, many European research institutes, universities and companies started the development of CIMEX-1 (Convection and Interfacial Mass Exchange), a project foreseen to take place in the International Space Station and sponsored by the European Space Agency. These entities form a consortium in which EADS-Astrium was selected as the prime contractor for developing the CIMEX-1 Experiment.

1.1 CIMEX–1 Fluid Cell Assembly overview

The scientific experiment will be executed inside the Fluid Cell Assembly which is composed by the followings elements:

-Reservoir for the experiment liquid with the capability to allow a refill on-ground.

-Reservoir for Nitrogen gas, which will be reused during the entire mission. The reservoir should allow a refill on-ground.

-The 3D Experiment Cell allowing the contact between the liquid and the gas through a free liquid surface. The liquid depth is adjustable thanks to a movable bottom. This device is the core of CIMEX-1 where the evaporation takes place.

-The Liquid Loop allowing a liquid level maintenance in the experiment cell.

-The Gas Loop allowing the selection of the gas pressure and flow rate over the liquid surface

-The Condenser Separator Subsystem (CSS) for the separation and the return of liquid and gaseous parts of the fluids after the separation area.

-Experiment Diagnostics for the liquid gas exchange incl. experiment liquid temperature diagnostics, performed by direct contact and via optical tomography, supported by infrared measurement. The flatness of the free surface is controlled by Schlieren diagnostic in reflection mode.

The following picture shows the fluid cell foreseen to be used in CIMEX-1 (Figure 1-1) and the Fluid Cell Assembly (Figure 1-2) at the Preliminary Design Review stage.
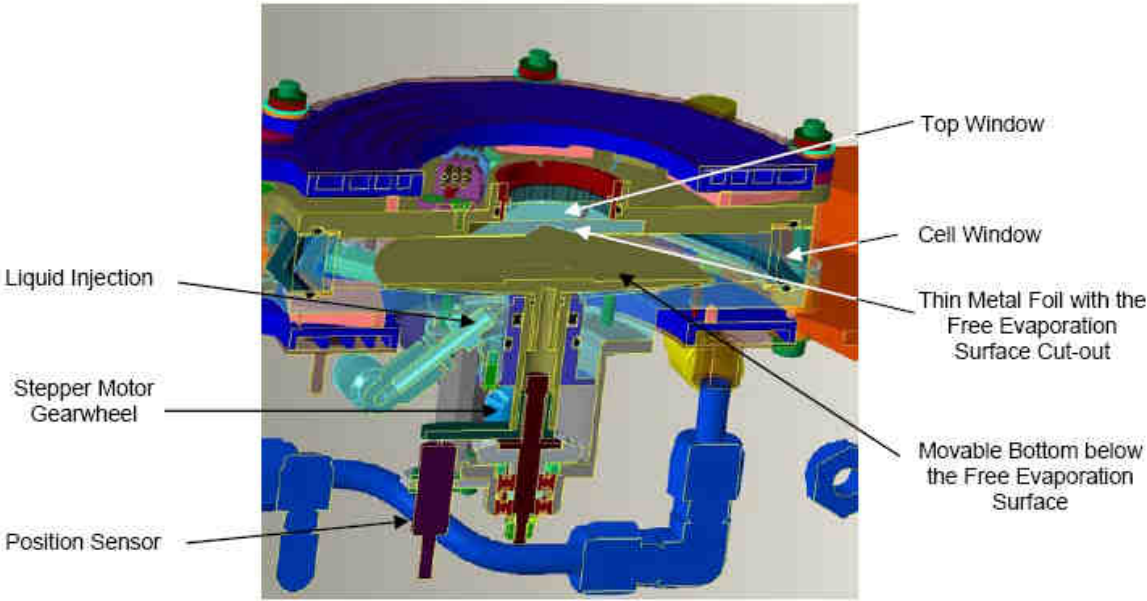
Figure 1-1: CIMEX-1 Fluid Cell cut [3]
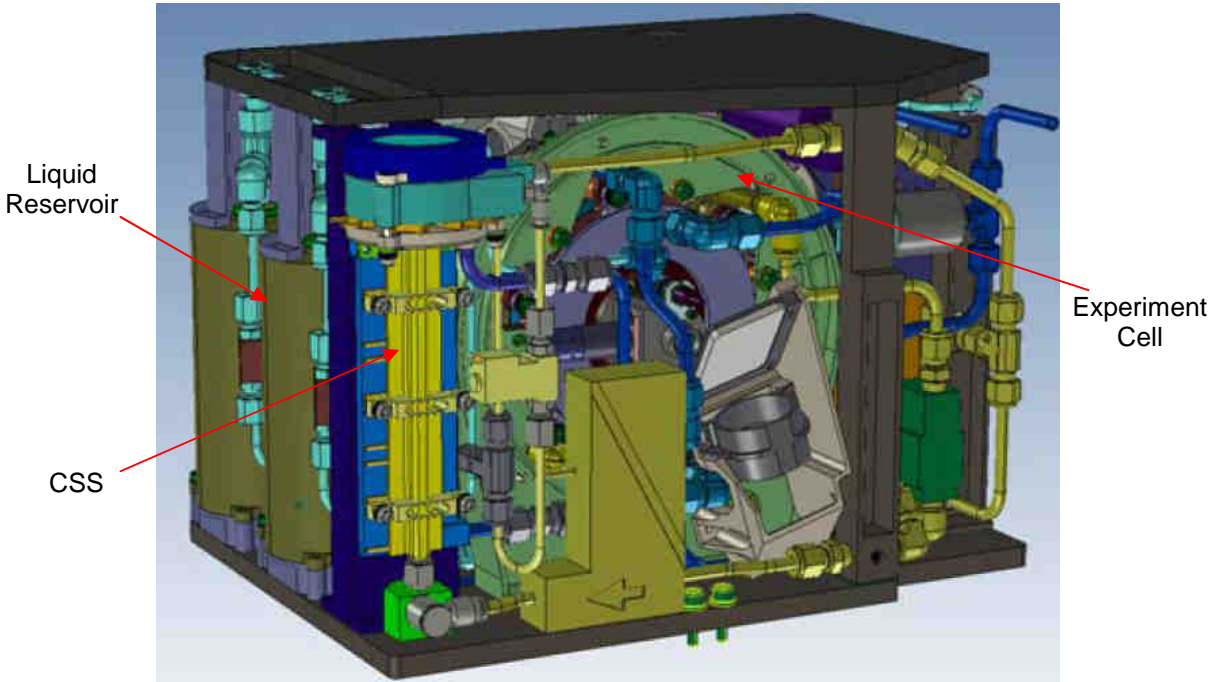
Figure 1-2: CIMEX-1 Fluid Cell Assembly from VERHAERT Space [14]

With a maximum mass of 40kg, the Experimental Container has dimensions of 400x270x280mm. The operative temperature range is between 0℃ and 60℃ and the connections to the FSL are the power I/F, the data and video I/F, the ground I/F and the water I/F.

1.2 Motivation

The project encountered an important setback after the Safety Review 1, when Ethanol, the foreseen operative fluid, was not considered safe. A new liquid was therefore needed and after the assessment of alternative fluids, HFE-7100 was selected. Since the CIMEX-1 components were designed or chosen for Ethanol, their functionality and operability had to be tested with the new liquid. Moreover, their behavior also had to be verified in the closed loop arrangement, since all of the equipment has to work together in CIMEX-1. If the system functionality of CIMEX-1 with the HFE-7100 was discovered to be limited, with a reduced range of the foreseen parameters, then finding a new solution would be necessary for the program to continue. This thesis aims to find answers to all of the previous open points.

1.2.1 Prior work

It has to be mentioned that some work towards this direction was already performed at the time this thesis project started. In fact, another student named Luis Ganuza, worked in 2010 at Astrium ST for CIMEX-1 [8], after the decision to change the operative fluid to HFE-7100 was made. The following points summarize the work he did and from which this thesis project started:

 -The Gas Concentration Sensor (GCS) was chosen after having tested different types

 -The GCS was calibrated for HFE-7100 with volumetric concentration

 -The "jump" problem of the GCS was found, but not solved via software

 -Some of the Bronkhorst instruments, which were used also for the closed loop test campaign, were purchased and tested

 -Many metallic foil coatings, developed by several institutes and universities were tested. However no one of them showed suitable performances with HFE-7100.

 -The fluid cell, which was used also for the closed loop test campaign, was designed

 -The Peltier elements for the fluid cell thermal controlling were already sized

 -Preliminary tests with the fluid cell were performed with an open loop configuration and without the appropriated anti wetting metallic foil. Moreover, the liquid was injected with a syringe and not with a liquid pump as it is foreseen for CIMEX-1.

Some of the above results were used during the thesis project in order to achieve the CIMEX-1 functionality in a closed loop.

1.2.2 Scientific purposes

<u>Primary Objectives</u>

CIMEX-1 is meant to study mass transfer processes through interfaces and their coupling with the surface tension driven instabilities that affect mass and energy transfer. The undertaken investigation is about both the macro convection, which occurs when heat or mass fluxes are imposed along an interface, and micro convection, which is about fluxes across an interface. Moreover, since the coupling between evaporation and convection has a direct effect on the evaporation rate, the study will be important for heat pipes and other industrial applications.

With this project it is expected that knowledge will be gained on different regimes of interfacial mass transfer processes in the presence of several effects:

- Evaporation in an inert gas atmosphere
- Marangoni convection (mass transfer along the interface due to surface tension gradient)
- Surfactants (compounds that reduces the surface tension of a liquid)

<u>Secondary Objectives</u>

Since the Condenser Separator System integrated in CIMEX-1 condenses the evaporated fluid, the device will be used to study the influence of the gravity effect on the heat transfer and on the pressure drop in the condenser tube.

1.3 Experimental facilities

CIMEX-1 Experiment will be carried out onboard the European Columbus module of the International Space Station. The ISS is the only existing platform which allows experiments to be performed in microgravity for extended periods of time. The ISS orbits around the Earth following a circular orbit inclined at 51,63° in respect to the Equator, at an altitude between 330Km and 400km and has an average velocity of 27.000Km/h. With a mass of 417.289Kg and with dimensions of 108x79x43 meters, it is the biggest orbiting construction ever built by human.

The Columbus module is one of the ESA main contributions to the ISS. It was carried by the space Shuttle Atlantis on February 7th 2008 from the Kennedy Space Centre, Florida.

The main purpose of this facility is providing an environment for scientific research to be carried out in microgravity conditions.

The internal laboratory includes the following payload racks [12]:

- ***BioLab -*** supports experiments on micro-organisms, cells and tissue cultures, and even small plants and small insects.
- ***The European Physiology Module (EPM)*** - a set of experiments that will be used to investigate the effects of long-duration spaceflight on the human body.

- ***The European Drawer Rack (EDR) -*** is a modular and flexible experiment carrier system for a large variety of scientific disciplines, providing basic accommodation and resources for experiment modules housed within standardized drawers and lockers.

- ***The European Transport Carrier (ETC)*** - accommodates items for transport and stowage. In orbit ETC will serve as a workbench and stowage facility.

- ***The Fluid Science Laboratory (FSL)*** - accommodates experiments in the strange behavior of weightless liquids. These too, could bring far-reaching benefits on Earth: better ways to clean up oil spills, for example, and even improved manufacture of optical lenses.
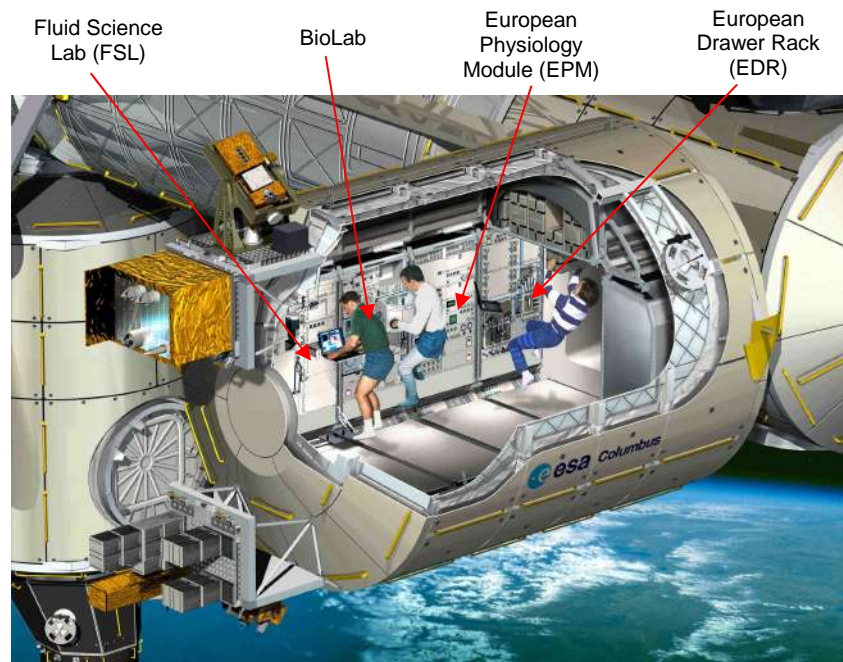
Figure 1-3: Columbus Module configuration

CIMEX-1 Experiment will be mounted in the FSL rack and the installation will be performed by the crew members. FSL can be operated fully automatic or semi-automatic on station by the flight crew or remotely controlled from ground. The FSL modular design consists of a/an [3]:

- *Master Control Unit (MCU),* controlling the facility and managing the ground / facility communication.

- *Video Management Unit (VMU),* synchronizing all cameras, capturing, processing and storing all video data.

- *Power Control Unit (PCU),* providing power at the appropriate voltage levels to the subsystems.

- *Thermal Environment Control System (TEC)* providing high cooling capacity to the test container using a secondary water loop and a liquid to liquid.

- *Optical Diagnostic Module (ODM).*

- *Central Experiment Module (CEM).*

- *Experiment Container (EC),* containing the object of study and generating the necessary stimuli to the fluid.

- *Optical Reference Targets*, serving as reference during calibration of the facility on-orbit.

- *Front Mounted Cameras (FMC),* enabling non-standard experiment observation.

- *Work Bench, containing a Laptop (LTU)* as crew interface to FSL facility (HCI/MMI).
- *Stowage Drawers*, serving for e.g. storage of the Optical Reference Targets, facility consumables etc.

The following picture shows the position of CIMEX-1 EC in the ISS.
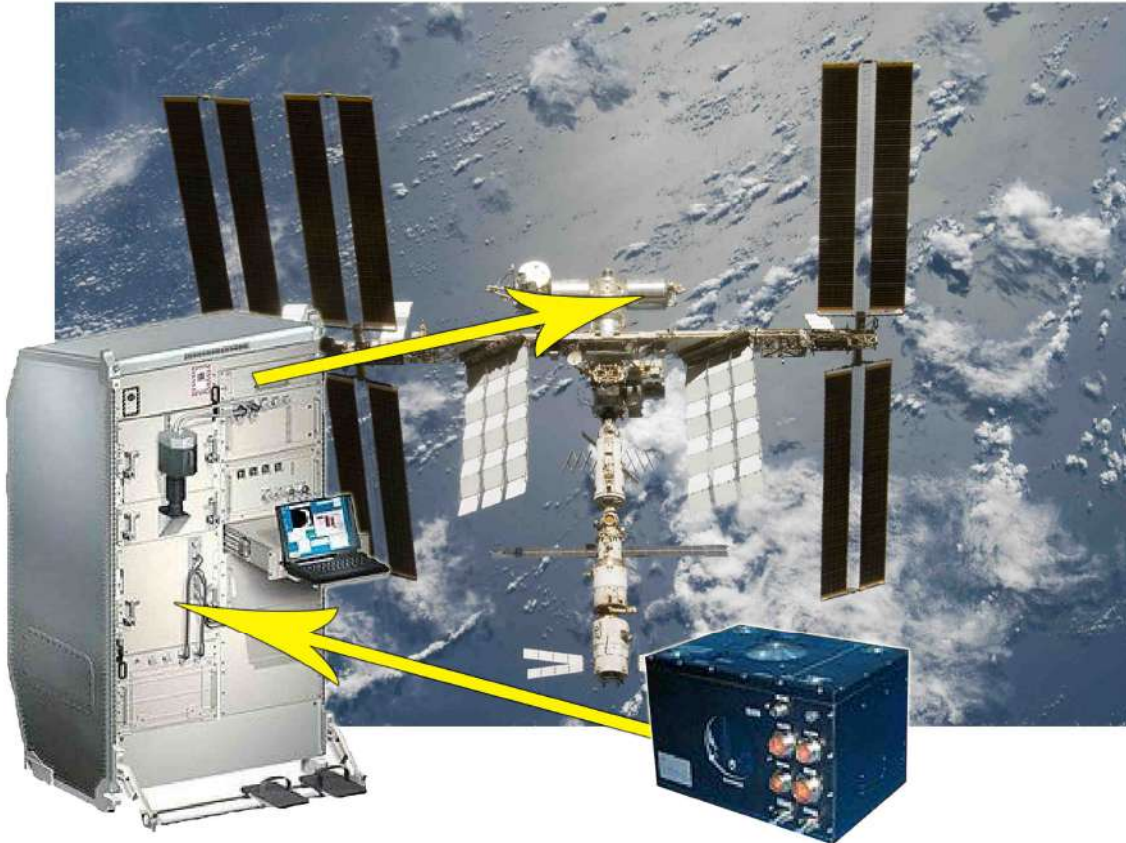
Figure 1-4: CIMEX-1 position inside FSL and the ISS

1.4 EADS

EADS (European Aeronautic Defence and Space Company) is the second largest Aerospace and Defence Company worldwide and the first one in Europe. It was formed on July 10th 2000 by the merge of Aérospatiale-Matra (France), DaimlerChrysler Aerospace AG (Germany) and Construcciones Aeronáuticas SA (Spain). The number of employees working in EADS was 119.500 in 2009.

The company produces civil and military aircraft, helicopters, missiles, communication systems, space rockets, satellites and components of the ISS.

EADS is formed by four divisions which are: Airbus, Astrium, Eurocopter and Cassidian.

Figure 1-5: EADS products portfolio

EADS Astrium is in turn divided into three departments which are Astrium Satellites, Astrium Services and Astrium Space Transportation. This thesis was carried out in TO-52; department of Astrium Space Transportation in Friedrichshafen, Germany. This department is in charge of developing Fluid Physics and Experimental Payloads for the International Space Station Columbus Laboratory.

1.5 Thesis objectives

The main assignments of this thesis project were building, testing and performing an analysis of the CIMEX-1 Closed Loop Breadboard. In the space industry Breadboards are ground tests which simulate the real experiment to be sent to orbit. Their purpose is to reduce the design risk and expand the knowledge of the system for a better understanding of its behavior.

In the particular case of the Closed Loop Breadboard (BB), the aim is to verify the closed loop performances of CIMEX-1 using the HFE-7100 fluid. This new liquid is meant to substitute the previous operative fluid which was Ethanol, as requested after the safety review 0/1. The target of this Breadboard is to test the foreseen parameters, previously established for Ethanol, to verify system compatibility and/or to eventually find new operative ranges in order to guarantee the system stability (this condition is essential to perform the scientific measurements).

1.6 Tasks performed

The main tasks undertaken during the thesis project were:

-Understanding the system design and the previous tests results.

-Ordering the missing components and finding/contacting the suppliers.

-Making a plan for performing the stand alone tests and for preparing the Breadboard on time for the test campaign.

-Assessing the characteristics/performances of the essential components (e.g. Gas Concentration Sensor, anti-wetting metallic foil with micro groove, liquid pump).

-Finding, together with the suppliers, the adequate settings for the instruments (in particular for the Bronkhorst meters/controllers).

-Building the Breadboard test setup according to the specifications.

-Performing the test campaign and collecting all of the experimental data.

-Making a post processing analysis and assessing the system behavior, operability and stability.

-Making a comparison between the project requirements (previously established for Ethanol) and the actual system performances/operability with HFE-7100.

-Proposing new requirements to ESA/Scientists teams.

-Creating a valuable experimental background for CIMEX-1 to be used both for future on ground tests and for the flight operations.

-Finding and solving eventual issues which were not encountered during the previous project steps.

2 CIMEX-1 Closed Loop test setup description

2.1 Introduction

This chapter is meant to explain the working principle of the Closed Loop Breadboard and to describe the main components functionality .Section 2.2 will give an overview on the main subsystems, clarifying their purposes and the concepts behind them. Afterwards, in section 2.3, all the elements taking part in the BB are explained in detail. For a better understanding of the subsequent paragraphs, it is advised to look at the BB schematic and pictures in Figure 2-2, Figure 2-3 and Figure 2-4.

2.2 Subsystems description

CIMEX-1 Closed Loop BB setup can be divided in different subsystems. This chapter is meant to give a general understanding while chapter 2.3 provides a deep insight of every component which was used for the setup. Graphical information about the subsystem are available in the schematic of Figure 2-2. The main Subsystems of CIMEX-1 Closed Loop BB are:

- ***The Evaporation Cell***. It is the core of CIMEX-1, providing the experimental volume within which the evaporation phenomenon to be studied takes place. The experimental liquid is placed in a chamber which is separated from the gas flow by a stainless steel thin foil. The project requirements specify that the liquid depth of the chamber should be adjustable, but no movable bottom is integrated in this experimental cell for this BB.
  The metallic foil has a square opening that represents the interface between the liquid and the gas flow. A gas channel allows the gas to flow over the liquid surface which is kept steady by constant injection of experimental fluid. More details about the cell design and configuration will be given in chapter 2.3.7.

Next sketch illustrates how the evaporation process takes place.
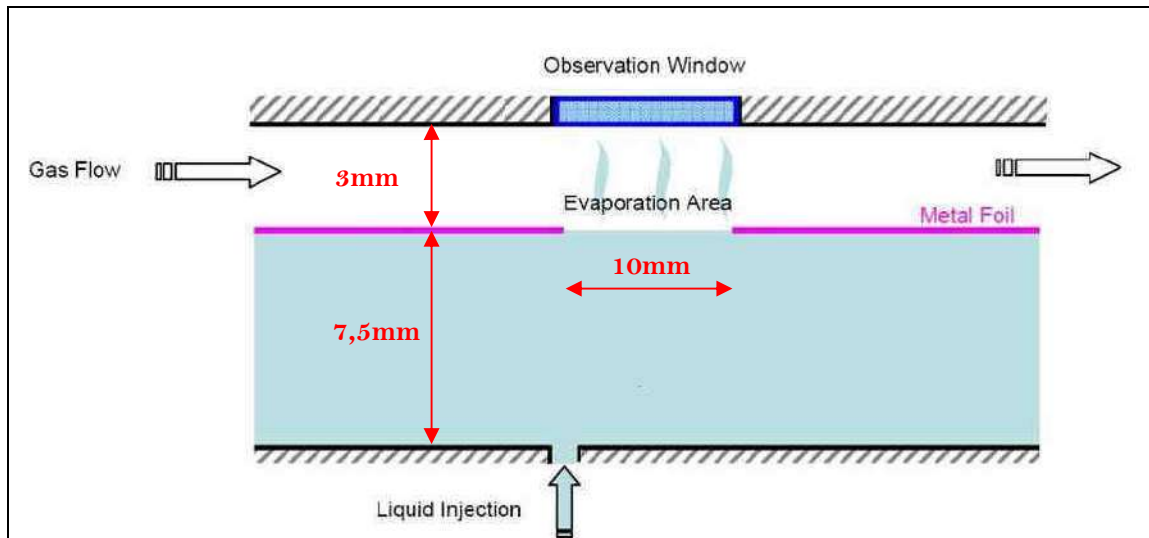
Figure 2-1: Evaporation concept

- ***The Condenser Separator Subsystem (CSS)***. The Condenser-Separator allows the CIMEX-1 experiment to be executed in a closed loop mode without the limitation caused by the use of consumables.

  The main objective of the CSS is to decrease the vapour quality and to separate the vapour phase to the gas phase. More information about this device will be given in section 2.3.8.

- ***The Liquid Loop Subsystem***. It provides the initial filling of both the evaporation cell and the CSS from the liquid reservoir, as well as feeding the liquid chamber while the evaporation phenomenon is taking place. Moreover it maintains the meniscus level of the CSS separator between two limits in order to assure the correct condensation, separation and extraction processes. This subsystem plays a key role in the whole BB steady state status.

- ***The Gas Loop Subsystem***. It guarantees the Nitrogen flow over the liquid surface of the evaporation cell chamber and it also permits adjustments of the flow rate according to the current experiment parameters. It provides the mixture gas flow from the evaporation cell to the CSS subsystem. Thanks to the Gas Concentration Sensor, the Mass Flow Meter and the Mass Flow Controller integrated in this loop, it is possible to establish the evaporation rate taking place in the evaporation cell. The Gas Pressure Control Loop is an essential part of the gas loop because it allows setting of different pressures in the gas loop subsystem. Indeed, it provides a real time controlling of the gas pressure in the circuit that avoids possible pressure fluctuations. It also permits the initial filling of Nitrogen from the gas reservoir to the gas circuit.

CIMEX Test campaign, June 2011

Breadboard configuration

Pressure controller

GL-PC

GL-SV2

Gas Pressure Control Loop

Camera to check the liquid level

Gas cell temperature

Gas temperature above the liquid level

Gas Loop

GL-GC

Cooling loop set @ 23.5°C (from Haake heat exchanger)

For degassing during initial filling of the separator

GL-GP

GL-SV3

GL-FC   GL-GCS

Gas inlet temperature

Air cooling

FC-TEC-gas   FC-TEC-gas

Air cooling

Fixed Bottom

Evaporation cell

Gas outlet temperature

To Separator

CS-TEC-C

CS-Cond

CS-V

Separator wall

CS-SEP

Camera to check the meniscus position

CS-TEC-C

FC-P-OUT

GL-FM

Condenser wall

GL-SV1

Liquid Loop

LL-LP

LL-SV1

GL-RES   GL-RES2

P

LL-SV2

GL-SV4

LL-RES1

GL-SV5

LEGEND

CS-COND	Condenser
CS-SEP	Separator
CS-V	Degassing Valve
FC	Fluid Cell
FC-P-OUT	Pressure Sensor
GCS	Gas Concentration Sensor
GL-FC	Gas Loop Flow Controller
GL-FM	Gas Loop Flow Meter
GL-GC	Gas Loop Gas Circulation pump
GL-GCS	Gas Loop Gas Concentration Sensor
GL-GP	Gas Loop Gas Retraction Pump
GL-PC	Gas Loop Pressure Controller
GL-RES	Gas Loop Reservoir
GL-SV	Gas Loop Valve
LL-LP	Liquid Loop Liquid Pump
LL-RES	Liquid Loop Reservoir
LL-SV	Liquid Loop Valve
MFC	Mass Flow Controller
MFM	Mass Flow Meter
TEC	Thermo Electric Cooler
T	Temperature Sensor

Figure 2-2: Breadboard schematic
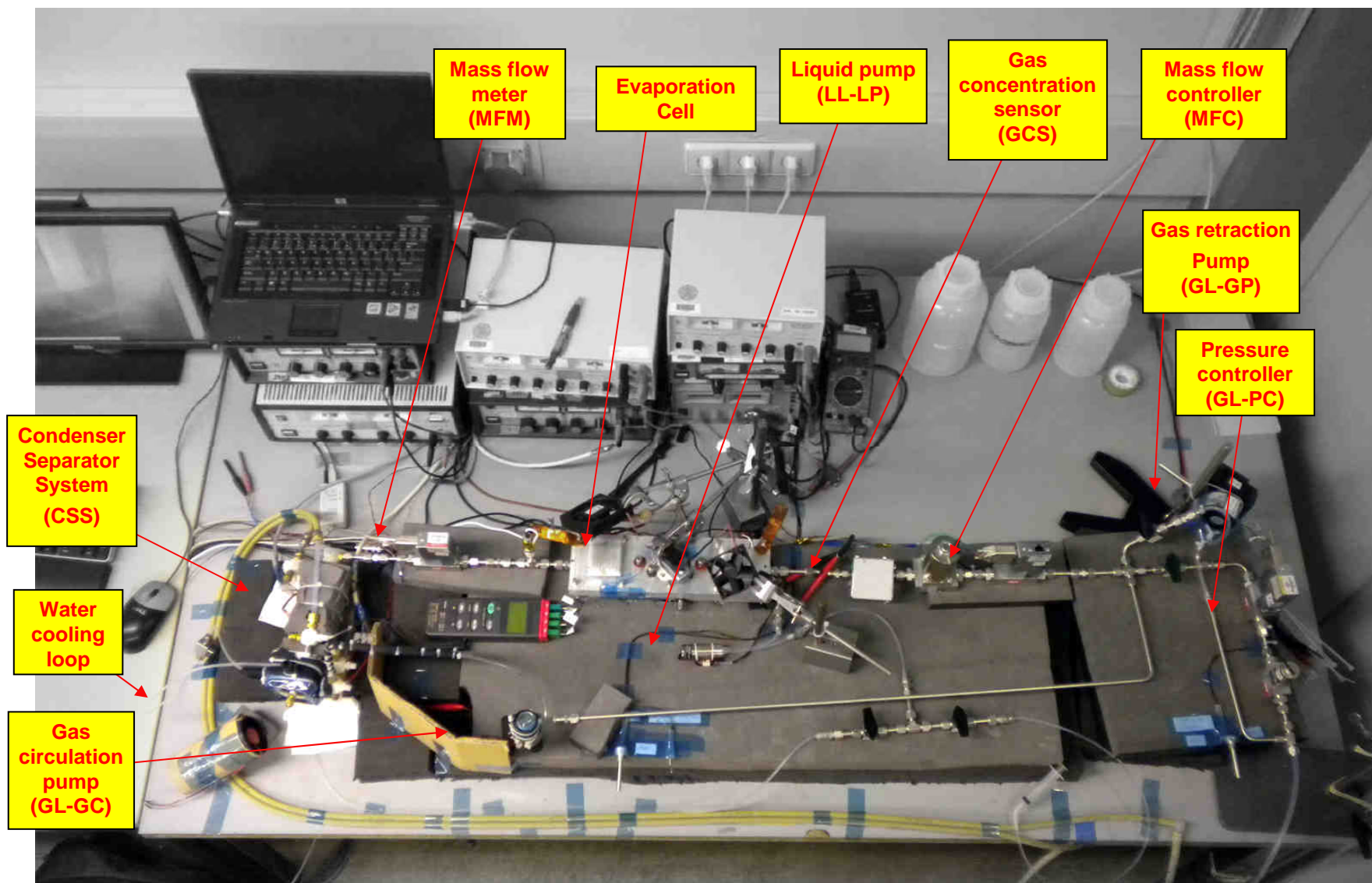
Figure 2-3: Breadboard setup top view
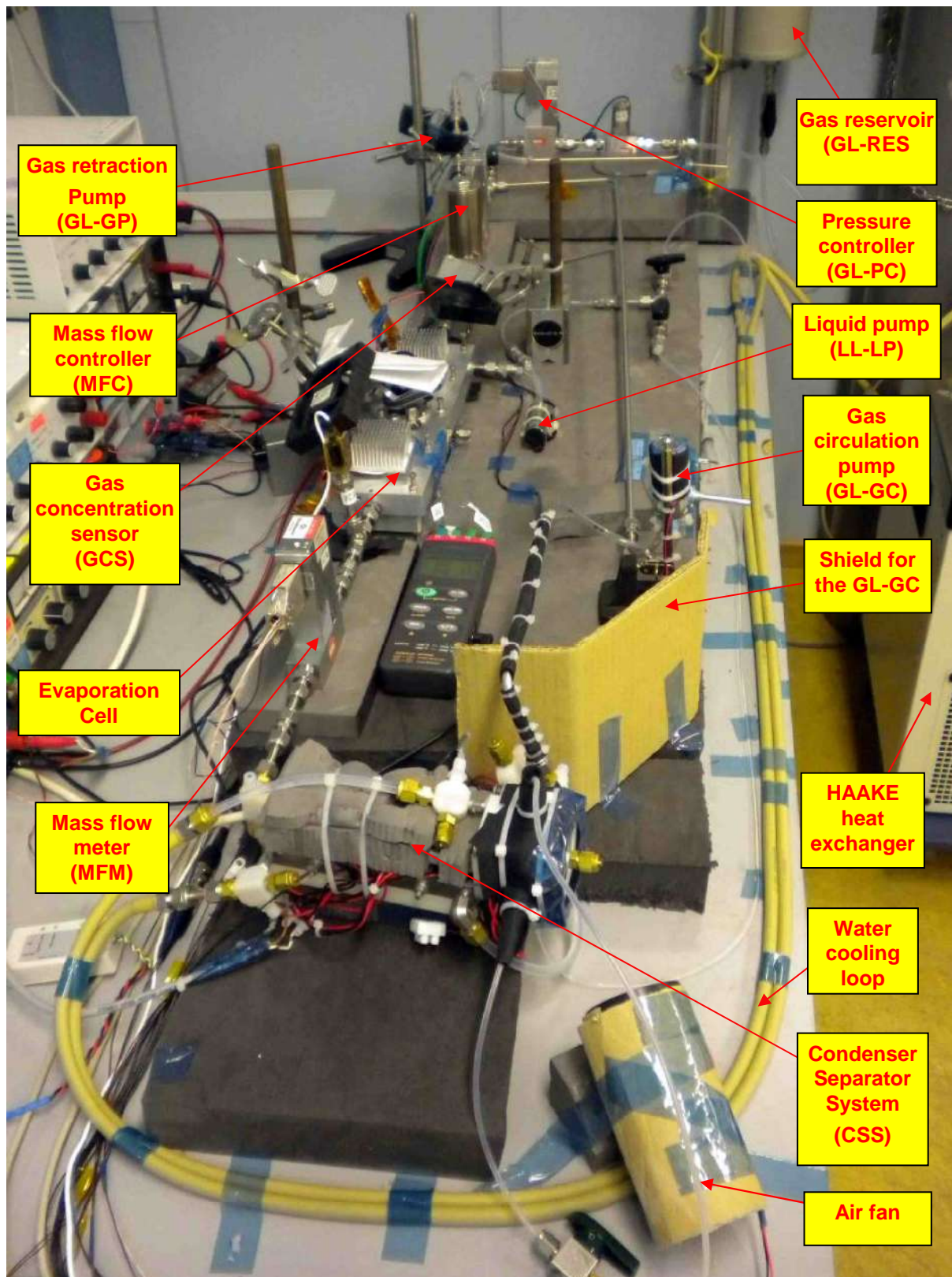
Figure 2-4: Breadboard setup side view

2.3 Components description

2.3.1 Liquid pump

The liquid pump (LL-LP) provides the liquid flow from the CSS to the evaporation cell in order to feed the liquid chamber when the evaporation phenomenon is taking place. The pump is also used to fill the cell during the system initialization, when the liquid chamber is still empty.

Figure 2-5: Liquid pump "HNP mzr-4661"

A new liquid pump, different from that was foreseen for CIMEX-1, was used during the test campaign. This newly selected pump is recent in the market and provides a high pumping resolution (minimum achievable flow rate of 4,8ml/min). This pump is recommended to be used in CIMEX-1, due to the hermetic properties and resolution. The main characteristics of the pump are summarized in the datasheet reported in Annex 6:. The pump has a micro annular gear and it is magnetically sealed. The speed control is possible thanks to a 0-10VDC input signal and the direction of the flow is reversible. This feature helps the operator to better maintain constant the liquid level of the square opening and to fill the line from the reservoir till the separator during the system initialization. This operation was possible by changing the state of the valves LL-SV1 and LL-SV2. An electric switch allowed changing the pump direction and a potentiometer permitted the pump speed setting, giving as an output a 0-10VDC signal. The pump was powered constantly at 15VDC. In Figure 2-6 is possible to see the mentioned components.
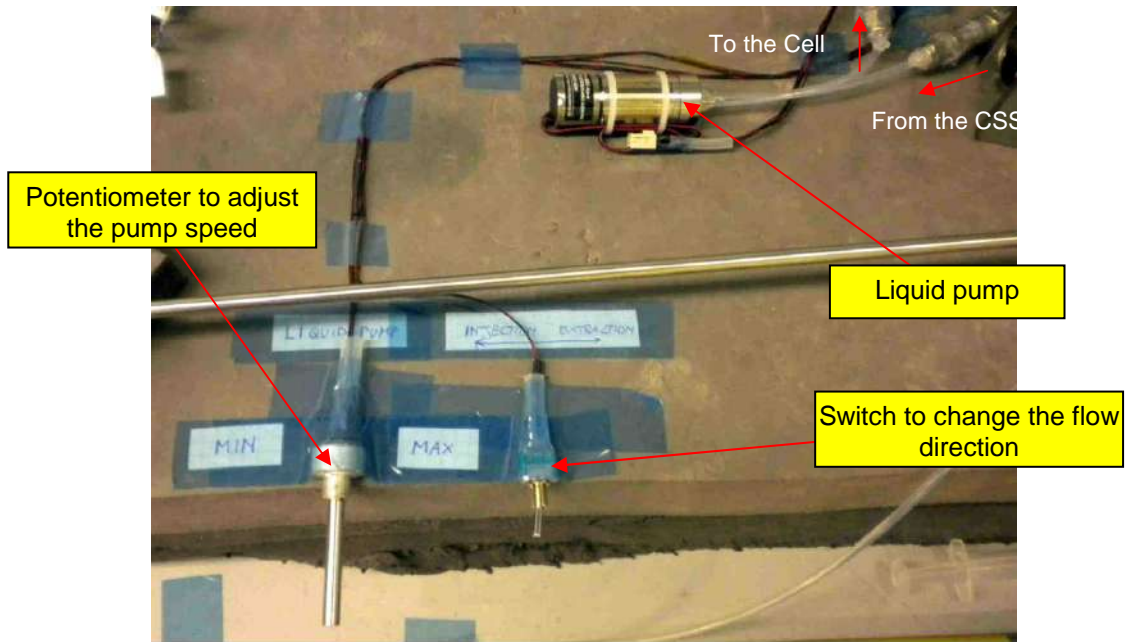
Figure 2-6: Liquid pump control devices

As it was suggested from the supplier a filter for $15 \mu m$ particles was integrated in the line before the liquid pump to prevent possible dirt to reach the pump mechanisms. Because of the small dimension of the gear even a small particle could damage the mechanism.

2.3.2 Gas circulator pump

The gas circulation pump (GL-GC) provides the gas flow passing over the experimental cell liquid and going from the evaporation cell to the CSS subsystem. The pump is a rotary vane pump provided by THOMAS (model no.BL-G-12/02-4 E110 D) and it was chosen because of the availability during tests and its hermetic characteristics. Figure 2-7 shows the device connected to the circuit.
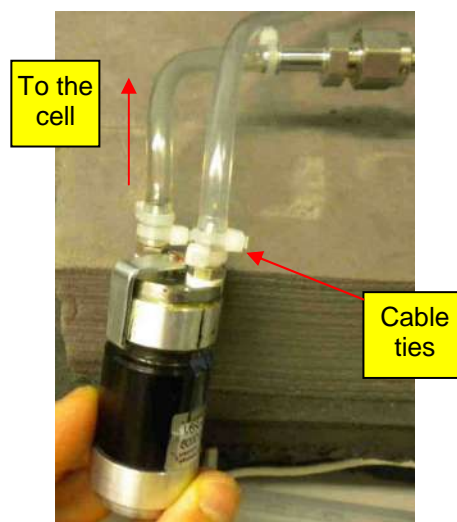
Figure 2-7: Gas circulation pump connections

The pump connections consisted of plastic tubes, as it is possible to see form the picture. It was not possible to use metal tubing because no proper fittings were available to connect the pump to the Swagelok tubes system. Cable ties where adopted in order to tight the plastic cables to the pump connections and to the Swagelok tubes.

2.3.2.1 Pump installation

The pump was installed in a vertical position and upside down to prevent the eventual HFE liquid coming out from the separator to go into the device. The following picture shows the pump configuration.
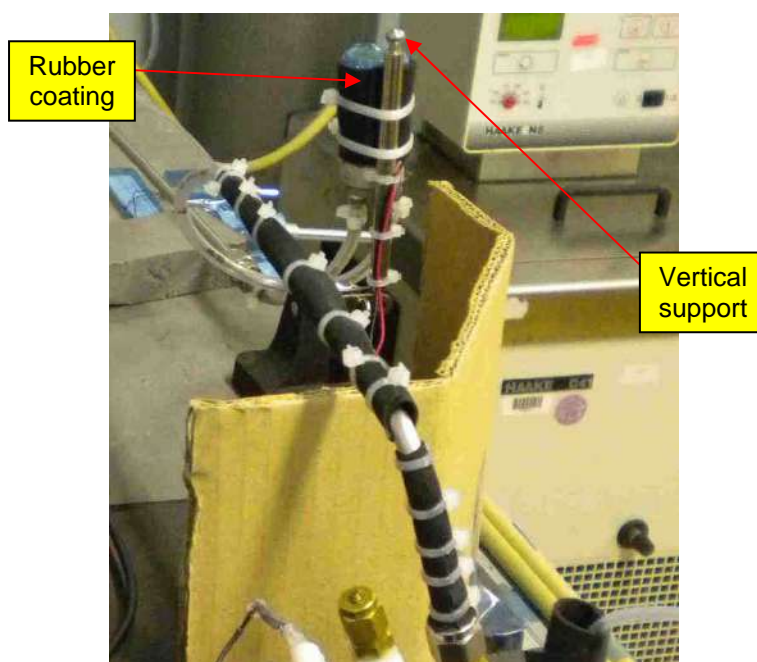
Figure 2-8: Installation of the gas circulation pump

A shield was mounted in order protect the liquid pump form the air jet coming from the fan used to prevent condensation in the separator window. The air flow could in fact cool down the pump with a consequent, unwanted condensation of HFE-7100 vapor. The shield is indicated in Figure 2-4 and it is also visible in Figure 2-8. Moreover, for a better protection of the pump from the air jet, a rubber foil was used to cover the device (see Figure 2-8).

2.3.3 Gas retraction pump

The gas retraction pump (GL-GP) allows, together with the pressure control loop, changing the system pressure. The selected pump, although it is not the one foreseen for CIMEX-1, is the micro-diaphragm gas pump NMP 850.1.2.KNDC B from the KNF Neuberger Company.
The working principle consists of an elastic diaphragm, fixed on its edge that moves its central point up and down by means of an eccentric. This way the gas is transferred using automatic valves.

The materials used for this pump are EPDM (Ethylene Propylene Diene Monomer rubber) for the valves and diaphragm and Ryton for the pump Head. The pump is capable of delivering a maximum volumetric flow rate of 4,2 l/min and the lowest achievable absolute pressure is 230mbar. The pump was powered at 12VDC and it was controlled by a 0-5VDC signal which was provided by a potentiometer.

Plastic tubes were used to connect the pump to the circuit because no Swagelok fittings were available. Moreover cable ties were used to better tight the connections.

In Figure 2-9 it is possible to see the pump installed in the pressure control loop and the potentiometer used to control the speed. The green arrows indicate the directions of the flows.
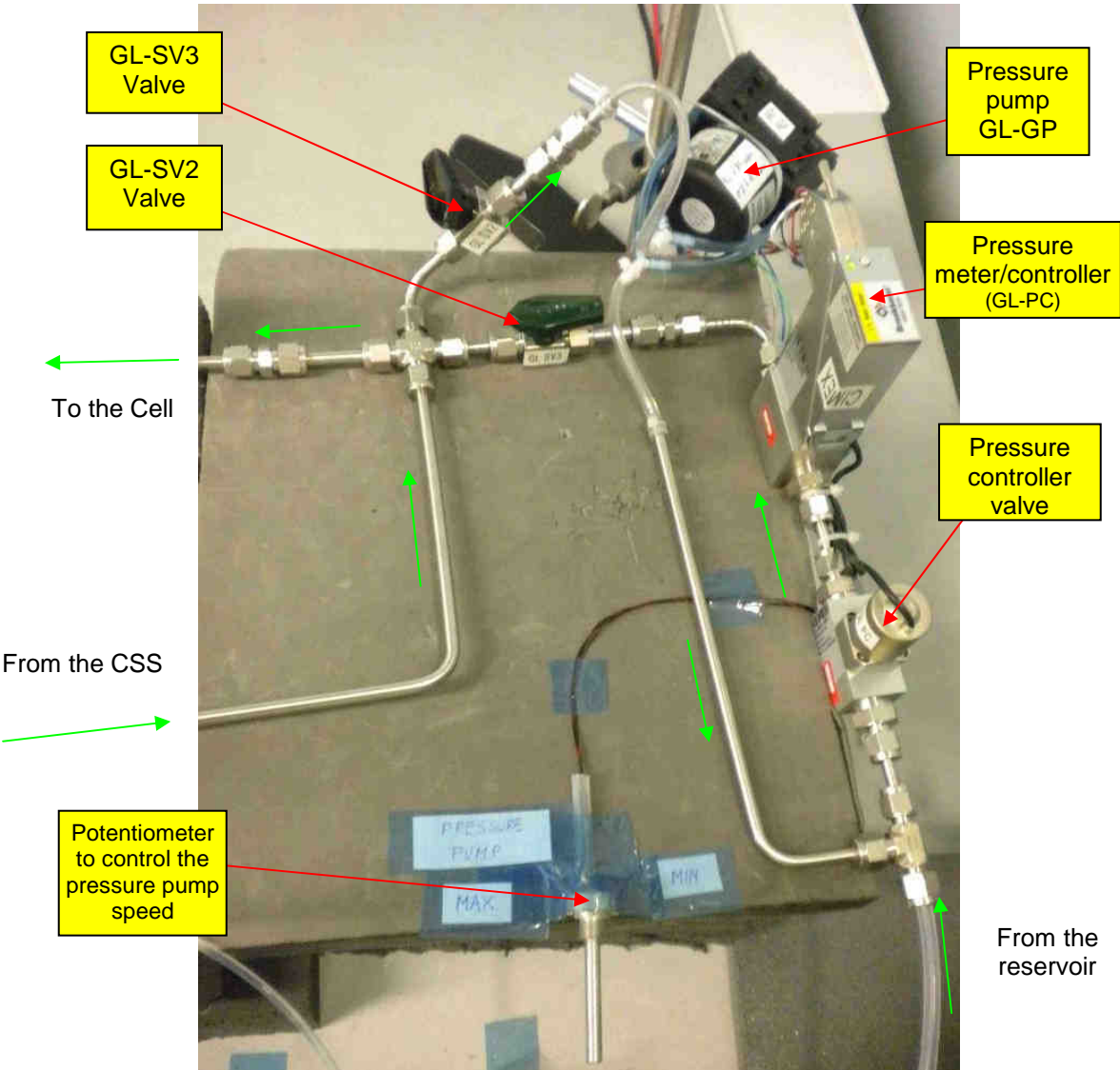
Figure 2-9: Gas retraction pump and pressure control loop

This pressure pump was oversized for the purpose of this experiment. It created in fact a lot of back pressure waves in the main gas loop, with the consequent loss of the liquid interface stability. In order to solve this problem two valves were installed: the first (GL-SV2) between the PC and the main circuit and the second (GL-SV3) between the pressure pump and the main circuit. During each test the

pressure was firstly set and then the valves GL-SV2 and GL-SV3 were closed in order to exclude the pressure pump from the main circuit. The main gas loop was sealed and so the pressure was foreseen to remain constant during the entire test.

2.3.4 Pressure controller

The pressure controller ensured, together with the pressure pump, the control of the pressure in the main gas loop. This was possible because of the action of a valve, controlled by the PC, which opens and closes depending on the pressure value of the main circuit that has to be controlled. The selected pressure controller is the one foreseen for CIMEX-1 from Bronkhorst Company (model number is: EL-PRESS –P502C). The data sheet is available in Annex 6:.

The measuring principle is based in a piezoresistive bridge on the surface of a silicon chip. When a pressure acts on this chip, the diaphragm bends, and the resistor values of the bridge alters in respect to the current pressure.

With the selected model it was possible to adjust the pressure in all the required range from 400 until 1000mbar.

In order to be able to operate the instrument and to read the values the pressure controller was connected to the computer by using the RS-232 serial connection. The instrument was powered with 28VDC, the same voltage available in FSL.

The instruments were sent to the supplier for the O-rings changing to the EPDM type in order to fulfill the material compatibility with HFE-7100.

The pressure controller is shown in Figure 2-9, Figure 2-3 and Figure 2-4.

2.3.5 Mass flow meter and mass flow controller

The mass flow controller (MFC) controls the gas mixture flow rate entering the experimental cell, while the mass flow meter (MFM) measures the mass flow rate exiting the cell. The instruments that were used were the Low-ΔP-Flow Controller and the Low-ΔP-Flow Meter from Bronkhorst Company, foreseen to be used in CIMEX-1.

These devices use a measuring principle based on the thermal bypass method which in turn adopts the heat conductivity of fluids to determine the mass flow. As it is shown in Figure 2-10, a small quantity of the main flow is directed through the sensor, which is warmed up by two heaters. Due to the heaters the measured temperatures T1 and T2 drift apart. The temperature difference is directly proportional to mass stream which flows through the sensor.

Both the instruments were calibrated with a mixture of 5% of Ethanol vapor and 95% of Nitrogen (mass fractions) because they were previously used for the Ethanol tests. A conversion was therefore needed to obtain the proper values referred to the HFE-7100. This transformation will be performed in chapter 5.3.

In order to fulfill the material compatibility with HFE-7100 the instruments were sent to Wagner for the O-rings changing to the EPDM type.
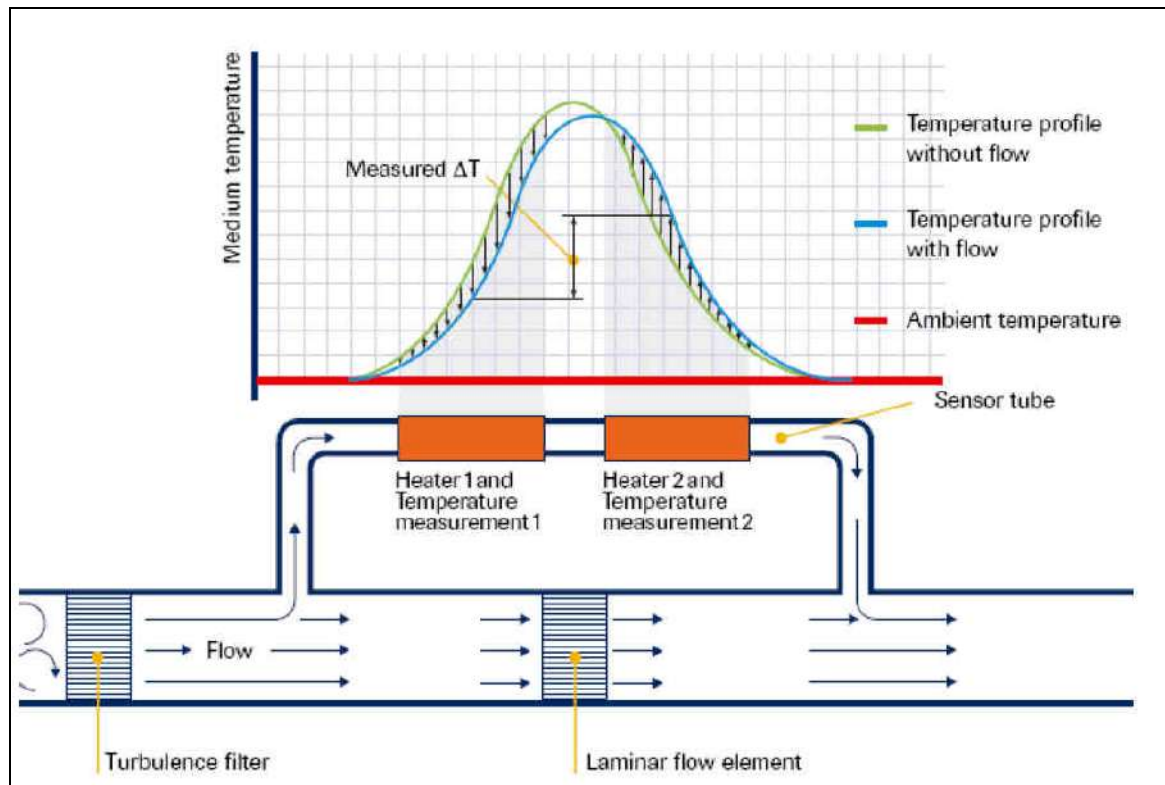
Figure 2-10: Bronkhorst Low-ΔP-Flow Meter measuring principle [11]

2.3.5.1 Bronkhorst instrument interface

The meters were connected to the computer using the RS-232 connection. The maximum number of Bronkhorst´ instruments that can be connected to one single computer is limited to two. Since the Flow Bus System, which allows multiple connections, was not implemented in this test setup two computers had to be used to operate the two Low-ΔP-Flow meters and the pressure controller.

The following programs (provided by Bronkhorst) were used for the communication with the instruments:

- FlowDDE (Dynamic Data Exchange): Used to establish communication between computer and the different devices. By using DDE commands, sent by software, to the DDE Server, data can be sent or requested from the FLOW-BUS.
- FlowView: Used to read and control the flow parameters.
- Flow-Plot: Used for signal monitoring program and for plotting up to four parameters versus time.

2.3.6 Gas concentration sensor

2.3.6.1 Sensor description

The Gas Concentration Sensor (GCS) is meant to measure the HFE-7100 vapor concentration at the entrance of the experiment cell. The device is a Non Dispersive Infra Red sensors and it was provided by SmartGas Mikrosensorik Gmbh. Its working principle is based on the infra-red gas technology.

Non Dispersive Infra Red sensors (NDIR) use a spectroscopique technique in order to measure the vapor quantity in the mixture. The main components of the sensor are an infra red lamp, a sample chamber, a wavelength filter, and an infrared light detector. The light that is emitted by the IR source passes through the mixture contained in the chamber. The detector is equipped with an optical filter which blocks all the light except the wavelength that the selected gas molecules can absorb.The amount of light that the detector can measure is therefore inversely proportional to the vapor concentration present in the flow. This is the physical principle used in the NDIR Gas Concentration Sensor.
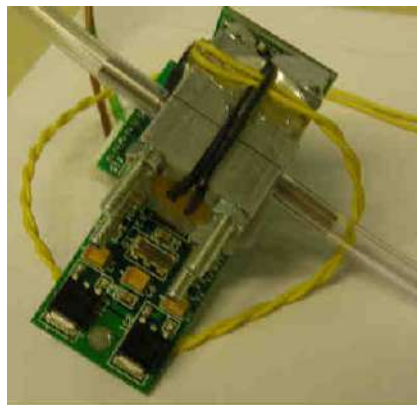
Figure 2-11: Smart Gas NDIR sensor

2.3.6.2 Sensor housing and fittings

The sensor was connected to the Swagelok tubes using Swagelok fittings. Next picture shows the GCS fittings/connections
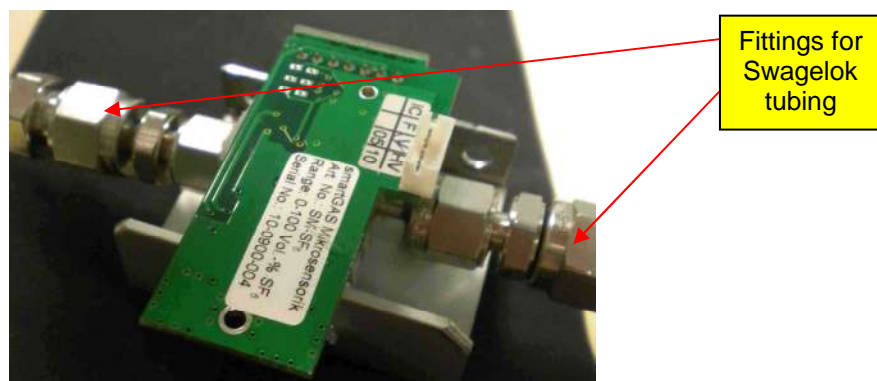
Figure 2-12: Gas concentration sensor with the mounted fittings

A dedicated metal housing was built for the sensor in order to prevent eventual damages. Next picture shows how the GCS housing looked like.
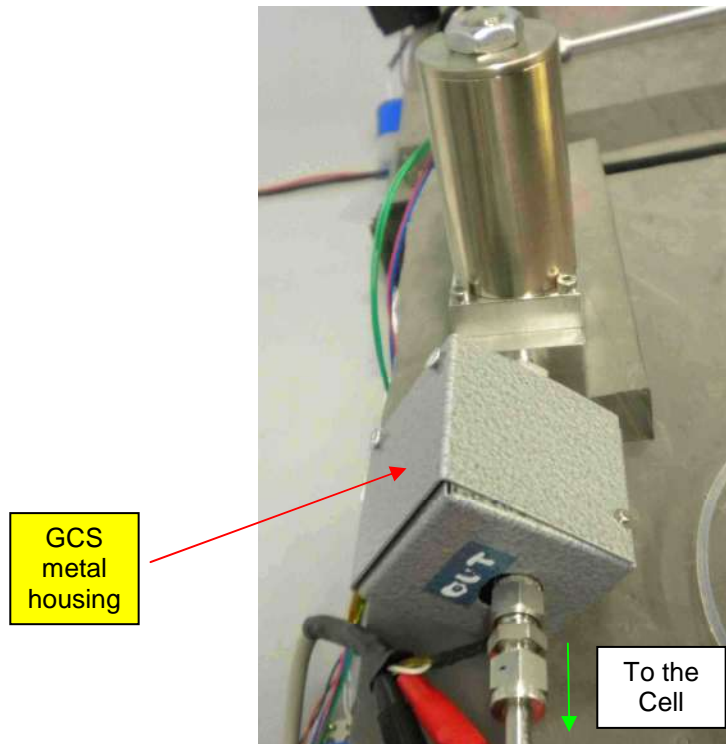
Figure 2-13: Gas concentration sensor mounted in the final circuit

2.3.6.3 Sensor interfaces

The sensor was connected to the PC using the USB connection and the data readout was shown in a program provided by Smart Gas. A post processing of the GCS readout value was needed since the sensor buffer was designed for another type of medium than HFE-7100 vapor. Due to the high sensitivity of the electronics to the HFE-7100 the numerical readout values exceeded the expected value and the buffer overflowed. Therefore the GCS readout experienced "jumps" each time the buffer became full. Since the value of the jumps was known a Java program was built in order to correct the readout values.

The program read constantly the readout data coming from the Smart Gas` program and detected automatically the jumps. The correct readout value was then obtained by summing the actual value with the eventual "jump" amount. The program performed another calculation: it converted the corrected readout value to the final volumetric concentration associated with that value. This transformation is performed using the following formula obtained from the previous GCS calibration campaign (see Reference [8]):

$$SR = 5,1266 \cdot p \cdot C + 632,79 \cdot C \qquad \textit{(Eq. 1)}$$

Where p is the pressure, SR is sensor readout and C is the concentration expressed in % Vol. The pressure had to be updated continuously in the program, for each test condition, in order to have to correct volumetric value. Figure 2-14 shows a screenshot of the two programs during a test.
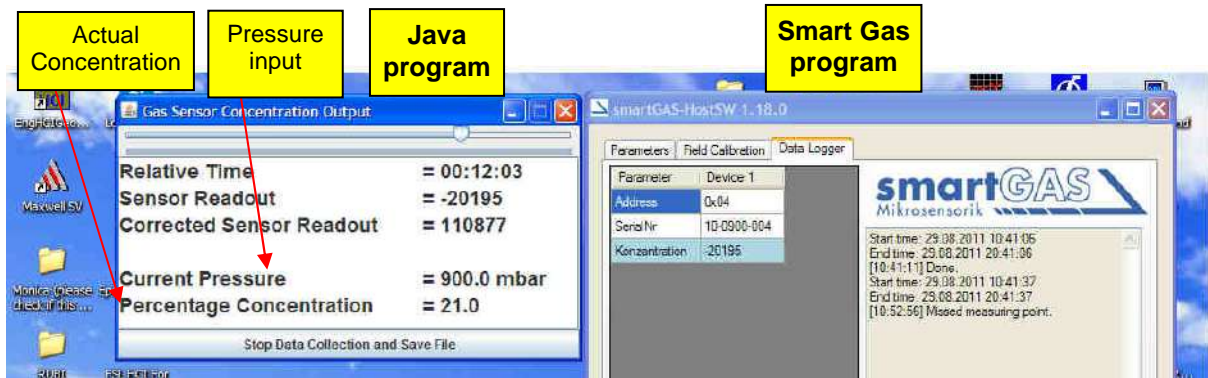
Figure 2-14: Java and Smart Gas programs

In order to have a correct sensor read out from the Java program the zero concentration value had to be set before the beginning of the tests. To do so the gas loop was firstly flushed with pure Nitrogen (prior to the liquid filling) and when the circuit was cleared from HFE particles the java program could be started from the zero value.

2.3.7 Evaporation cell

The Evaporation cell is the heart of CIMEX-1 in which the evaporation process takes place. It has in particular to provide similar conditions of the evaporation cell foreseen for the project (see Figure 1-1). Windows are installed on the top and on the bottom of the cell for the optical interface (i.e. cameras). Thermal controlling is provided to maintain the fluids in the evaporation area at temperatures within the range from 10℃ to 60℃. The cell supports flow rat es between 10 ml/min and 1000 ml/min at pressures between 400 mbar and 1000 mbar, as described in the requirements.

The variable liquid depth, requested from the requirements [2], was not implemented in this version of the cell. A constant liquid dept of 7,5mm was used instead. The Nitrogen cavity of the cell had the same shape as the one designed for CIMEX-1. Thereby laminar flow takes place in the evaporation area (estimated Reynolds' number about 150) under all the possible operating ranges of the experiment, as it is foreseen to be for CIMEX-1. Furthermore the square opening of the metal foil had the same dimensions and thickness than the original one of CIMEX-1. Sealing of the cell is done by means of EPDM O-rings.

Figure 2-15 and Figure 2-16 show an isometric view and a cut view of the cell, respectively.
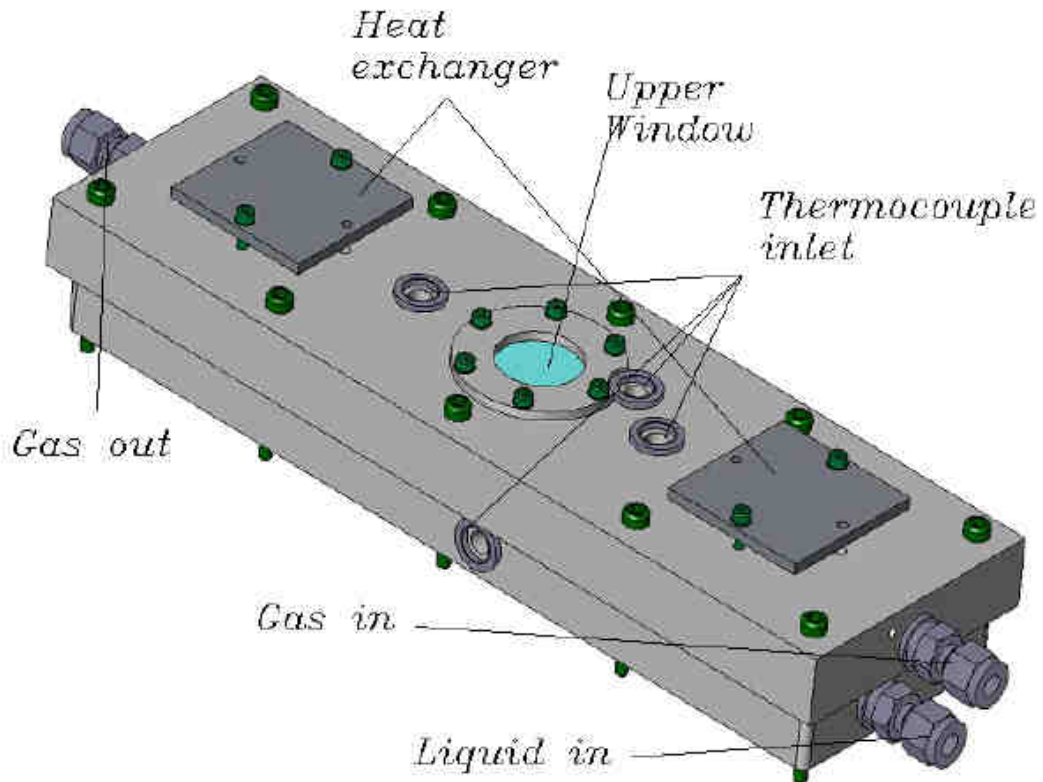
Figure 2-15: Isometric view of the designed evaporation cell
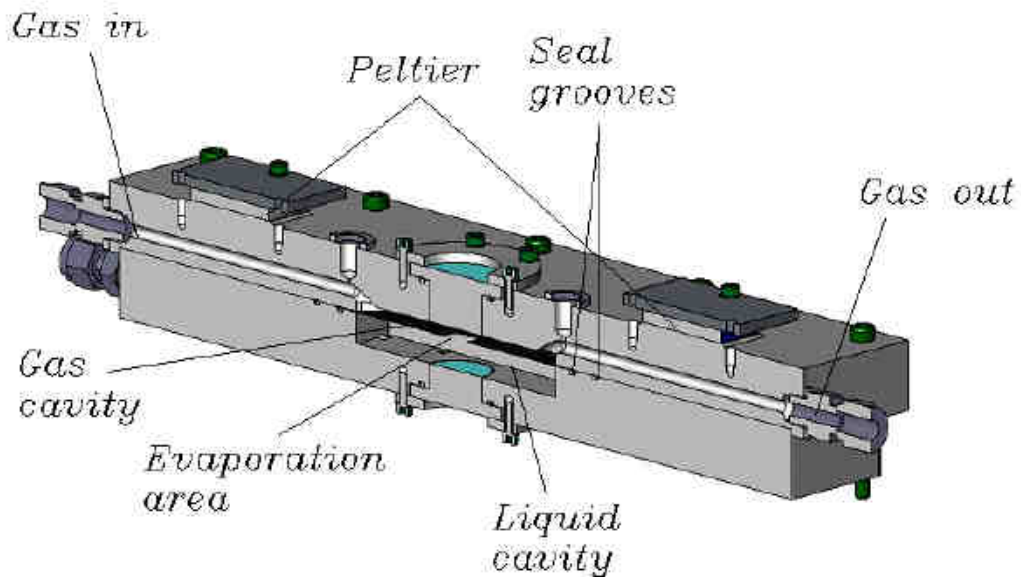
Figure 2-16: Cut of evaporation cell
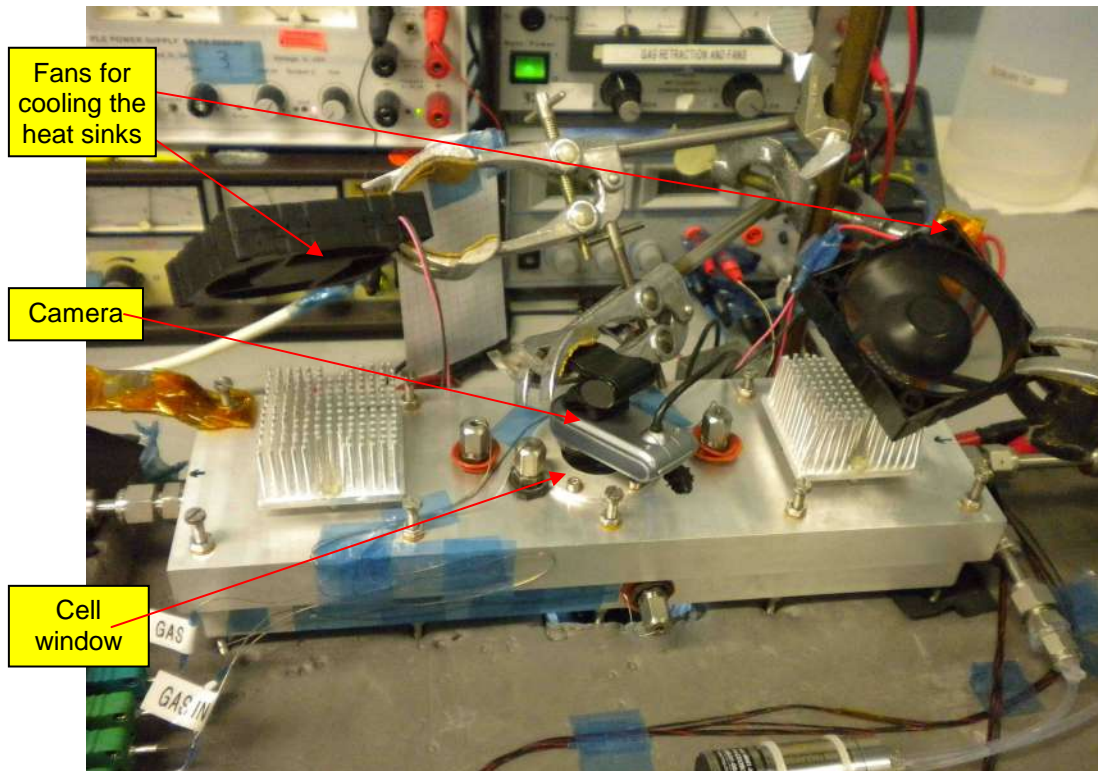
Figure 2-17: Experimental cell used in the test campaign setup

The material selected for the cell body (upper part and lower part) and the fixing rings for windows, was aluminum. The thin plate, on the contrary, was manufactured in stainless steel, the same material as the plate foreseen for CIMEX-1.

Windows were made by Polycarbonate, a material with good optical properties that has been already used in other Astrium Breadboards.

The thermal control of the cell was performed by means of two Peltier elements (electrical heating/cooling devices) situated on the top side of the cell. However with these devices the cell was only heated up till 50℃. Temperatures below the en vironment temperature were not reached because the cell was not thermally isolated. Heat sinks were used to dissipate the heat exchanged by the Peltier elements. Two fans were used to cool down the heat sinks. See Figure 2-17 for a better understanding of the arrangement. The cell temperature controlling was performed manually by changing the power supply settings.

Temperatures were measured by means of 4 thermocouples, situated at the gas inlet, at the gas outlet, at the evaporation area and in the middle of the liquid interface. The selected thermocouples were K-type from TC-Direct. Their diameter was 0,5 mm, small enough to avoid disturbances to the laminar flow.

One camera was placed above the cell upper window to check the liquid level surface and another one was placed underneath the cell to see the eventual liquid bubbling or the eventual leaks.

Figure 2-18 shows the sketch of the evaporation area, the liquid pool, the gas channel and the thermocouples positions. One thermocouple was placed in the middle of the evaporation area, 1mm above the metal foil surface, as indicated in the sketch. In this way it was possible to detect the liquid

level of the liquid interface (the procedure is explained in detail in section 3.2.3) since no optical diagnostics (Schlieren) were installed.
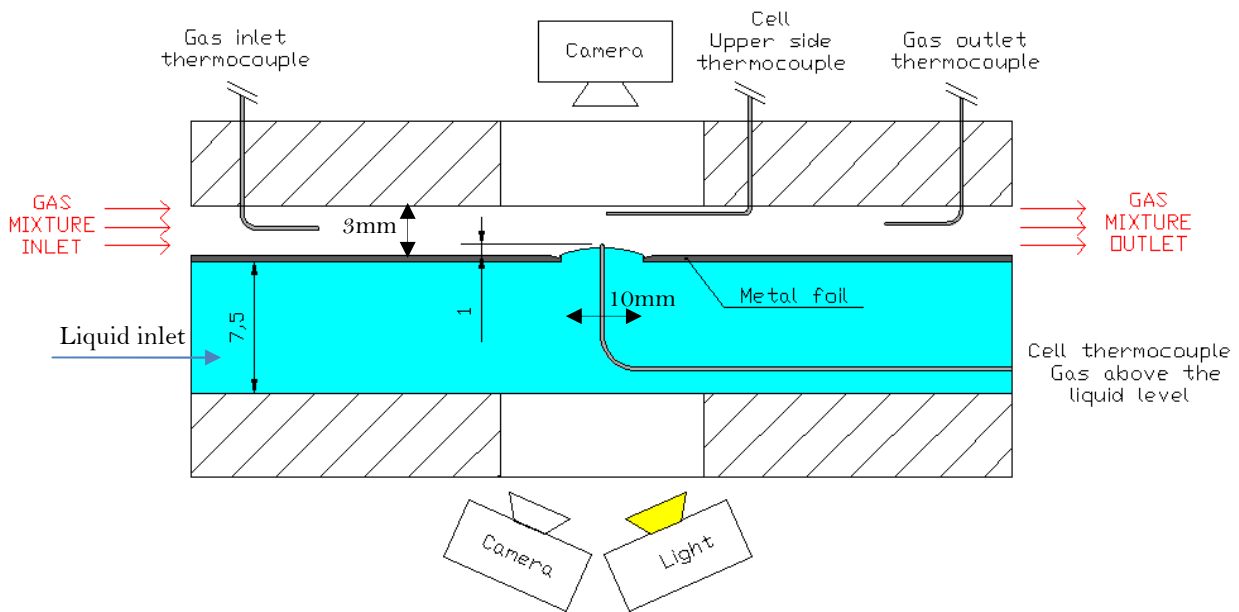
Figure 2-18: Experimental cell sketch and thermocouples positions.

2.3.7.1 Metallic foil with the anti-wetting groove

The metallic foil, seen in Figure 2-21, separates the liquid chamber from the Nitrogen flow and provides a square opening (10x10mm of dimension) through which the liquid evaporates. In order to permit a correct evaporation, the liquid interface must be flat. The requirements specify a surface flatness of ±0,1mm.

For this reason the metallic foil has to behave ideally as a non-wetting system. Wetting is referred to the ability to maintain contact with the solid surface and it is quantified by giving the angle θ at which the liquid-gas interface meets the solid liquid interface. Next picture shows the angle θ and the concept of wettability.
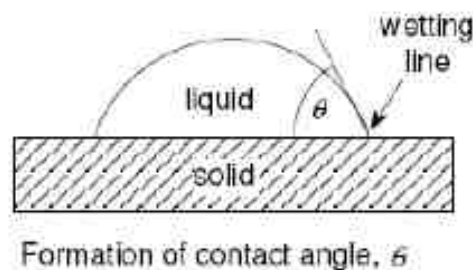
Figure 2-19: Wettability of a surface, contact angle.

An angle of 0° defines a perfect wetting system, wh ile an angle of 180° is referred to an ideal non-wetting system. In order to keep the liquid interface above the surface, the metallic foil should behave as an ideal non-wetting system.

Various solutions, like covering the metallic foil with special coatings, were tested in the past, but the results were not sufficient. A new anti-wetting concept was therefore introduced, which consists of creating a groove all around the edge of the square opening. This new metallic foil was tested prior to the test campaign. The results and the description of the specific stand alone test are available in section 3.2.

The geometry of the groove is shown in Figure 2-20, while Figure 2-22 shows the micro groove captured with the microscope.
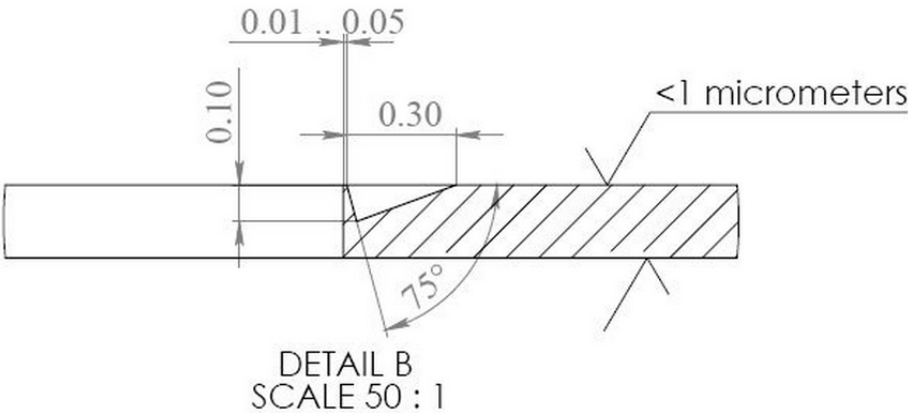
Figure 2-20: Geometry of the micro groove
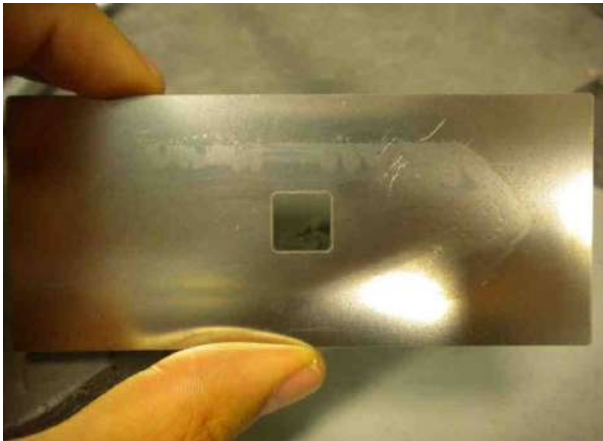
Figure 2-21: Metallic foil with micro groove
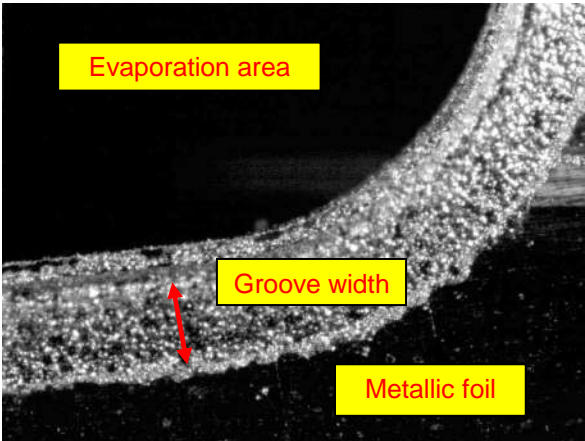
Figure 2-22: Picture of the groove captured with the microscope (scale 40:1)

The functionality of the anti-wetting system is essential for the whole project since it would not be possible to perform any experiment, according to the requirements, if the liquid interface flatness was not guaranteed. The performances of the new anti wetting system will be demonstrated with a dedicated stand alone test (see section 3.2).

2.3.8 Condenser separator system

The CSS main components are the separator and the condenser. The Condenser decreases the quality of the vapor while the separator divides the liquid phase to the gas phase. The following sketch shows the CSS arrangement.
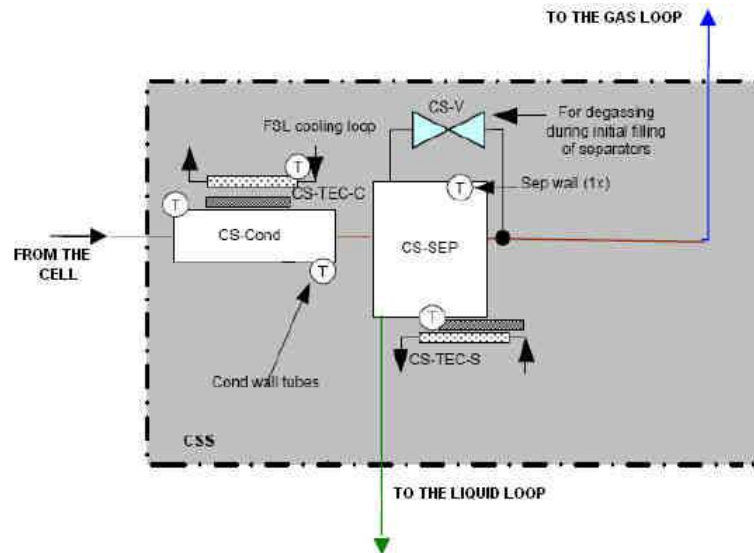
Figure 2-23: Functional schematic of the Condenser Separator System

The vapor from the evaporation cell enters the condenser, kept at a temperature of -10℃, and condensates due to the low temperature. A capillary channel film separator collects the liquid which is extracted from the bottom. Figure 2-24 shows the functionality of the CSS. To ensure and to maintain proper condensation, the film separator is also cooled via thermo electric cooler elements (TECs). The heat exchanged by the TECs is then delivered to a liquid cooling loop thanks to two cold plates. The cooling liquid is constantly provided by an heat exchanger (see Figure 2-27). The valve CS-V is installed between two separator connections for the de-gas during initial filling (on ground and in orbit). The condensed liquid in the film separator meniscus is retracted by the liquid pump LL-LP and transported back to the experiment cell.
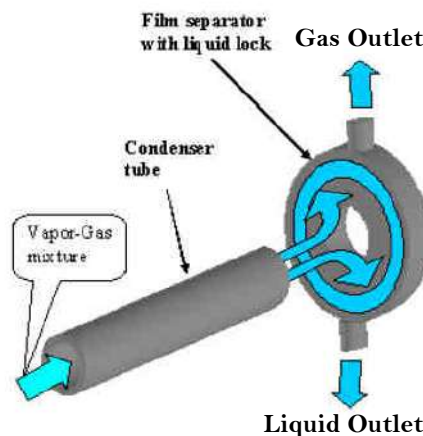
Figure 2-24: Functional principle of the Condenser-Separator

Next pictures show the condenser on the left side and the separator cut view on the right side.
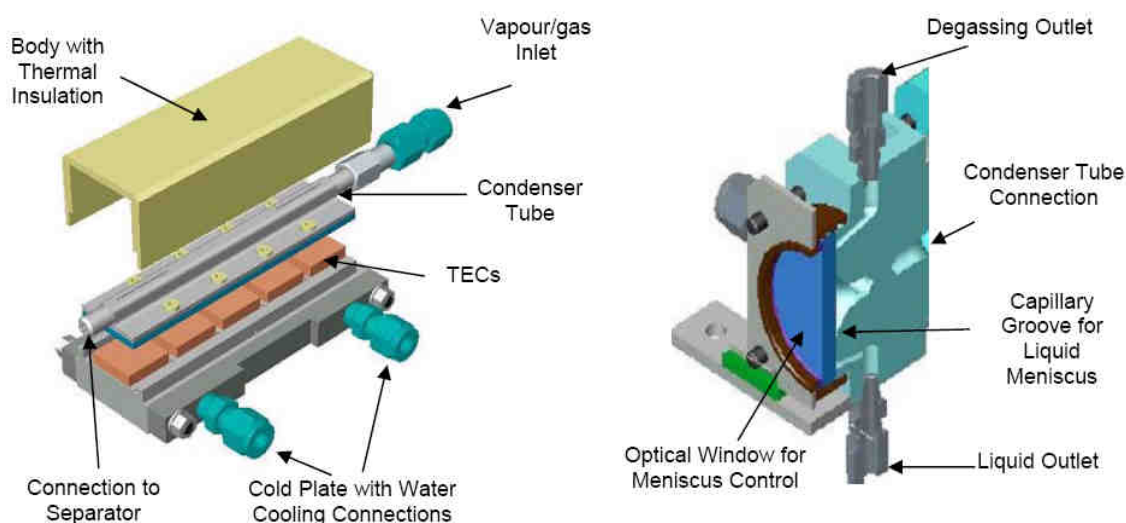
Figure 2-25: Condenser and Separator views

The TECs were divided in two groups: the condenser TECs and the separator TECs. In both groups the TECs were connected in series and powered with two different power supplies. The temperature adjustments were performed by changing the power settings until the desiderated values of temperature were reached. The maximum power limit, from the FSL requirements, for both the TECs channels, was 17V and 4,4A.

The cold plates were cooled with water which was provided by HAAKE heat exchanger (see Figure 2-27). The flow rate of the water was 22,5l/h and the temperature of the CSS water inlet was set to 23,5℃ . The Condenser and the Separator cold plate s were connected in series: the water entered the condenser and exits from the separator. Figure 2-2 helps to understand the arrangement.

The condenser was terminally isolated by a layer of foam which also prevented the condensation of the most air (of the lab environment) on the condenser walls. For the same reason the Separator was covered with a layer of rubber. Note that if air condenses on the condenser/separator walls ice would form and the CSS performances would be consequently reduced.

PT-1000 temperature sensors were installed for measuring the condenser and separator temperatures. Two other sensors were placed on the condenser inlet side, corresponding to the incoming mixture side. One was attached to the condenser wall and the other was attached on the cold plate, right above the previous one. Other two sensors were placed at the condenser outlet using the same arrangement as the other two. This way, it was possible to monitor the temperature gradient along the condenser due to the heat flux exchanged between the condenser and the cold plate. Another Pt-1000 sensor was attached to the separator wall.

Pt-1000 temperature sensors were also used to measure the cooling water inlet and outlet temperatures. Particular fittings, marked with green circles in Figure 2-26, were used to connect the Pt-1000 sensors.

A fan pointing to the separator window was installed, otherwise condensation would have occurred. The meniscus position has in fact to be visible in order to allow a correct extraction process.

The following picture shows the CSS during the tests.
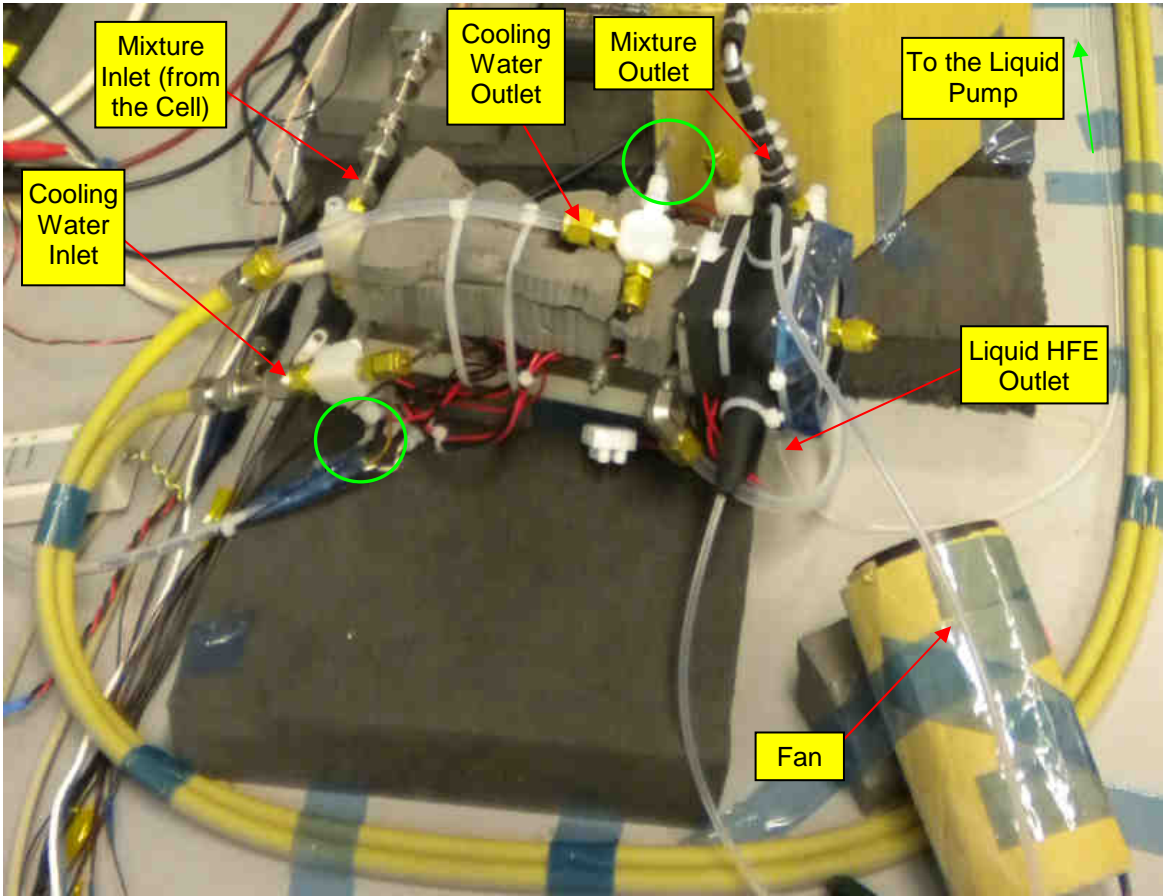
Figure 2-26: CSS Arrangement during the test campaign
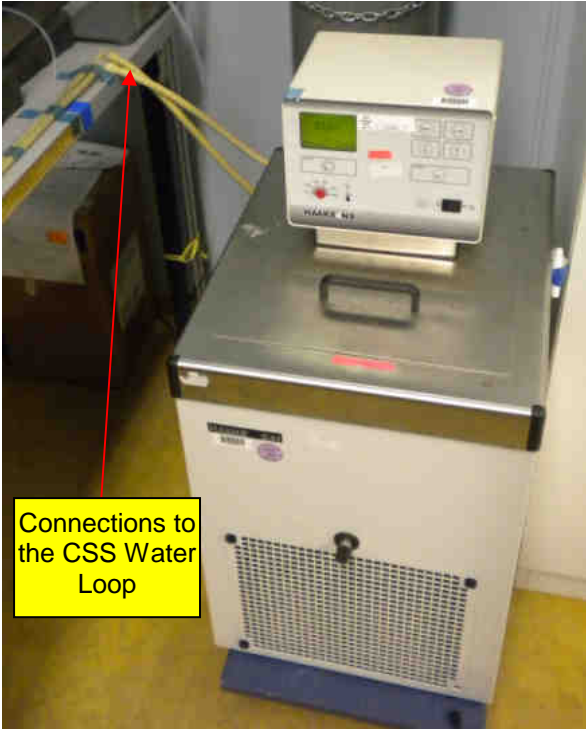
Figure 2-27: HAAKE heat exchanger

2.3.9 General circuit integration

The circuit integration was done by means of Swagelok tubing and fittings. The Bronkhorst instruments needed 6mm tubing while other components like the CSS and the cell needed ¼" tubing. Therefore, particular fittings were used to connect the 6mm tubes to ¼"tubes.

The connections between the gas circulation pump, the gas retraction pump and the Swagelok tubes were done by means of plastic tubes. At the time of the tests this solution was used, but in the future metal tubing or very rigid plastic should be used for the connections.

PFA tubes with 1/8" diameter were used for the liquid loop. The transparency of these tubes was very useful to check the presence of eventual bubbles in the liquid loop.

The metal tube that connected the CSS gas outlet to the Gas circulation pump was covered with a layer of rubber in order to isolate it from the air coming from the fan, otherwise condensation would have occur (see Figure 2-4 and Figure 2-8). CSS fittings were tight with Teflon.

2.3.10 Pressure sensor

A pressure sensor was installed for measuring the cell pressure. The selected instrument was the ETM-375 from Kulite. Next picture shows how it was mounted.
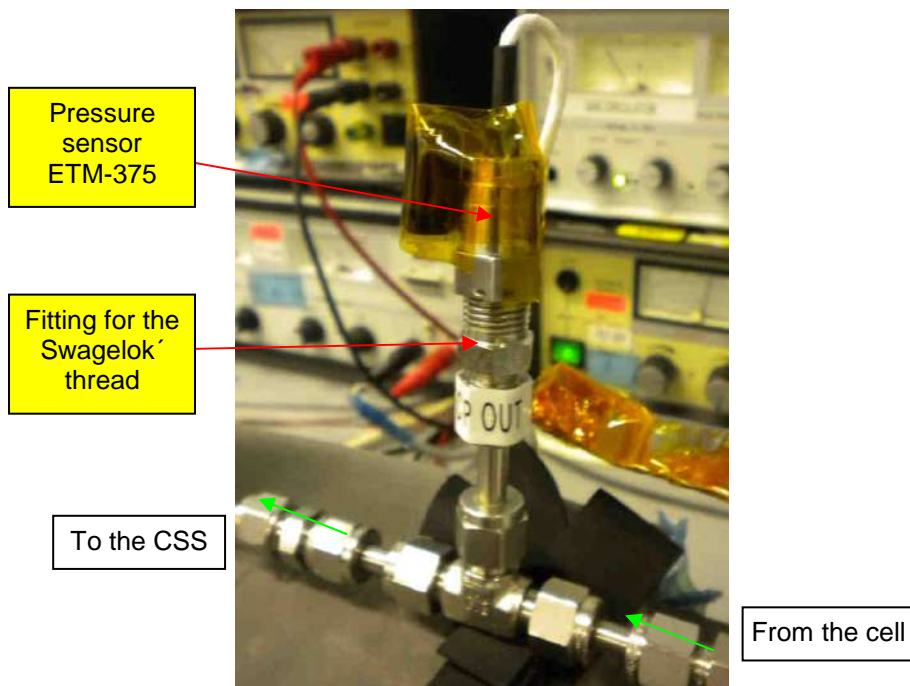
Figure 2-28: Kulite ETM-375 mounting configuration

A particular fitting, shown in Figure 2-28, allowed the transition from the pressure sensor thread to the Swagelok thread system.

The sensor was powered with 28VDC provided by the computer rack (see 2.3.11). The output signal was acquired by the computer rack as well.

The pressure range of this sensor was 0-1700mbara. The calibration of this sensor was performed prior to the closed loop test campaign. The specifications of the sensor are reported in the datasheet attached in Annex 6:.

31

2.3.11 Data acquisition system

In order to acquire the analog data from the pressure sensor and from the temperature sensors a computer rack was used. Then a Lab VIEW [16] program showed the data on the computer screen and saved all the information into a spreadsheet file. The computer rack provided also the 28VDC needed for the pressure sensor.

The four thermocouples were connected to a digital readout instrument which was in turn connected to the computer by an USB connection.

The Bronkhorst instruments were operated with FlowView and FlowPlot programs (see 2.3.5.1). With the last one was also possible to save the data into an excel file.

3 Stand alone tests

3.1 Introduction

The behavior of the specific components had to be checked before the final integration of the closed loop test setup. Therefore dedicated tests, with different setups, were performed. This section is meant to show what these tests were about and which results were achieved with them.

3.2 Metallic foil test with the anti-wetting groove

3.2.1 Introduction and purposes

This test was performed in order to check the behavior of the anti wetting groove (see 2.3.7.1). According to the requirements, the new metallic foil should allow a liquid surface flatness of ±0,1mm. To prove this a thermocouple was placed in the middle of the metallic foil window and its tip was placed 1 mm above the metallic foil level. The liquid interface height was therefore measured by making a comparison with the thermocouple tip.

Figure 2-18 shows the thermocouple arrangement. The final results of this test are very important for the whole project for the following reasons:

- The liquid interface flatness has to fulfill the requirement.
- The liquid interface stability has to be guaranteed by assuring that the liquid does not spill out during the measurements. Moreover the liquid has to be kept inside the window even when the cell is eventually shaken.

3.2.2 Test setup

The setup for this experiment is composed by the evaporation cell (the same used for the closed loop test) the MFC (see section 2.3.5), the pressure controller (see section 2.3.4), the pressure pump (see section 2.3.3) and a camera. A reservoir provides the Nitrogen for the experiment and a syringe was used to inject the HFE-7100 inside the cell. The gas that entered the cell was pure Nitrogen and the flow rate was controlled by the MFC. The pressure was set thanks to the pressure controller and the pressure pump installed after the cell. The liquid was injected in the cell by using a syringe. In order to check the level of the liquid interface a camera was placed above the top window of the cell. Figure 3-2 shows the setup that was built for this stand alone test and Figure 3-1 shows the functional schematic.
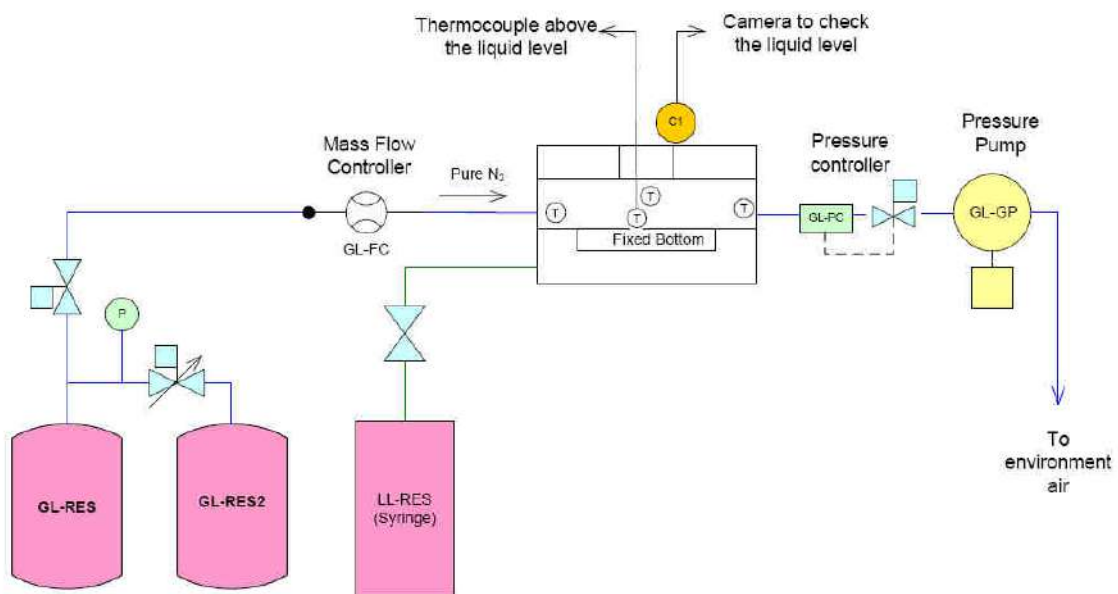
Figure 3-1: Anti wetting groove test, sketch of the setup
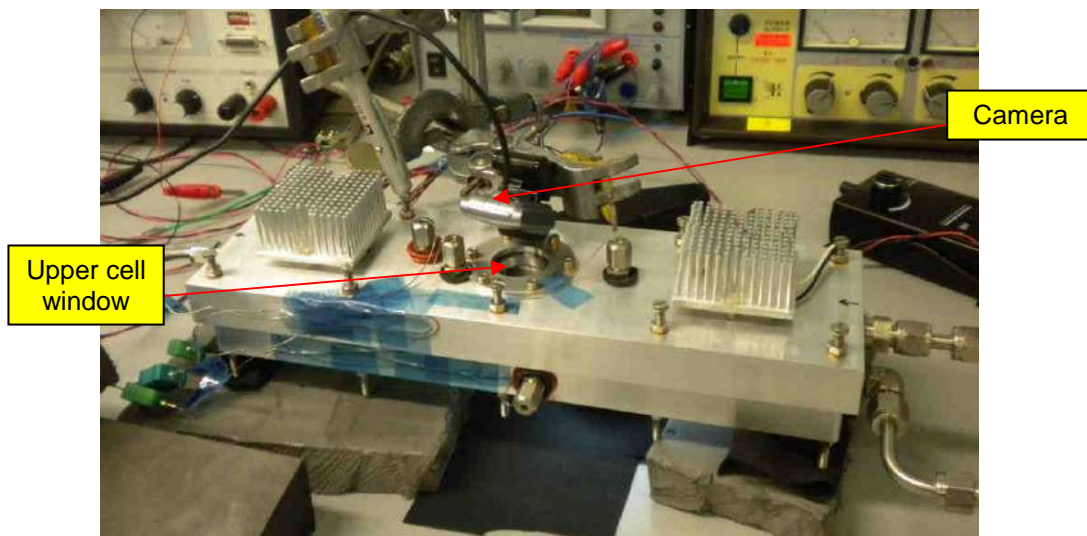
Figure 3-2: Cell configuration during the anti wetting groove test

3.2.3 Test results

The tests were performed at the maximum flow rate 1000 $[ml/min]_n$ and at a pressure of 960mbar (correspondent to the worst case condition).

The liquid level was checked by using the thermocouple, placed in the middle of the square opening, since no optical diagnostic was installed in this test setup. The liquid creates in fact a small circle, all around the thermocouple, which permits to estimate the height of the liquid by making a comparison with the probe tip. In the following table it is possible to see the filling sequence and the main meniscus positions.
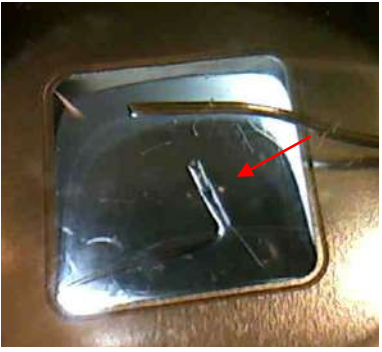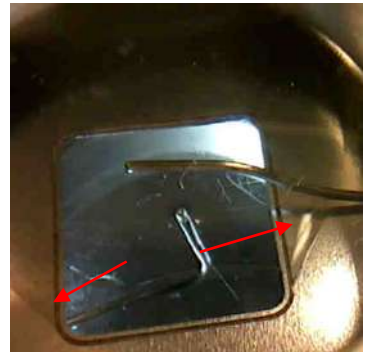
The liquid has the same height of the metallic foil level	The liquid level starts rising (check the circle around the thermocouple)	The liquid is now well above the metallic foil level
Now the over filling is evident also from the liquid reflex	The maximum liquid height of about 1mm is achieved. The liquid reflexes around the window are well evident.	Spilling after having injected more liquid.

Table 1: Anti-wetting groove results and main cell meniscus positions

3.2.4 Comparison with the simple metallic foil

A comparison with the behavior of the metallic foil without any type of anti wetting system permits a better assessment of the micro groove performance. Table 2 shows the results obtained with the simple edge metallic foil. From the sequence of pictures it is possible to see that as soon as the liquid interface height reaches the metallic foil level a further injection of liquid causes the spilling. This

means that the creation of a proper liquid meniscus is not possible and the requirements are not satisfied.

On the contrary, the metallic foil with the groove is able to keep the liquid inside the square window even when the liquid interface is well above the foil level. As it is possible to see there is a considerable difference between the maximum heights achieved in the tests shown in Table 1 and in Table 2.

Initial under filling.	The liquid is now at the same height as the metallic foil.	As soon as more liquid is injected the spilling occurs. The creation of a proper interface in not possible.

Table 2: Simple edge behavior

3.2.5 Comments and conclusions

The anti-wetting groove tests were successfully completed. The good performances with the new metallic foil can be summarized as follows:

- In the middle of the evaporating area, a maximum height of about 1mm was achieved. In the Table 1 and Table 2 the comparison of performance (with/without groove) has been provided with a performance improvement estimated at 0,8mm. Additionally, it has to be mentioned that the requirement for surface flatness is +/-0,1mm (which will be performed with a closed control loop Schlieren observation and liquid pump injection velocity). This means that the anti-wetting groove clearly covers/exceeds the required performance. Figure 3-3 helps to understand the good achievement.
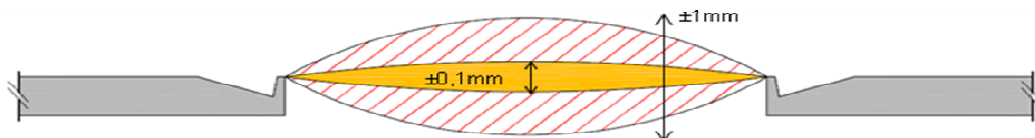
Figure 3-3: Sketch showing the required flatness range (yellow area) and the achieved range (red area). The requirement is well satisfied.

- Stable behavior within the entire requirement ranges of gas flow and pressure. Even with induced vibrations (e.g. shaking of the sample cell manually), the liquid was kept inside the evaporating area. These vibrations were widely exceeding any kind of external influence

that might be expected on-orbit. This characteristic enhances the system capability to maintain stable conditions;

- A further test was performed, to observe the performance of the micro-groove under saturated conditions. In this case, the actual test setup, did not allow perfect saturated conditions, since the loop tightness and pressure performance were a limiting factor. The loop lower limit pressure was 400mbar, which means that Nitrogen was present in the loop. Nevertheless, it was observed that the microgroove performance was kept and no performance degradation was observed with these semi-saturated conditions;

- In the cases where spilling was forced e.g. overfilling (above 1mm of plain surface or very rough shaking), then after drying out the spilled fluid, it was possible to re-generate the meniscus without observing any performance reduction (even after 2 weeks of testing).

The new anti wetting system is suitable for CIMEX-1. Moreover its characteristics allow a good controlling of the liquid interface permitting the stabilization of the whole system.

3.3 Gas pressure control loop test

3.3.1 Introduction and purpose

This test was performed prior to the closed loop test setup integration to better understand how the pressure loop can be operated. The pressure controller is required to be set differently depending on the type of controlling that it has to perform. In fact there are two possible operating modes: the forward pressure controlling and the backward pressure controlling. "Forward" and "backward" refer to the mutual position of the meter/controller and the controlled valve (see Figure 3-5). The aim of this test was to choose the correct pressure controller settings, to verify the adjustable range of the experimental pressure (400-1000mbar) and to gain knowledge on the system behavior.

3.3.2 Test setup

The devices used for this test setup were the pressure controller (see 2.3.4), the pressure pump (see 2.3.3) and the gas circulation pump (see 2.3.2). Nitrogen, provided by the G-RES reservoir, was used as operative gas. Tubing, fittings and manual valves were all from Swagelok. For this test the pressure control loop was connected to a simple gas loop which aimed to simulate the gas loop used in the

Breadboard. Therefore if the system works with this setup it would work also with the Breadboard complete setup. Figure 3-4 shows the scheme that represents the test setup.
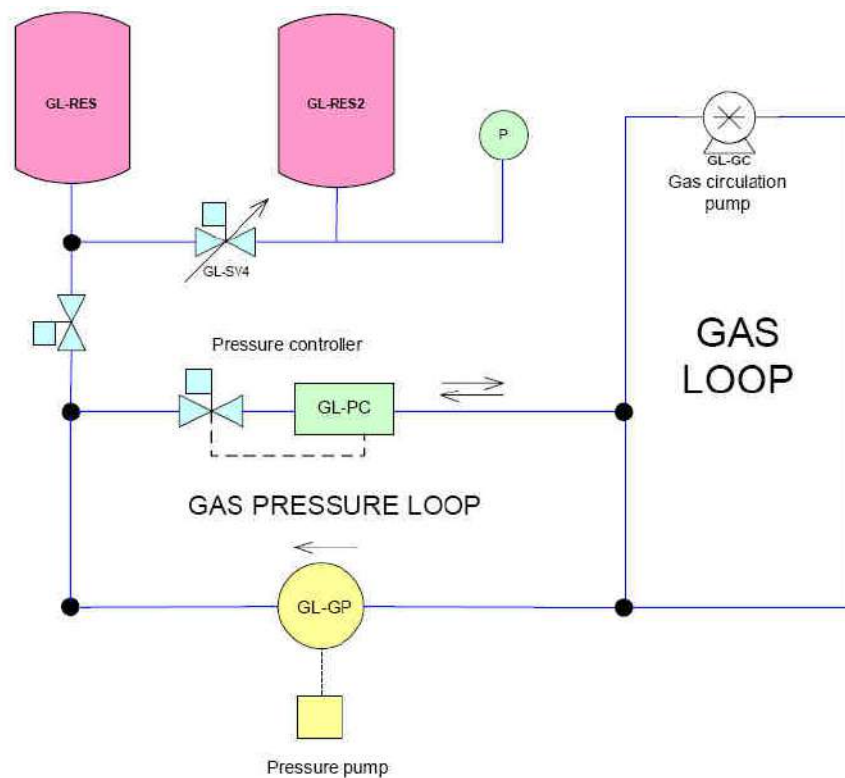
Figure 3-4: Gas pressure loop test schematic

3.3.3 System functionality

The gas retraction pump and the pressure controller must work together in order to control the pressure of the gas loop. The pump is meant to reduce the pressure of the loop and therefore the pumping direction has to be from the gas loop to the reservoir, as indicated in Figure 3-4. The pressure controller is used to adjust the pressure in the gas loop when the pressure is higher or lower than the set one. In order to do this the PC has a valve that opens or closes depending on the signal received from the controller. The pressure of the gas loop is measured by the meter section of the PC (Figure 3-5 helps to recognize the PC elements). When the pressure in the gas loop is too high the controller closes the valve and the pump lowers the pressure by pumping the Nitrogen back to the reservoir. When the pressure is too low the controller opens the valve and the gas flows from the reservoir to the loop, raising the pressure. Obviously the reservoir pressure has to be higher than the maximum pressure that has to be controlled. When the pressure of the circuit is constant the controller set the valve position in such a way that all the gas quantity that is sucked by the pump comes back to the gas loop. The system would therefore be stabilized.
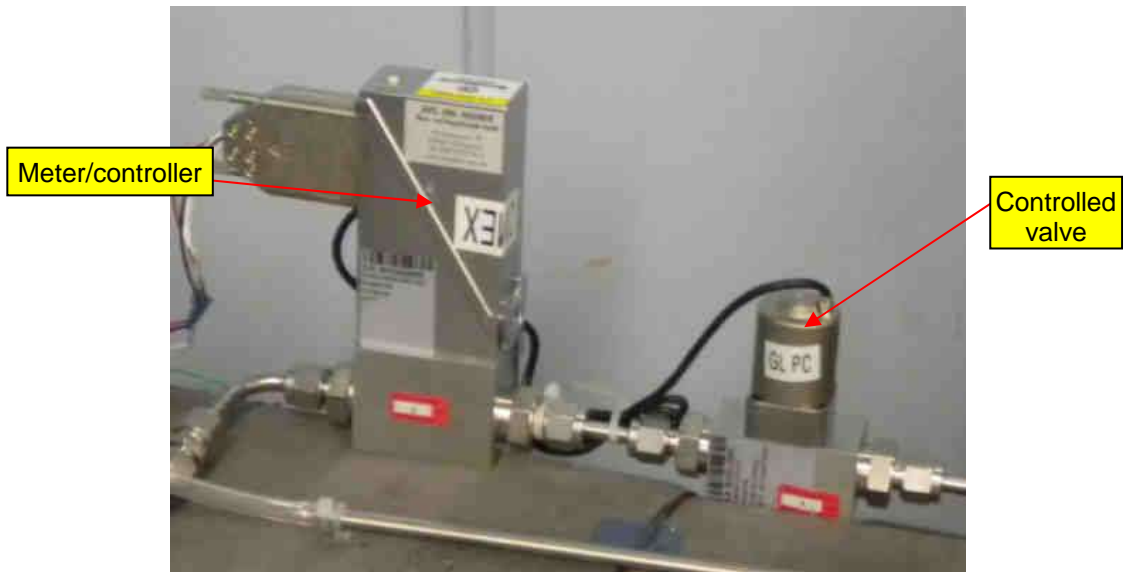
Figure 3-5: Pressure controller elements

3.3.3.1 Pressure controller settings

The meter section of the pressure controller has to be connected to the gas pressure loop and the controlled valve has to be attached in the way shown in Figure 3-4. If the mutual position of the controller and the valve was inverted the controlling would not work anymore because the pressure that the meter measured would not be the one present in the gas loop. This arrangement is referred to the forward pressure controlling. The pressure controller settings were changed by using FlowDDE.

3.3.4 Results

The pressure loop was able to set the gas loop pressure within the required pressure range of 400-1000mbar. Figure 3-6 shows the results of one test (comments are reported in the next page). In the graph in Figure 3-6, which was obtained with the Flow PLOT program (see section 2.3.5.1), there are three different plots: the set pressure value, the current pressure value and the valve position of the pressure controller. Their colors are yellow, green and red, respectively. The x axis is the time axis. Looking at the graph it is possible to see a sharp change of the pressure set point from 40% to 54% (percentages in respect to the maximum controllable pressure, 1,2 bar) which was commanded by the operator. After some instants the valve changed its status to raise the pressure and correspondently the pressure increased. Moreover, after a period of about 5 seconds during which the pressure is subject to two pressure oscillations (with maximum amplitude of 3%), the new desired pressure was reached.

The system experienced the same behavior for other pressure settings, up to 1000mbar, therefore the pressure control loop was installed in the final BB circuit.
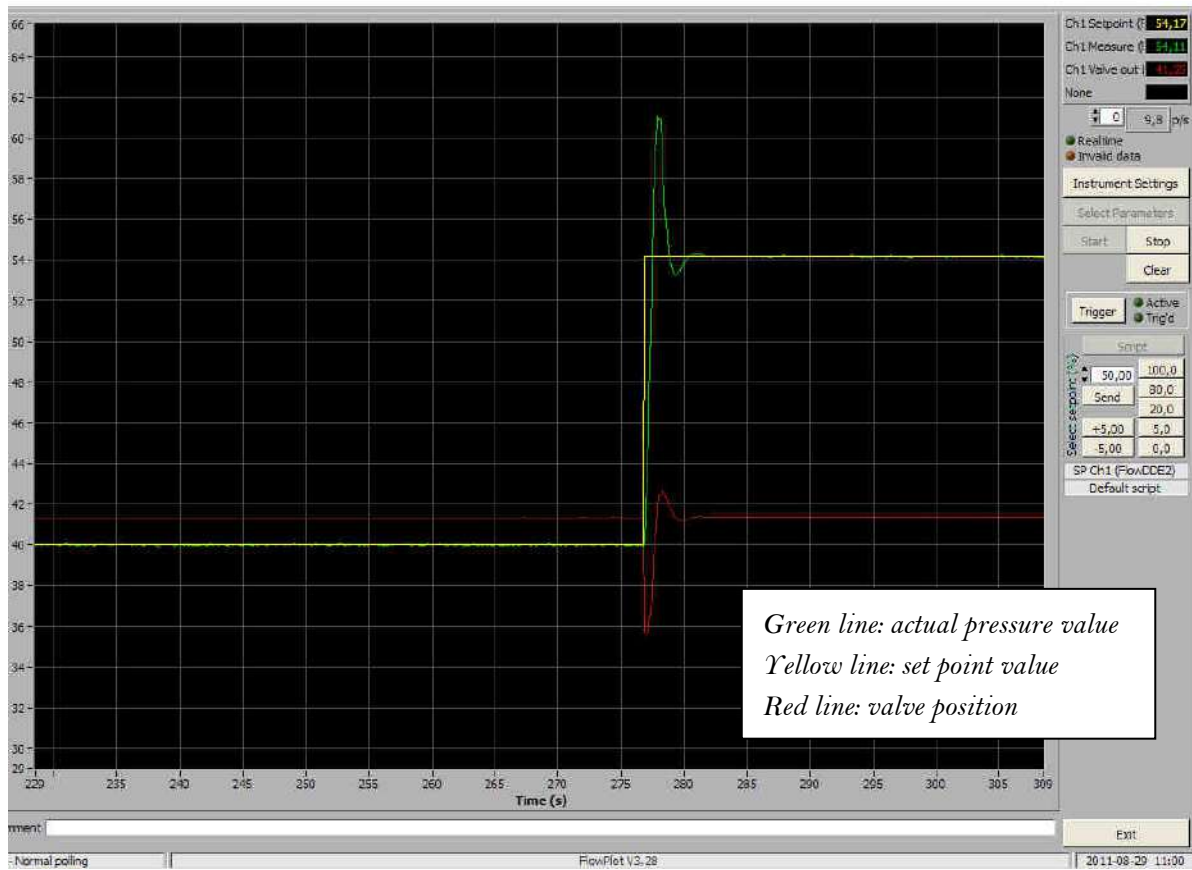
Figure 3-6: Pressure setting from 0,5 to 0,65bar. The time for the pressure to be stable again was about 5seconds.

4 Closed loop behavior evaluation

4.1 Introduction

This chapter contains an important part of the Breadboard test campaign results. The achievements that will be considered are related to the way the system behaved and to the way it was operated. The main objectives of the Breadboard were in fact assessing the closed loop stability and finding/evaluating the procedures which allow operating the system for the experimental conditions. The filling of the liquid loop procedure, the settings of the experimental parameters procedure and the system stability will be also assessed and discussed in this chapter.

4.2 Filling of the liquid loop

4.2.1 Introduction

An important procedure to be investigated is the filling of the liquid loop with HFE-7100. Once the EC is sent to the ISS, the system has to automatically fill the liquid chamber of the evaporation cell and the entire liquid loop. If this procedure fails, it would not be possible to perform any experiment. Knowing therefore how to perform this operation, firstly on the ground, during a Breadboard campaign is essential.

4.2.2 Procedure

At the initial conditions the circuit is cleared from HFE-7100 and only Nitrogen is present in both the gas and the liquid lines. The first step of the procedure was therefore the filling of the cell liquid

chamber. The valve LL-SV1 (see Figure 2-2 and Figure 4-1) was closed and the valve LL-SV2 was opened. The pump was operated in the forward direction (i.e. cell direction), pumping liquid from the liquid reservoir to the cell. The liquid chamber was filled until half of its volume.

The second step was filling the liquid line between the valve LL-SV1 and the CSS and filling the meniscus of the Separator. This operation was possible by inverting the pump direction and by inverting the status of the two valves.

Once all the liquid line and the meniscus of the Separator were filled and free from bubbles the cell was filled again until the maximum height allowed by the anti wetting groove.

The final status of the valves was: LL-SV1 opened and LL-SV2 closed. The liquid loop was then ready to be operated.
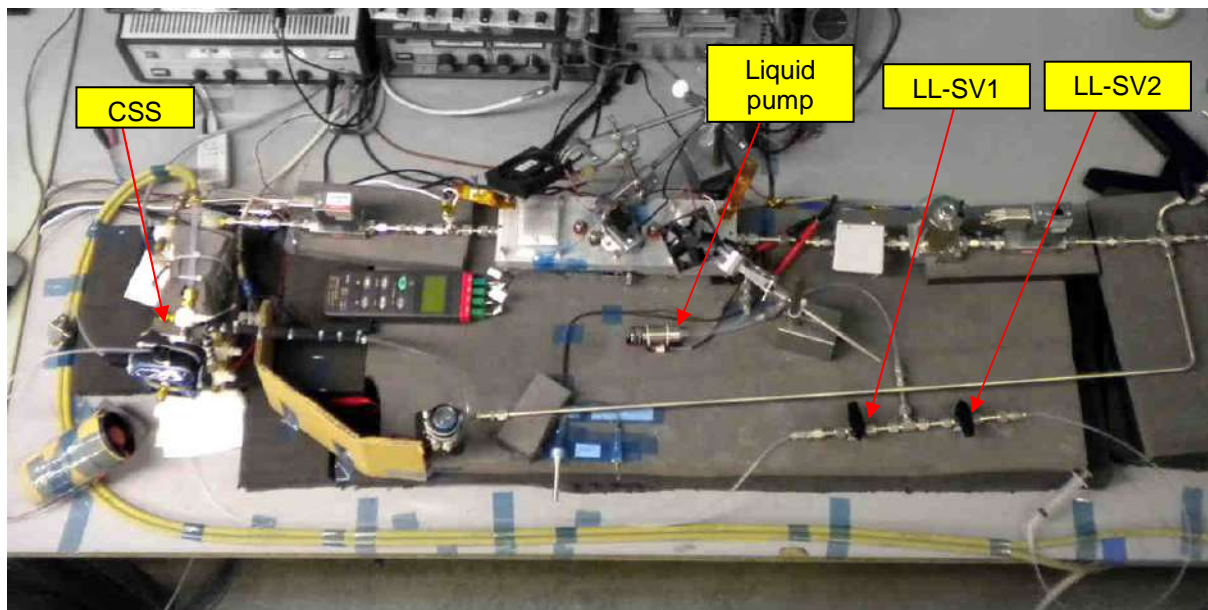
Figure 4-1: Liquid loop

4.2.3 Comments

The filling procedure took about 10 minutes to be performed and no bubbles were seen in the lines. The procedure worked correctly and therefore it was used during the entire test campaign.

4.3 Setting of experiment parameters

4.3.1 Introduction

This procedure is a sequence of actions explaining the necessary steps needed to perform a single measurement. The method had to be tested and documented for future tests and improvements. The know-how that was gained is essential for developing the automatic control system that will control all the main CIMEX-1 components such as the pumps, the flow controllers and the temperatures.

4.3.2 Procedure

The first operation to be performed, even before the filling of the liquid loop with HFE-7100, was reaching stable temperatures at the condenser, separator, evaporation cell and water cooling devices. Then the cell and the liquid loop were filled, the pressure controller was set to the environment pressure, the gas retraction pump was activated and the valves GL-SV2 and GL-SV3 (see Figure 2-2 and Figure 2-9) were opened.

Afterwards the pressure was slowly decreased to the desiderated value and when the pressure was stable the valve GL-SV3 was closed. The MFC was then set to the experimental value of flow rate and the circulation pump was powered with the minimum current needed to have the desired flow rate.

During all these steps the liquid interface and the CSS meniscus positions were constantly controlled by operating the liquid pump.

When stable conditions were achieved the measurement could be started.

4.3.3 Comments

This sequence of actions is the result of all the trials and the tests that were performed during the campaign. The reasons for all of the choices that have been mentioned before will be clarified in the next chapters.

4.4 System Stability

4.4.1 Introduction

The system stability is an essential condition that has to be verified for each single test, both during ground campaigns and during flight operations. Each measurement needs stable conditions for all of the experimental parameters such as temperatures, pressures, flow rates and gas concentration. Only when this situation is verified, the measurement can be considered valid.

Reaching system stability and gaining knowledge about it, was one of the priorities of the closed loop BB test campaign. This chapter encompasses this priority.

The stability will be analyzed for the main components of the BB and the main causes that perturb this condition will be discussed. Moreover, alternative solutions will be proposed in case stable conditions were not completely achievable.

The last paragraph of this chapter is about the boiling curve of the liquid. The eventual bubbling is an issue that affects the system stability and therefore a dedicated section was added in this part of the thesis.

4.4.2 CSS Stability

The CSS is one of the most important elements of CIMEX-1. Its scope is to ensure that the HFE-7100 vapor condenses correctly and to deliver a limited value of vapor to the gas loop, according to the requirements.

The parameters that could be operated to control the CSS were:

- the condenser and separator temperatures
- the inlet cooling water temperature
- the flow rate of the extracted liquid (changeable by operating the liquid pump). It was also possible to inject liquid.
- the degassing valve status (open/close)

The temperature of the condenser and the separator were set constant at -10℃ or at -20℃ during all the test campaign. The cooling water inlet temperature was set to 23,5℃ in order to simulate the FSL cooling system. The degassing valve was opened for almost all the measurements. Therefore the only parameter that was effectively set was the flow rate of the extracted liquid.

In order to assess the functionality of the CSS, the gas concentration value and the separator meniscus position were considered.

4.4.2.1 Extra liquid within separator

In some cases it happened that the quantity of liquid HFE-7100 in the separator meniscus was too much. Because of this the gas concentration (read by the GCS) increased, exceeding the expected value and the system become consequently unstable. For the system to be stable again the extracted liquid flow rate had to be increased until the meniscus reached the normal position. This process had to continue until the entire extra vapor present in the circuit was condensed.

The following pictures show the meniscus positions during the tests. The meniscus dimension can be seen by the red arrow in the first picture of Table 3.

Meniscus at the normal position	Sketch: meniscus at the normal position	Sketch: meniscus full
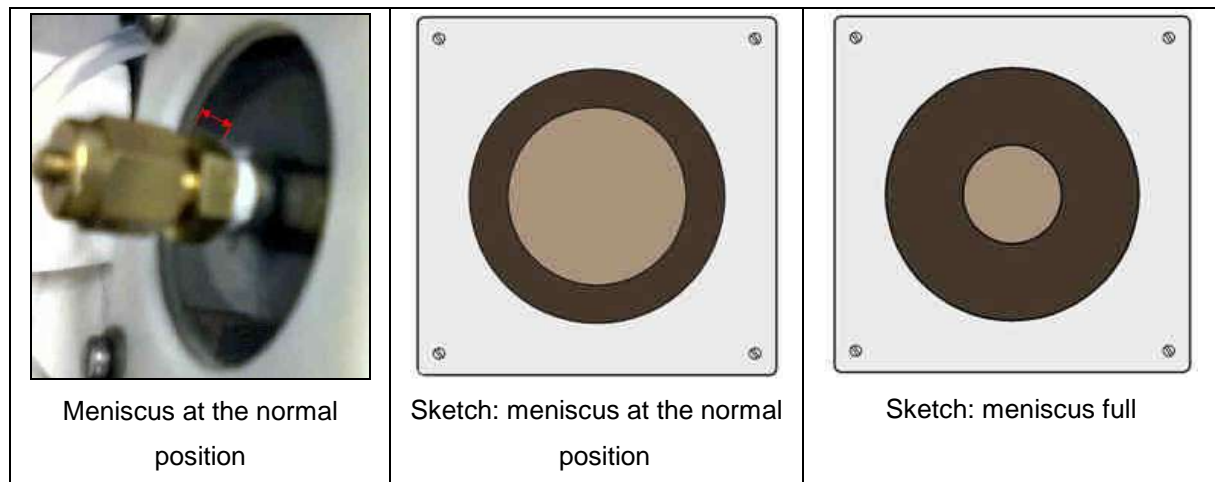
Table 3: Main meniscus positions

Moreover, if the liquid quantity in the separator was too much the liquid could be sucked by the gas circulation pump and could therefore go into the line between the CSS and into the pump (Figure 4-2 helps to identify the line). Therefore, the HFE inside the pipe had to evaporate to stabilize the system again.
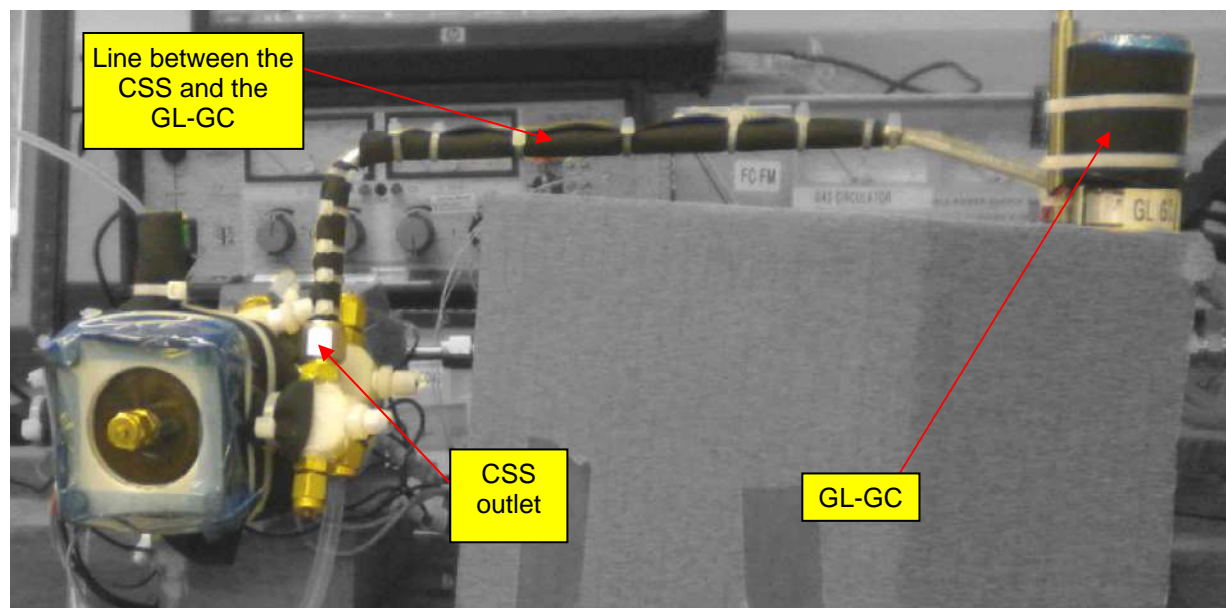
Figure 4-2: Gas line between the CSS and the circulation pump

In order to avoid the eventual sucked liquid to go inside the gas circulation pump the device was mounted in a vertical position (see Figure 2-8).

4.4.2.2 Separator channel issue

The channel around the separator chamber is designed to collect the condensed liquid and to permit a correct extraction of liquid from the separator outlet (blue arrow in Figure 4-3). This happens only when the channel is filled enough by the condensate HFE i.e. when the liquid level reaches the points indicated by the red arrows in Figure 4-3. During the tests it was seen that if the level was too low (i.e. when too much liquid was extracted) the outgoing stream would contain also gas that would consequently be injected in the liquid loop. The presence of the gas in the liquid loop would then create pressure fluctuations that could affect the liquid interface stability in the cell. Therefore it is essential to check continuously the height of the liquid channel in order to extract only liquid from the CSS
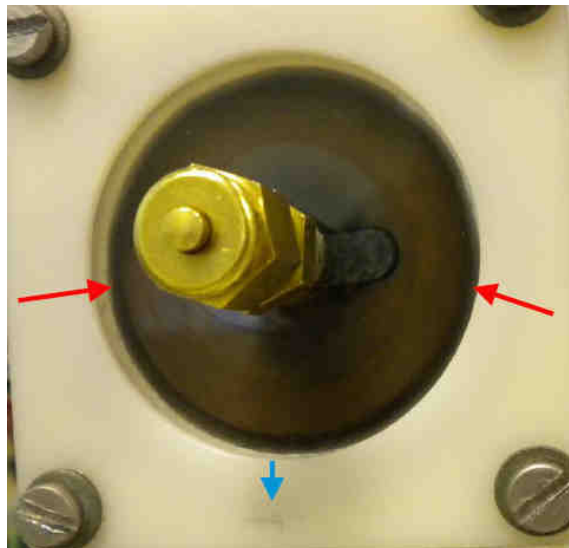
Figure 4-3: Separator channel ideal position

When an adjustment of the channel liquid level was needed (i.e. when it was too low) the liquid direction was inverted and the liquid was pumped in the separator either from the cell or from the reservoir, until the ideal level was reached. This procedure was done manually by means of the switch visible in Figure 2-6.

Both the meniscus and the channel liquid level positions were constantly monitored by the operator using the camera C2 (see the Breadboard schematic in Figure 2-2). The camera position has to be adjusted in order to have a good contrast for the meniscus position to be visible.

4.4.2.3 Extra liquid within condenser

When the liquid in the cell boiled or when the pressure gradient (which was needed to change the pressure in the system) was too high, some liquid went inside the gas circuit and in the CSS condenser. This caused a rising of the condenser temperature and the system became unstable. Only when all the extra liquid drained out from the condenser the system was able to stabilize again at the nominal temperature conditions.

This instability will not affect the real CIMEX-1 because the liquid will not boil and because the pressure gradient will not affect the liquid position.

4.4.3 Stability of the evaporation cell

The evaporation cell is the heart of CIMEX-1 in which the evaporation phenomenon takes place. Assuring stable conditions for this component is essential to perform correct measurements. In this chapter the major causes that perturb the cell stability will be analyzed.

4.4.3.1 Influence of the gas retraction pump

A significant cause of instability was due to the gas retraction pump. In fact it generated big pressure fluctuations which in turn produced waves on the liquid interface. The presence of these waves had to be completely avoided since the surface flatness had to be achieved. Furthermore these fluctuations caused the spilling of the liquid with the consequent loss of the system stability. In order to avoid this problem it was decided to exclude the pressure control loop once the desired pressure was reached. This was possible by closing the valves GL-SV2 and GL-SV3 (see Figure 2-2 and Figure 2-9). Figure 4-4 shows the effects of the gas retraction pump on the liquid surface.

| Liquid level conditions with the gas retraction pump on. The waves on the surface are quite evident. | Liquid level excluding the pressure control loop. The surface flatness is achieved. |
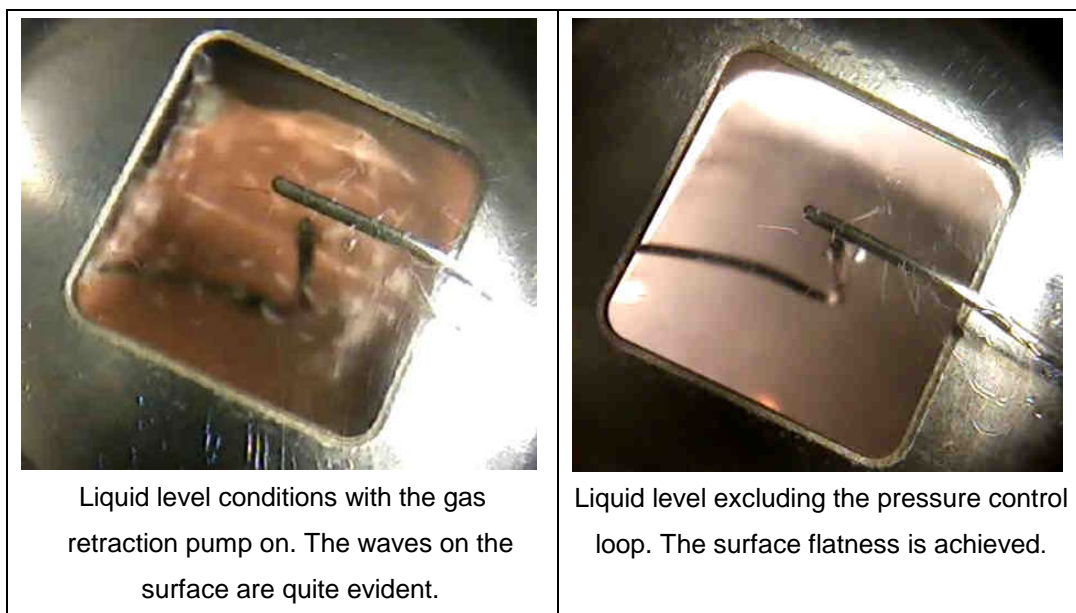
Figure 4-4: Pressure pump influence on the cell liquid interface

Once the pressure control loop was excluded from the circuit the pressure of the system was not controlled anymore. The presence of leaks in the circuit caused therefore a rising of the pressure and produced instable conditions. However the pressure rising was small enough to allow the operator to perform the test. At 500 mbar the leak rate was about 20mbar/min.

However, if this procedure would be implemented in CIMEX-1, the pressure will not rise because of the complete leak tightness of the final circuit.

4.4.3.2 Influence of the gas circulation pump

Also the gas circulation pump was a cause of waves on the cell liquid level surface because of its induced backpressure. In this case the problem was solved by finding the pump speed that minimizes the wave intensity. Despite the different pump speeds, the mass flow rate was kept constant, at the desired value, by the MFC.

In all of the cases the waves were almost totally reduced. Figure 4-5 show the results of the pump speed adjustment.

| Liquid level before adjusting the pump speed: waves are present on the surface | Liquid level after having adjusted the pump speed: the surface is now cleared from waves |
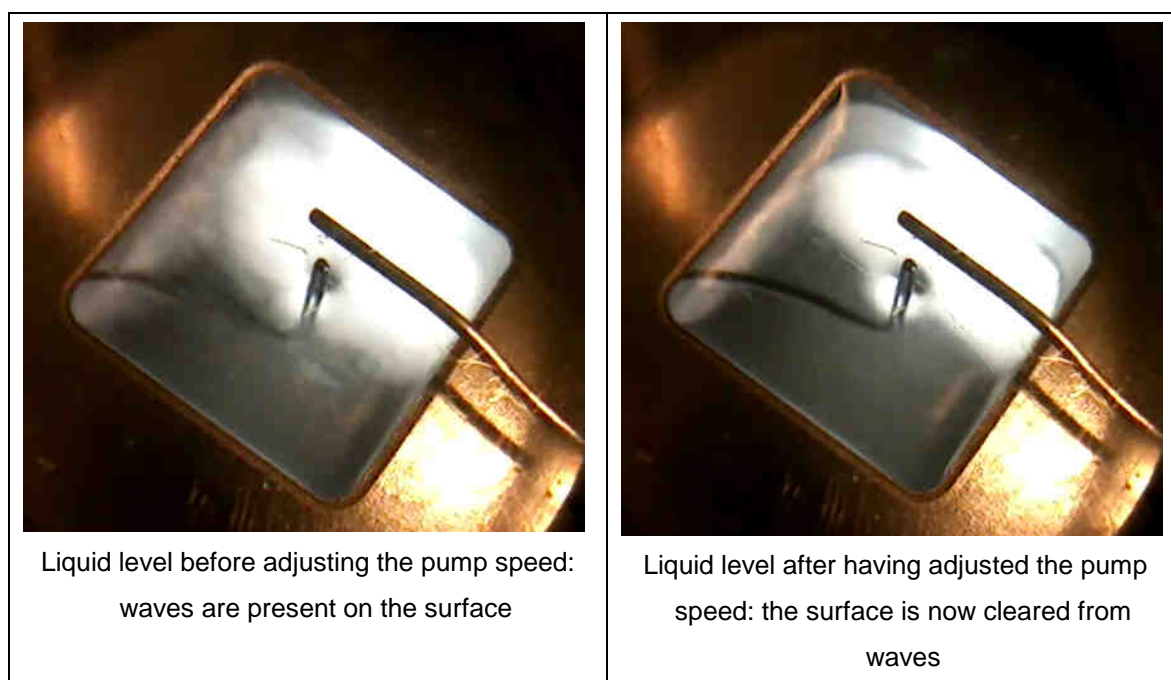
Figure 4-5: Gas circulation pump influence
Operative conditions: p=1010 mbar, flow rate = 300 (ml/min) and cell temperature = 25℃

Other tests were performed for different experimental conditions to be sure that the surface flatness was achievable for the whole experimental range of parameters. Table 4 demonstrates that the liquid level flatness was achieved for all the presented conditions which include high and low pressures, high and low cell temperatures and high and low flow rates. The surface stability was achieved for the worst operative conditions: high flow rates and low pressure. These achievements were reached only by finding the optimal gas circulation pump speeds.

T_{cell} =25℃ p=1000mbar Flow rate=419(ml/min)$_{N2\ normalized}$	T_{cell} =25℃ p=1000mbar Flow rate=838(ml/min)$_{N2\ normalized}$	T_{cell} =45℃ p=1000mbar Flow rate=838(ml/min)$_{N2\ normalized}$
T_{cell} =25℃ p=800mbar Flow rate=838(ml/min)$_{N2\ normalized}$	T_{cell} =40℃ p=600mbar Flow rate=838(ml/min)$_{N2\ normalized}$	T_{cell} =25℃ p=400mbar Flow rate=838(ml/min)$_{N2\ normalized}$

Table 4: Experimental cell liquid surface flatness at various conditions of temperature, pressure and flow rate

4.4.3.3 Influence of the pressure gradient

Another cause of instability was the variation of the liquid level interface when the gas pressure changed. If the pressure gradient was too big (for example from 1000mbar directly to 500mbar) and if the liquid level was kept at the top, the liquid spilled out and the system became unstable until all the spilled liquid evaporated.

The reason of this behavior was the presence of plastic tubes in the gas loop line which were used to connect the gas circulation pump to the system. When the under pressure was applied to the system the tubes contracted, due to the low stiffness of the plastic material, and therefore the total gas loop volume decreased. Consequently every time the pressure in the loop changed also the total gas loop volume changed and so did the liquid interface level.

The problem was solved by applying a low pressure gradient when a new pressure was needed for a new test. Moreover, before performing this operation, the liquid interface level was slightly decreased to prevent the eventual spilling.

This issue will not interest the final version of CIMEX-1 because only metal tubing will be used for the assembling.

4.4.3.4 Influence of the leaks

Even if much care was taken during the integration of the Breadboard, leaks were still present in the loop and it was not completely possible to avoid them.

The presence of leaks was an important cause of system instabilities during the test campaign because of the following reasons:

- *Rising in pressure.* The leaks slowly increased the pressure in the gas loop. This problem was solved by imposing the initial pressure controller set point slightly below the desiderated value of pressure. In this way the operator had time to stabilize the system, until the pressure rose up to the wished experimental pressure value. Clearly, the measurements were not totally correct, since the pressure was not completely stabilized. However, performing very precise tests was not the aim of the test campaign, and for the purpose of the closed loop BB, this approximation can be accepted.

- *Presence of bubbles in the cell.* Bubbles coming out from the liquid inlet of the cell affected the liquid interface stability. This problem was very important at lower pressures, while at 900-1000mbar bubbles did not appear, because of the low difference in pressure between the external pressure and the cell pressure. The problem was solved by sealing the cell liquid inlet fitting. The leaks were detected by performing a leak test. The sealing process was done by means of grease. In the next page, it possible to see a sequence of pictures showing how the bubbles affected the liquid level interface.

- Liquid Loop instabilities. The leaks caused a fictitious "increasing" of the liquid quantity contained in the liquid loop, even if no liquid was injected. This happened in particular, at low pressures. Due to the leaks, small volumes of gas entered the liquid loop and the respective volume of liquid, which was before previously in the loop, went to the CSS. The meniscus separator therefore became full, and an extraction to the external reservoir was needed. When the pressure increased for other test conditions, the gas in the liquid loop disappeared and therefore an injection of liquid from the external reservoir was necessary.

In Table 5, it possible to see a sequence of pictures showing how the bubble inside the liquid chamber grew affecting the liquid level interface.
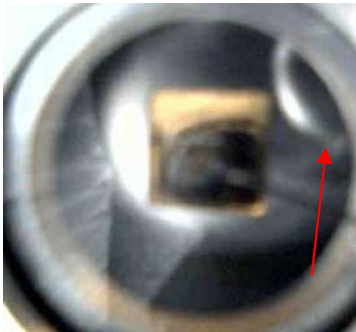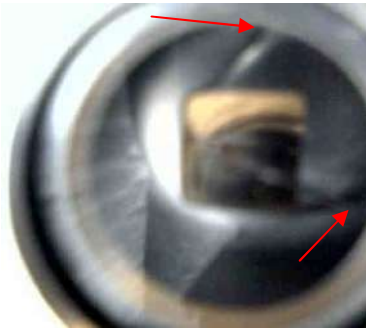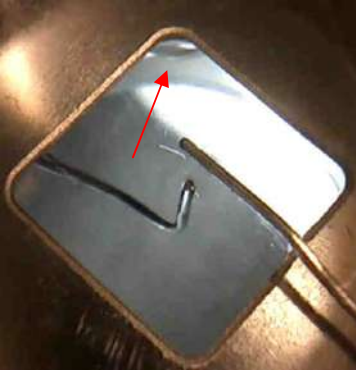
Instant 1	Instant 2	Instant 3
The liquid level is reached, but a bubble coming from the liquid inlet is placed under the metal foil.	During the filling adjustment the bubble is about to interfere the square opening of the metal foil.	The bubble has expanded in the square opening and now there is a strong under filling.
The liquid surface is still at the normal position	The bubble is rising from the corner	The liquid level decreases because of the bubble

Table 5: Sequence of pictures showing the effects of the leaks on the liquid interface. Bubbles rose from the bottom because of leaks.

4.4.3.5 Influence of boiling

Liquid boiling in the cell was observed at different conditions of temperature and pressure. Obviously, when bubbling occurs, it is not possible to do any measurements due to the high surface instability.
The observed causes of instability due to the bubbling were the following:

- *Some drops of HFE liquid flowed from the cell to the MFM and to the MFC*. The devices were not able to work correctly and the readout/controlling were not possible anymore. The liquid in the meters had to be evaporated in order to stabilize the system again.
  The valve of the MFC was therefore fully opened and the gas circulation pump was operated at the maximum speed. In about 20 minutes the devices became dry and ready for other tests.
  It is a very important remark that the gas loop was not opened for drying the meters and all the operation was done only by changing the gas pump speed and the MFC valve status. This

aspect is essential for CIMEX-1 since once the Experimental Container is on orbit, hardware operations like the previous one will not be possible.

- *Liquid spilling*. Bubbles wet the metallic foil which had to become dry before performing other tests. In the next picture it is possible to see the cell liquid surface during bubbling and the wet metallic foil (check the drop between the metallic foil and the thermocouple line).
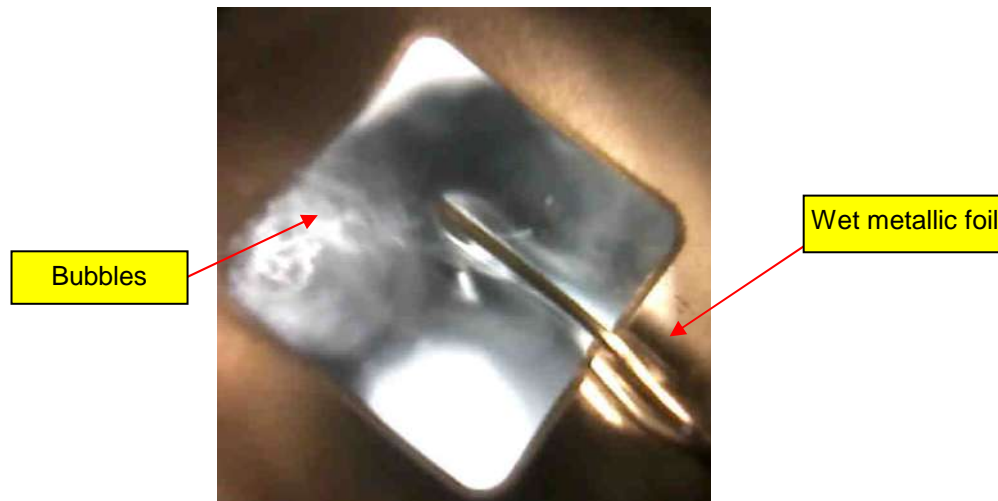
Figure 4-6: Bubbling effects on the cell meniscus surface

4.4.4 GCS stability

When strong bubbling occurred or when the pressure gradient was too strong some drops of liquid went inside the GCS. As a consequence of this the Java program crashed and its readout showed a sharp drop, to negative values. A software reset was therefore needed by flushing all the circuit with Nitrogen only. This program behavior will be considered for future developments. For further information see chapter 2.3.6.3.

Since in CIMEX-1 many measurements are foreseen for the flight test campaign it is useful to know, for time management reasons, how long it takes for the sensor readout to stabilize between two measurements.

The graph in of Figure 4-7 shows the GCS behavior between two different tests at two different pressures. The considered tests are the 32nd and the 33rd (see Table 9 for further information). As it is possible to see the concentration for the 32nd test was stable at 8% (Vol). Than, the graph shows a transitory period in which the concentration rises up to 30% (Vol). This was due to the spilling of the cell that was provoked by the pressure change from 800mbar to 600mbar. When the pressure was set to 600mbar and when the valve GL-SV3 was opened, the plastic tubes used in the loop contracted. The consequent volume reduction was the cause of the spilling.
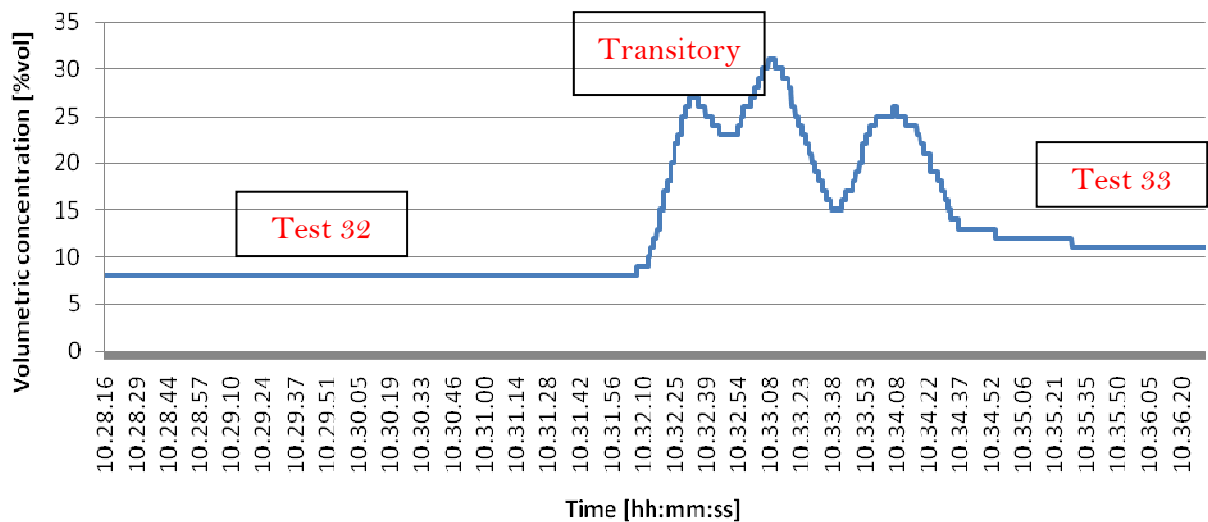
Figure 4-7: GCS behavior between two different measurements

The transitory lasted for about 3 minutes. After this time the new stable conditions, of the 33rd test, was achieved at a concentration of 11% (Vol).

4.4.5 Pressure stability

The pressure is one of the main parameters which has to be controlled in order to fulfill the requirements. Knowing the reasons that affect the pressure stability is therefore very important for the project.

During the test campaign it was seen that the pressure stability was influenced by the following causes:

- *The gas circulation pump back pressure*. The problem was solved by finding the optimal speed which minimizes the surface vibrations for each test (see chapter 4.4.3.2 for more information).
- *The presence of leaks*. The pressure continued rising at a rate of 20 mbar/min. In section 4.4.3.4 it is described how this problem was solved.
- *The extra HFE condensation/evaporation*. Due to the spilling of the liquid the amount of vapor present in the gas loop changed. When the spilled liquid was evaporating the vapor quantity in the gas loop increased and consequently the pressure rose up. Moreover, when the extra vapor was condensing the gas pressure decreased. Every time there was a change in the HFE gas concentration the pressure could not be stable. Therefore the concentration stability has to be firstly reached in order to have the pressure stability. This was not a serious matter during the test campaign since the spilling was most of the times prevented by carefully injecting the liquid in the cell.

4.4.6 MFM/MFC stability

The stability was mostly conditioned by the presence of liquid drops in the meters. This could happen both when a strong bubbling occurred and when the pressure gradient was too strong. In order to stabilize the meters again the valve of the MFC was fully opened and the gas circulation pump was operated at the maximum speed. In about 20 minutes the devices were able to work correctly again.

4.4.7 Time to stability

This value is important for scheduling the operations on-orbit and therefore a first estimation was done during the test campaign. An average time required for the system to stabilize, after having set the new experimental parameters, was about 10 minutes. This time does not include the time to stabilize the cell temperature since the cell body is not the one foreseen for CIMEX-1 (Figure 1-1 shows the foreseen experimental cell while Figure 2-15 shows the cell used for the closed loop BB).
For the most difficult cases of high cell temperatures and low pressures (i.e. high evaporation rates) the time to stability was longer, about 20 min.
These values are only first estimations. Further developments will allow better evaluations of the stability time.

4.4.8 Conclusions

It was demonstrated that it is possible to control both the CSS meniscus and the liquid interface using only the liquid pump. Moreover, it was seen that, in order to avoid the back pressure waves of the pressure pump, the device has to be excluded from the circuit using the valves GL-SV2 and GL-SV3. This means that, before every measurement, the pressure must firstly set. Due to the leaks, the pressure raised at a rate of 20mbar/min, but in CIMEX-1 the system will be completely tight and therefore the pressure will not change because of the leaks.
The GCS demonstrated to be stable at all conditions. However, the Java program must be reviewed to avoid drops in the readout value when liquid HFE goes inside the sensor.
The system was successfully operated by hand and therefore it is expected that an even better controlling may be achieved with the implementation of the automatic controlling system (Schlieren). At the end of the test campaign, overall system stability was achieved.

4.5 Boiling curve

4.5.1 Introduction

The operability of CIMEX-1 is largely influenced by the physical properties of the HFE-7100. In fact, it is not possible to guarantee the interface flatness when the liquid starts boiling.

Boiling occurs when the vapor pressure equals the pressure that is exerted to the liquid. It is therefore related both to the pressure applied to the closed loop and to the temperature of the cell.

This means that it is not possible to apply any indiscriminate combination of pressure and temperature to the system, while requiring the surface to be flat.

Finding the boiling curve is hence essential for knowing the limits up to which CIMEX-1 can be operated. This is the focus for this chapter.

4.5.2 Results

Various tests were performed in order to find the pressure-temperature points for which the liquid starts boiling. For each test the evaporation cell temperature was first set for and then the pressure was smoothly decreased until boiling was observed. Four measurements with four different cell temperatures were performed. The graph in Figure 4-8 shows the obtained results.
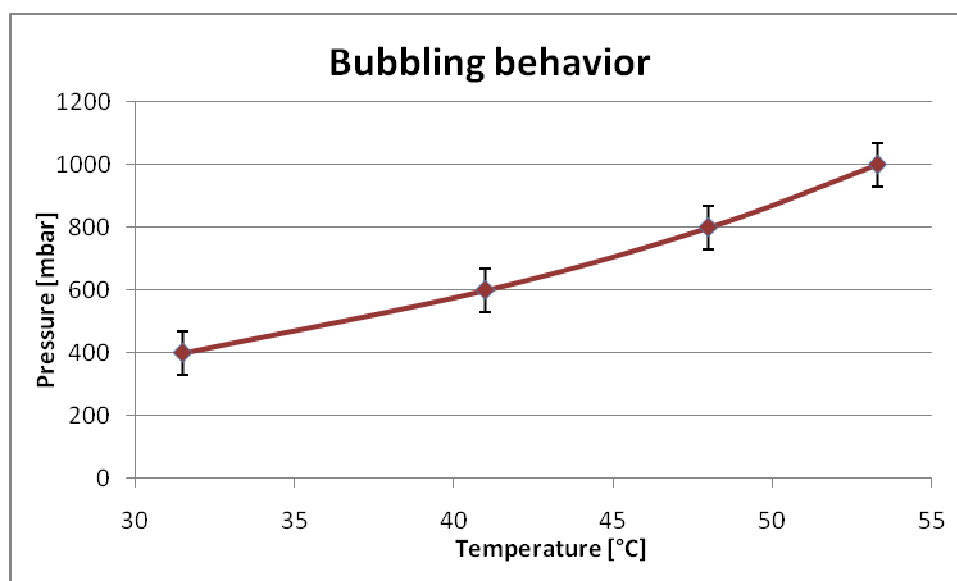
Figure 4-8: Experimental boiling curve (2mbar of accuracy on the pressure values)

In the Figure 4-9 it is also possible see the differences between the obtained experimental curve and the data from the pure HFE-7100 saturated case (from the literature).
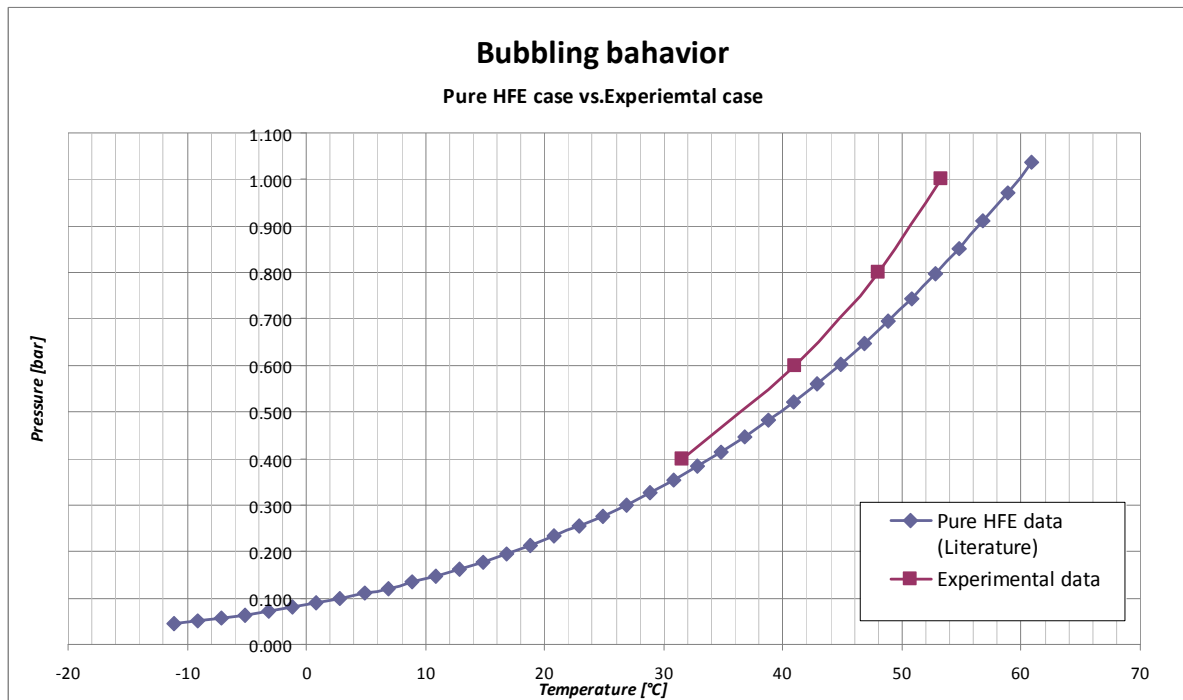
Figure 4-9: Bubbling curve vs. pure HFE boiling curve

From the graph in Figure 4-9 it is possible to see that the boiling occurs, for the same pressure values, at lower temperatures than the pure HFE-7100 case. This behavior could be explained because of the Nitrogen dissolved in the liquid. In fact, when the HFE-7100 is bubbling, the liquid also degasses. This leads to different values than the ones obtained from the literature. Anyway, it has to be mentioned that there are many other causes for which the experimental values differ to the ones from the literature. One of them could be, for instance, the different roughness of the surfaces in contact with the liquid.

5 Measured raw data conversion and calculations

5.1 Introduction

The raw values from the MFM, the MFC and the GCS had to be converted, since the instruments were calibrated for other operative conditions, more precisely:

- The GCS was calibrated for volumetric gas concentrations. Since the requirements impose limitations on the mass concentration, a conversion from volumetric to mass concentration was necessary.

- The MFM and the MFC were calibrated for a mixture of 95% of Nitrogen and 5% of Ethanol vapor. A conversion is therefore needed to obtain the values for the measured mixture of Nitrogen and HFE-7100 vapor. If the values were not changed, the post-processing analysis would be completely wrong.

Moreover, the only available value for the outcome flow of the evaporation cell was the mass flow rate. Knowing the concentration at both sides of the cell allows a better analysis of the performance of the subsystem, especially of the CSS. Therefore, calculations must also be performed in order to obtain the gas concentration after the evaporation cell.

This chapter focuses on the mentioned conversions and calculations. The outcome results will be used for the post processing analysis of chapter 6.

5.2 Gas concentration conversion

5.2.1 Introduction and objectives

The GCS used for the test campaign was calibrated for volumetric concentrations. The project requirement 3267 (see Annex 1:) states that the "CSS shall deliver at the outlet a gas phase composed of at least 50% of gas" in which the composition is intended as a mass fraction. Therefore a conversion method had to be found in order to obtain the mass concentration value.

A theoretical model based on the ideal gas theory was used to perform this transformation. The HFE-vapor and Nitrogen will be considered as a mixture of ideal gases.

In the ideal gas theory there are two different models that can be used for mixtures of gases [1] :

- The Dalton model
- The Amagat model

The Amagat model was chosen for the calculation because the Dalton one was not suitable for the current problem.

In fact the Dalton assumption states that:

> "each mixture components behaves as an ideal gas as if it were alone at the temperature T and the volume V of the mixture" [1]

Since the HFE volumetric concentration is defined as:

$$C_{Vol} = \frac{\dot{V}_{HFE}}{\dot{V}_{HFE} + \dot{V}_{N_2}}$$

(Eq. 2)

then the concentration would remain every time equal to 0,5 because, according to the Dalton model, all the volumetric flow rates would have been considered equal:

$$\dot{V}_{HFE} = \dot{V}_{N_2} = \dot{V}_{mixture}$$

(Eq. 3)

Therefore the Amagat model is considered for the conversion.

The model states that:

> "each mixture components behaves as an ideal gas as if it existed alone at the temperature T and the pressure p of the mixture" [1]

5.2.2 Analytical calculations

The partial volume that the component "i" of mixture occupies, according to the Amagat model, could be calculated as follows:

$$V_i = \frac{n_i \cdot \overline{R} \cdot T}{p} \qquad \textit{(Eq. 4)}$$

Where n_i is the number of moles of the component "i", p is the pressure of the mixture, T is the mixture temperature and $\overline{R}$ is the universal gas constant.´

The HFE volumetric concentration could therefore be expressed as following:

$$C_{Vol} = \frac{\dot{V}_{HFE}}{\dot{V}_{HFE} + \dot{V}_{N_2}} = \frac{\dot{V}_{HFE}}{\dot{V}_{MIXTURE}} = \frac{\dfrac{\dot{n}_{HFE} \cdot \overline{R} \cdot T}{p}}{\dfrac{\dot{n}_{MIXTURE} \cdot \overline{R} \cdot T}{p}} = \frac{\dot{n}_{HFE}}{\dot{n}_{MIXTURE}} = y_{HFE} \qquad \textit{(Eq. 5)}$$

Where y_{HFE} is the mole fraction of the HFE-7100.

The sum of the partial volumes has to be equal to the mixture volume, therefore:

$$\dot{V}_{HFE} + \dot{V}_{N_2} = \dot{V}_{MIXTURE} \implies \quad \frac{\dot{V}_{HFE}}{\dot{V}_{MIXTURE}} + \frac{\dot{V}_{N_2}}{\dot{V}_{MIXTURE}} = 1 \implies \quad y_{HFE} + y_{N_2} = 1 \implies \quad y_{N_2} = 1 - y_{HFE}$$

$$\implies y_{N_2} = 1 - C_{vol} \qquad \textit{(Eq. 6)}$$

From the mass concentration definition it is possible to obtain the following relation:

$$C_{Mass} = \frac{\dot{m}_{HFE}}{\dot{m}_{HFE} + \dot{m}_{N_2}} = \frac{1}{1 + \dfrac{\dot{m}_{N_2}}{\dot{m}_{HFE}}} \qquad \textit{(Eq. 7)}$$

The mass of the Nitrogen and the HFE-7100 can be calculated as following:

$$\dot{m}_{N_2} = \dot{n}_{N_2} \cdot M_{N_2} = \dot{n} \cdot y_{N_2} \cdot M_{N_2} \qquad \textit{(Eq. 8)}$$

$$\dot{m}_{HFE} = \dot{n}_{HFE} \cdot M_{HFE} = \dot{n} \cdot y_{HFE} \cdot M_{HFE} \qquad \textit{(Eq. 9)}$$

M is the molecular weight of each component and " $\dot{n}$ " is the mole flow rate of the Mixture.

Combing *(Eq. 5)*, *(Eq. 6)*, *(Eq. 7)*, *(Eq. 8)* and *(Eq. 9)* it is finally possible to obtain the mass concentration:

$$C_{Mass} = \frac{\dot{m}_{HFE}}{\dot{m}_{HFE} + \dot{m}_{N_2}} = \frac{1}{1 + \dfrac{M_{N_2}}{M_{HFE}} \cdot \dfrac{1 - C_{Vol}}{C_{Vol}}} \qquad \textit{(Eq. 10)}$$

From this final equation it is possible to see that, according to the Amagat model, the mass concentration of the mixture is function only of the volumetric concentration and of the molecular weights of the Nitrogen and the HFE-7100. The temperature and the pressure of the mixture do not affect the conversion.

Therefore the mass concentration can be easily calculated with this formula knowing only the gas concentration sensor readout value.

5.2.3 Analysis of the results

Using Eq. 10 to perform the conversion, it is possible to obtain the graph shown in Fig.5-1, considering:

$$M_{N_2} = 28,01 \frac{kg}{kmol} \qquad\qquad M_{HFE} = 250 \frac{kg}{kmol} \qquad\qquad (Eq.\ 11)$$

The HFE molecular weight value was found in the datasheet attached in Annex 6:
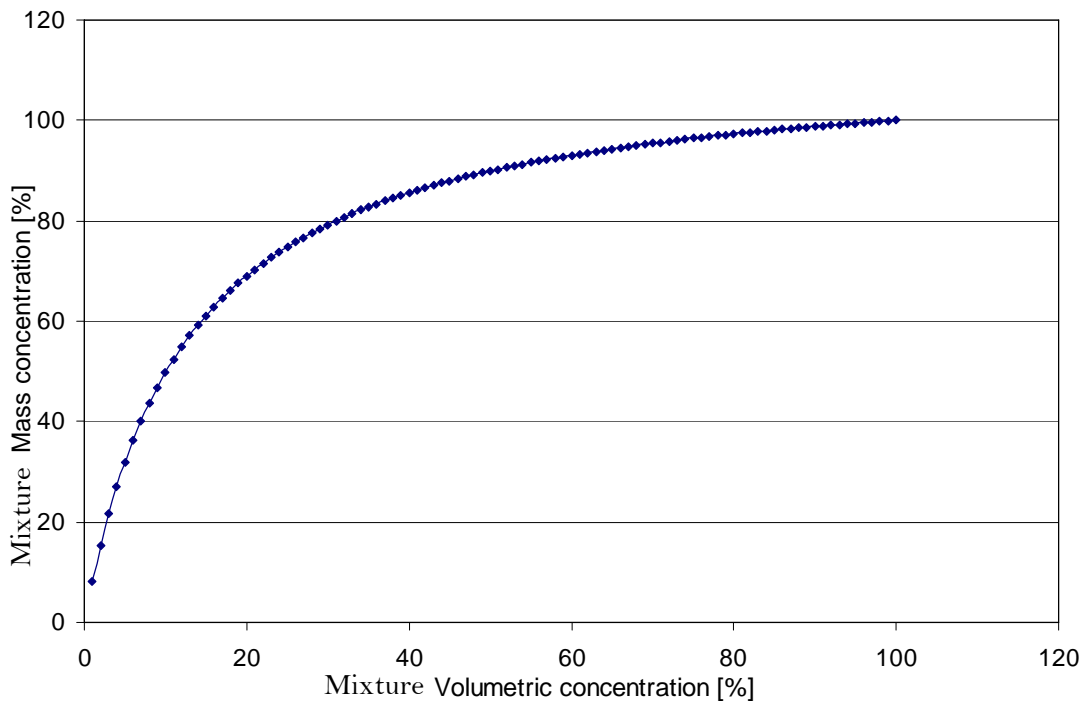
Figure 5-1: Conversion from volumetric to mass concentration. Values obtained theoretically using the Amagat model.

These results are very important because they show that the mass concentration becomes relatively big even at small volumetric concentrations. In fact already at 10% of volumetric concentration the mass fraction is 50%. This means that every test for which the volumetric concentration value was above 10% it would be out of the mass fraction requirement 3267 of Annex 1:.

5.2.4 Validation of results using an experimental test

The curve reported in Figure 5-1 is purely theoretical and it is based on the preliminary assumptions: the Amagat and the ideal gas models. In order to rely on this conversion method, an experimental validation test was performed. The test setup consisted of a temperature controlled chamber which mixed the measured amounts of Nitrogen and liquid HFE-7100, in order to deliver to the GCS (placed after the mixer) a precise mass mixture quality. For each test, the volumetric concentration was obtained from the sensor readout through Eq. 1, which was a result of a previous sensor calibration. This value was then compared with the known mass concentration. Tests were performed at different mixture pressures and temperatures.Figure 5-2 shows the validation results.
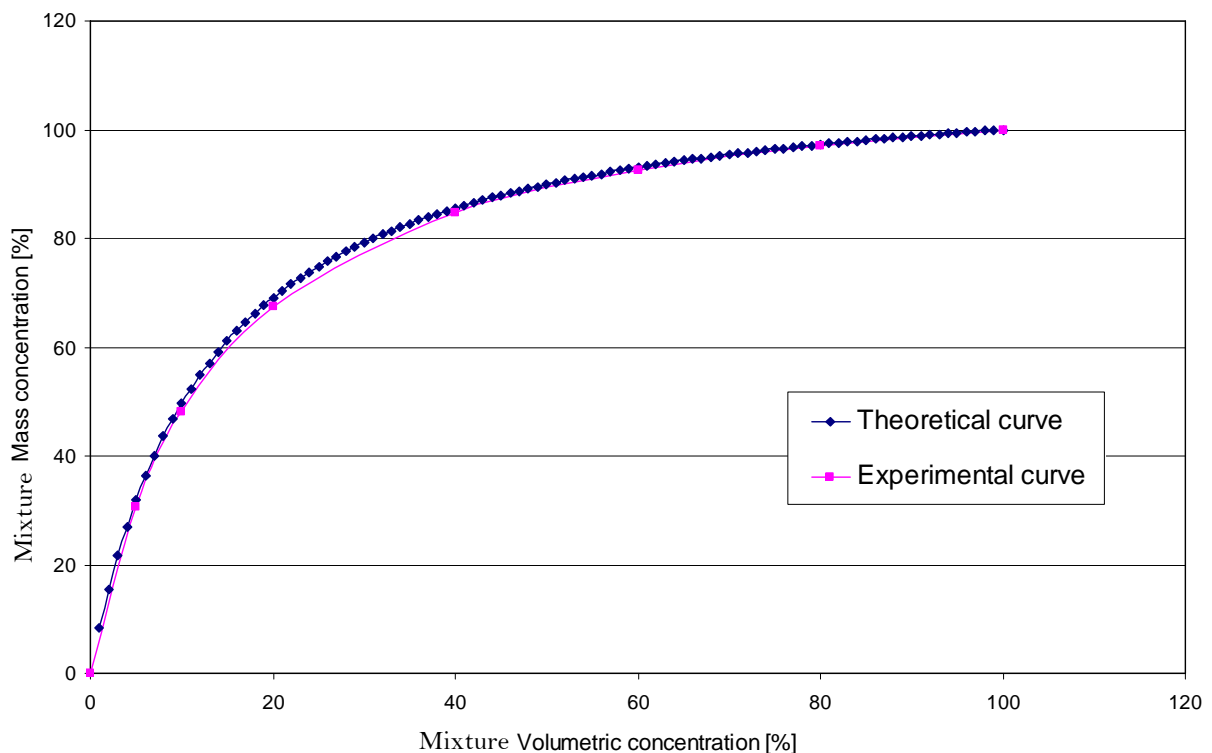
Figure 5-2: Conversion curve between the mass and the volumetric concentrations.
Comparison between the experimental and the theoretical values.

During the tests, it was observed that both the temperature and the pressure did not affect the conversion. This is an important result because it proves the accuracy of the theoretical relationship (Eq.10), which is also not dependent on the pressure and temperature. Moreover, the points of the two curves in Figure 5-2 are very close to each other and the trends are the same. However there are little differences between the curves. The possible reasons are the presence of dissolved Nitrogen in the HFE and the accuracy of the instruments used to feed the mixer. The maximum difference between the experimental and theoretical values was 5%. It is therefore possible to say that the theoretical method approximates the real values very well. The Amagat and the ideal gas assumptions are therefore correct.

The following deductions can be made looking at the conversion relationship (Eq.10):

- The transformation curve gives higher mass concentrations in respect to the volumetric ones, because the molar mass of the HFE is much more (almost 10 times) than the Nitrogen molar mass.
- The only parameters that appear in the conversion are the volumetric concentration and the molar weights of the mixture components.

5.3 Calibration of the MFM and MFC

5.3.1 Introduction and objectives

The MFM and the MFC were calibrated for a mixture of 95% of Nitrogen and 5% of Ethanol. During the test campaign, the meters measured a mixture of Nitrogen and HFE-7100. Therefore a conversion was necessary in order to have correct results. The values were firstly converted to the fictitious case of pure Nitrogen passing through the meters. This transformation was done by using a program from Bronkhorst, named FLUIDAT[15], which provided a conversion factor of 1,048. Once the values were converted to the pure Nitrogen case it was possible to perform the calculation to obtain the final value for the mixture of HFE-7100 and Nitrogen. This chapter is about this calculation.

Even before computing the transformation, it could be easily noticed that, if the meters readouts were converted as if the flow was pure Nitrogen, the error made would be relevant. In fact, considering that the obtained mass concentration of the mixture was around 50% most of the time, and considering that the molar mass of the HFE-7100 is almost 10 times the Nitrogen one, the real readout values are expected to be quite different from the case with the Nitrogen calibration.

5.3.2 Calculations

The conversion factor cannot be calculated with FLUIDAT because the HFE-7100 fluid was not loaded in the program archive. Moreover even if FLUIDAT had the HFE-7100 fluid properties, the concentration of the HFE vapor would not be constant throughout all the tests range, and it would be not convenient to perform the conversion for every one of the 55 measurements.

Therefore an alternative way was chosen by using a model proposed in the Bronkhorst` LOW-ΔP-METER instruction manual [6]. This choice was also suggested by a supplier expert.

The proposed formula in the manual for a gas mixture is:

$$\frac{1}{C_{mix}} = \frac{V_1}{C_1} + \frac{V_2}{C_2} + \dots \frac{V_n}{C_n}$$ (Eq. 12)

Where C_{mix} is the conversion factor for the whole mixture, C_i is the conversion factor for the "i" component of the mixture and V_i is the volumetric fraction of the "i" component in the mixture.

For the mixture used in CIMEX-1 (HFE vapor and-Nitrogen) Eq.12 becomes

$$\frac{1}{C_{mix}} = \frac{V_{N_2}}{C_{N_2}} + \frac{V_{HFE}}{C_{HFE}}$$ (Eq. 13)

For the MFC V_{HFE} is simply the volumetric concentration read by the GCS, namely C_{vol}, and $V_{N_2} = 1 - V_{HFE}$, therefore $V_{N_2} = 1 - C_{vol}$.

For the second conversion factor to be used for the MFM, positioned after the cell, another volumetric concentration is needed for V_{HFE} because the HFE vapor quantity increases, due to the evaporation in the cell. Since is not possible to calculate this concentration, because it depends on the MFM readout (see chapter 5.4, Eq.28), the same volumetric concentration, read by the GCS, is used also for the MFM. Clearly, this is a source of error which has to be avoided in the future measurements, for example implementing a second GCS after the cell or characterizing the liquid pump behavior.

Note: The following calculations are intended for the pure Nitrogen data (already converted from the Nitrogen-Ethanol mixture calibrated data) to the desired HFE7100-Nitrogen data.

5.3.2.1 C$_{N_2}$ calculation

According to the Bronkhorst manual [6], the conversion factor for each component of the mixture has to be calculated as following:

$$C_{(1\rightarrow2)} = \frac{c_{p(1)} \cdot \rho_{(1)}}{c_{p(2)} \cdot \rho_{(2)}}$$ (Eq. 14)

Where (1) is the gas to be calibrated and (2) is the gas to be measured. c_p is the specific heat at constant pressure and ρ is the gas density. The formula contains the thermal properties of the flow since the working principle of the meters is based on the thermal bypass method. For further information see section 2.3.5 and [6].

> _Note_: according to the manual c_p has to be taken at a temperature 50°C higher than the one at which the conversion factor is calculated. This recommendation will be applied for all the following calculations, also for the C$_{HFE}$ calculations.

In the case of C_{N2} both the gas to be calibrated and the measured one are Nitrogen. Therefore the conversion factor is 1.

$$C_{N_2} = 1$$ (Eq. 15)

5.3.2.2 C_{HFE} calculation

In this case, according to Eq.14, the gas to be calibrated is HFE vapor and the gas to be measured is Nitrogen. Therefore:

$$C_{(N2 \to HFE)} = \frac{c_{p(N_2)} \cdot \rho_{(N_2)}}{c_{p(HFE)} \cdot \rho_{(HFE)}} \qquad \text{(Eq. 16)}$$

$c_{p(N_2)}$ is calculated from the relationship valid for ideal gases provided in table A-21 of Reference [1]:

$$c_{p(N_2)} = \frac{\overline{R}}{M_{N_2}} \cdot (3{,}675 - 1{,}208 \cdot 10^{-3} \cdot T + 2{,}324 \cdot 10^{-6} \cdot T^2 - 0{,}632 \cdot 10^{-9} \cdot T^3 - 0{,}226 \cdot 10^{-12} \cdot T^4) \qquad \text{(Eq. 17)}$$

Where $\overline{R}$ is the universal gas constant and M_{N_2} is the Nitrogen molar mass, equal to $28{,}01 \dfrac{Kg}{Kmol}$

The Nitrogen density $\rho_{(N_2)}$ can be easily calculated using the ideal gas state equation:

$$\rho_{(N_2)} = \frac{p \cdot M_{N_2}}{\overline{R} \cdot T} \qquad \text{(Eq. 18)}$$

Where p and T are the gas mixture pressure and temperature, respectively.

Also the HFE-7100 density $\rho_{(HFE)}$ can be calculated using the ideal gas state equation:

$$\rho_{(HFE)} = \frac{p \cdot M_{HFE}}{\overline{R} \cdot T} \qquad \text{(Eq. 19)}$$

P and T are again the gas mixture pressure and temperature.

Unfortunately a formula like Eq.17 is not available for the HFE-7100 specific heat. Therefore this quantity has to be calculated using the definition and the HFE-7100 vapor table that is possible to find in Annex 4:.The specific heat at constant pressure is defined as:

$$c_p = \left. \frac{\partial h}{\partial T} \right|_p \qquad \text{(Eq. 20)}$$

Where h is the mass specific enthalpy and T is the temperature

Since the vapor table provides all the enthalpy values for the correspondent temperatures, it is possible to calculate the HFE-7100 specific heat by approximating the derivative in Eq.20 with the forward finite difference as following:

$$c_{pHFE}(T, p) = \left. \frac{h_{HFE}(T + \Delta T) - h_{HFE}(T)}{\Delta T} \right|_p \qquad \text{(Eq. 21)}$$

With this approximation it was found that c_{pHFE} varies from $0{,}94 \dfrac{KJ}{Kg \cdot K}$ to $0{,}99 \dfrac{KJ}{Kg \cdot K}$ throughout the full tested pressure range (400-1000 mbar) and the full tested temperature range (25-50℃). A verification of these values was also performed in the pressure-enthalpy chart included in Annex 5:.

5.3.3 Results evaluation

The influence of the temperature and pressure on the conversion factor is negligible compared to the influence of concentration. In fact, the graphs reported in Annex 2: show that the conversion factor variations are only 1,5% throughout the temperature range, and only 1,4% throughout the pressure range. The conversion factor was therefore correlated only with the volumetric concentration, being sure that the final error will be negligeble.

Figure 5-3 presents the final results of the calculation, showing the conversion factor as a function of the volumetric concentration, only.
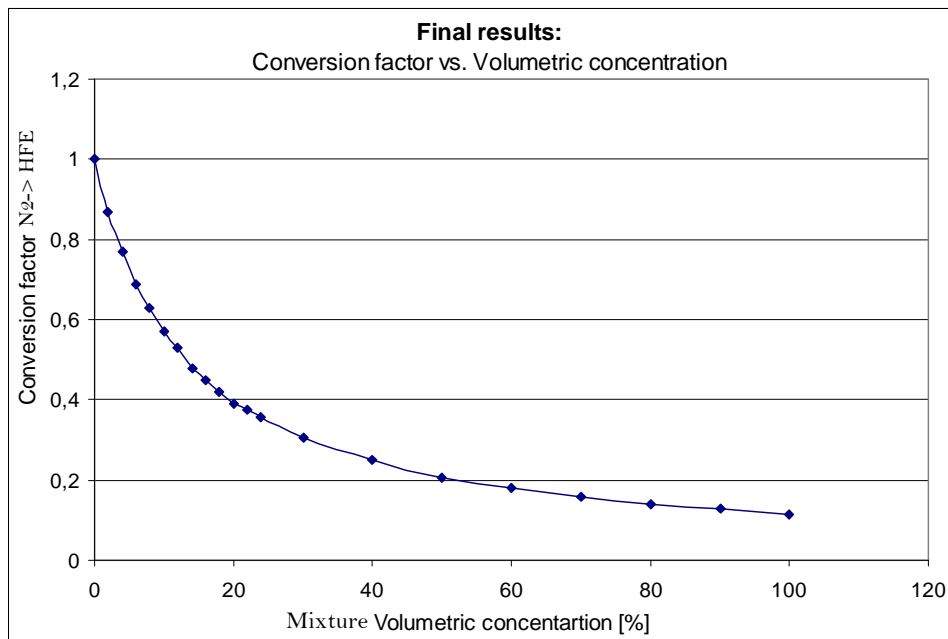
Figure 5-3: Conversion Factor for the MFM and the MFC

This data was finally used for the data conversion of the MFM and the MFC pure Nitrogen values. For example 500 [mg/min] with the pure Nitrogen calibration, considering a volumetric concentration of 20 %, would correspond to:

$$\text{Real HFE flow rate} = 500\left.\frac{\text{mg}}{\text{min}}\right|_{N2\,calibrated} \cdot 0,39 = 195\left.\frac{\text{mg}}{\text{min}}\right|_{HFEcalibrated} \qquad \textit{(Eq. 22)}$$

5.3.4 Comments and recommendations

The concentration of the HFE is the main driver of the conversion factor calculation. Therefore, it is not possible to adopt only one single conversion factor value for all of the test cases. Moreover, even if the meters were calibrated for HFE-7100, with a specific concentration, a conversion factor would be still needed because of the concentration variation during the tests. The conversion formula, according to

Bronkhorst, is affected by an error which, in the worst case during the tests, was about 5%. This inaccuracy cannot be avoided because it is prescribed in the formulas.

A more refined relationship for calculating the conversion factor should be found, taking into account the temperature and the pressure influences. Moreover, the liquid pump behavior has to be characterized to know exactly the volumetric concentration after the cell. With this value it will be possible to calculate a more precise conversion factor for the MFM (see the comments after Eq.13*(Eq. 13)*).

5.4 Calculation of the mass concentration after the cell

5.4.1 Introduction and objectives

This chapter is meant to explain how the concentration at the cell outlet was calculated. This value is important, because it allows a better assessment of the performances of the CSS (see chapter 6.4).

A mass balance will be applied to the evaporation cell.

5.4.2 Calculations

All the following calculations are based on the next scheme showed in Figure 5-4.
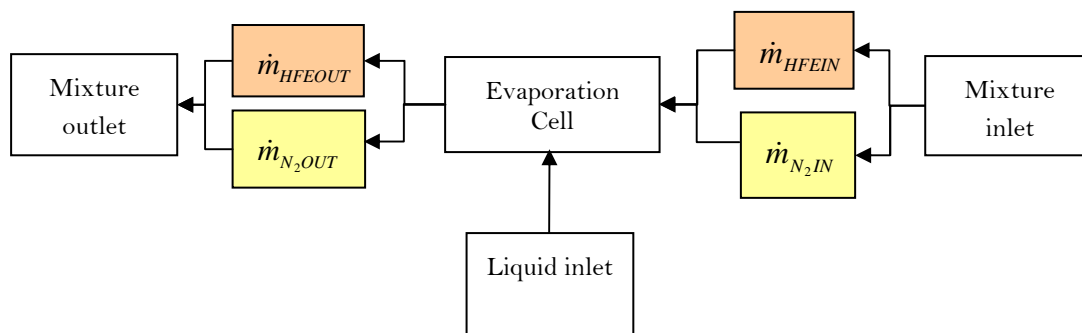
Figure 5-4: Scheme showing the cell inlets and outlet

At the inlet and at the outlet of the cell the mixture flow rate is:

$$\dot{m}_{MIXTUREIN} = \dot{m}_{HFEIN} + \dot{m}_{N_2IN} \qquad (Eq.\ 23)$$

$$\dot{m}_{MIXTUREOUT} = \dot{m}_{HFEOUT} + \dot{m}_{N_2OUT} \qquad (Eq.\ 24)$$

Since the Nitrogen flow rate entering the cell is the same that leaves the cell (the liquid HFE contained inside the liquid chamber is not supposed to absorb gas at steady state conditions):

$$\dot{m}_{N_2 IN} = \dot{m}_{N_2 OUT} = \dot{m}_{N_2} \qquad (Eq.\ 25)$$

Form Eq.23 and from the definition of the mass concentration it is possible to calculate the Nitrogen flow rate:

$$\dot{m}_{N_2} = \dot{m}_{MIXTUREIN} - \dot{m}_{HFEIN} = \dot{m}_{MIXTUREIN} \cdot (1 - C_{mass}) \qquad (Eq.\ 26)$$

Rearranging Eq.24 with Eq.26 it is possible to say that:

$$\dot{m}_{HFEOUT} = \dot{m}_{MIXTUREOUT} - \dot{m}_{N_2} = \dot{m}_{MIXTUREOUT} - \dot{m}_{MIXTUREIN} \cdot (1 - C_{massIN}) \qquad (Eq.\ 27)$$

Considering the definition of mass concentration and Eq.27 it is finally possible to calculate the gas concentration before the CSS:

$$C_{massOUT} = \frac{\dot{m}_{HFEOUT}}{\dot{m}_{MIXTUREOUT}} = \frac{\dot{m}_{MIXTUREOUT} - \dot{m}_{MIXTUREIN} \cdot (1 - C_{massIN})}{\dot{m}_{MIXTUREOUT}} = 1 - \frac{\dot{m}_{MIXTUREIN} \cdot (1 - C_{massIN})}{\dot{m}_{MIXTUREOUT}}$$

$$(Eq.\ 28)$$

5.4.3 Comments and recommendations

C_{massIN} is calculated using Eq.10. Moreover, $\dot{m}_{MIXTUREOUT}$ is calculated from the MFM readout converting the value to the HFE case. This calculation was performed considering the same volumetric concentration as at the cell inlet (see the comments of Eq.13). Since the MFM converted value is an approximation to the correct mass flow rate, also $C_{massOUT}$, calculated from Eq.28, represents an approximation to its real value.

More precise results will be available when the liquid pump behavior is characterized.

6 Analysis of the test data

6.1 Introduction

The aim of this section is to present the calculated results of the closed loop BB test campaign. The data obtained directly from the instruments will be converted, according to the indications reported in chapter 6.2. These conversions are important for a better assessment of the system performances.

Although the calculated results of CIMEX-1 are the main purpose for the real mission, they are not the primary target for this BB test campaign. Anyway, they are the first results obtained with the HFE-7100; the fluid replacing the previous Ethanol, and therefore they will be useful for the requirements redefinition or for the first eventual design iteration of some components like the CSS.

The results are graphically reported in section 6.3 and 6.4. Tables containing all of the partial calculation and additional information are reported in Annex 3:.

6.2 Used formulas

All the results that will be presented were obtained using the following calculations:

- *Change from volumetric to mass gas concentration.*
  The theoretical background and the performed calculation are presented in chapter 5.2.

- *Conversion from the "apparent" volumetric flow unit readout of the Bronkhorst meters to the mass flow unit.*
  The instruments readouts are expressed in units of Volume, ml/min, but they are normalized to a constant temperature and pressure: 0℃ and 1,013b ar. This means that, although the readouts are in units of volume, the measurement is a mass flow.

To convert the result in units of mass the Nitrogen density at 0℃ and 1,013bar was calculated. Its value was 1,2504mg/ml and it was used for both the MFM and the MFC.

$$\text{Example}: \quad 200\frac{ml}{\min}\bigg|_{n} = 200\frac{ml}{\min}\bigg|_{n} \cdot 1,2504\frac{mg}{ml} = 250,08\frac{mg}{\min} \qquad Eq.\ 29$$

> *Note:* in order to highlight that the MFM readout is a mass flow, even if it expressed in unit of volume, a subscript n (meaning "normalized") will be used.

- *Conversion from the N2+Ethanol calibration to the pure Nitrogen calibration.*
This calculation was performed for both meters. The used conversion factor was 1,048, and it was provided by the supplier.

$$\text{Example}: \quad 500\frac{mg}{\min}\bigg|_{N2+Ethanol} \cdot 1,048 = 524\frac{ml}{\min}\bigg|_{pureN2} \qquad Eq.\ 30$$

- *Conversion from the pure N2 calibration to the HFE calibration.*
This calculation was performed for both the MFM and the MFC using the conversion factor calculated in chapter 5.3. The factor depends on the volumetric concentration and it is therefore different for each test case.

> Example of conversion: 500 [mg/min] with the pure Nitrogen calibration, considering a volumetric concentration of 20 %, would correspond to:

$$\text{Real HFE flow rate} = 500\frac{mg}{\min}\bigg|_{N2calibrated} \cdot 0,39 = 195\frac{mg}{\min}\bigg|_{HFEcalibrated} \qquad Eq.\ 31$$

See chapters 5.3.3 and 5.3.4 and check the comments of this conversion method

- *Calculation of the mixture volumetric flow rate.*
This calculation was performed only for the MFC using the following mixture density:

$$\rho_{(Mixture)} = \frac{p \cdot M_{Mixture}}{\overline{R} \cdot T} \qquad Eq.\ 32$$

T is the temperature of the mixture which is equal to the ambient temperature (26℃) since the line was not thermally isolated. P is the test pressure. $M_{Mixture}$ is the molar mass of the mixture and it is equal to:

$$M_{Mixture} = y_{HFE} \cdot M_{HFE} + y_{N2} \cdot M_{N2} = C_{vol} \cdot M_{HFE} + (1 - C_{vol}) \cdot M_{N2} \qquad Eq.\ 33$$

Finally the volumetric flow rate was calculated from the mass flow rate by using:

$$\dot{V}\bigg|_{HFEmixture} = \frac{\dot{m}\big|_{HFEmixture}}{\rho_{(Mixture)}} \qquad Eq.\ 34$$

- *Calculation of the gas concentration after the cell.*
  Eq.28 in chapter 5.4 was used for this calculation.

- *Gas concentration percentage reduced by the CSS (or CSS efficiency)*:
  This parameter was considered for a better assessment of the CSS performance because it is independent on the flow rate. In fact, the efficiency is the ratio between the mass concentration reduced by CSS and the mass concentration that enters in the condenser.
  The definition of the efficiency is the following:

$$\eta = \frac{C_{massIN} - C_{massOUT}}{C_{massIN}} \qquad \textit{Eq. 35}$$

- *Evaporating HFE flow rate.*
  This calculation is performed by subtracting the MFC mass flow to the MFM mass flow:

$$\text{Evaporating HFE flow rate} = \text{MFM}_{HFEcalibrated} - \text{MFC}_{HFEcalibrated} \qquad \textit{Eq. 36}$$

6.3 Cell behavior

The calculated results of the cell are about the evaporation rate as a function of the main parameters: the cell temperature, the gas loop pressure and the mixture flow rate. Figure 6-1 and Figure 6-2 summarize the results of the tests. In the graph below, it is possible to see that as the volumetric flow rate increases, the evaporating liquid flow rate also increases. Moreover, the lower the pressure, the higher the evaporation rate.
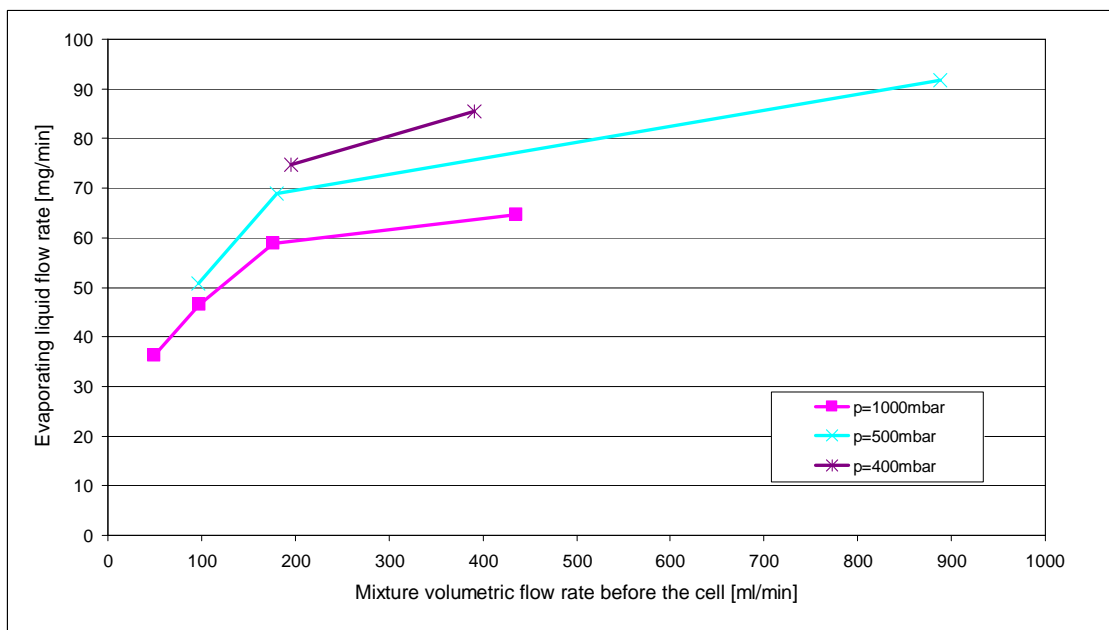
Figure 6-1: Evaporating fluid flow rate vs. mixture volumetric flow rate @ T=25°C

The following second graph shows that, the higher the temperature, the higher the evaporation rate, and the higher the volumetric flow rate, the higher the evaporation rate.
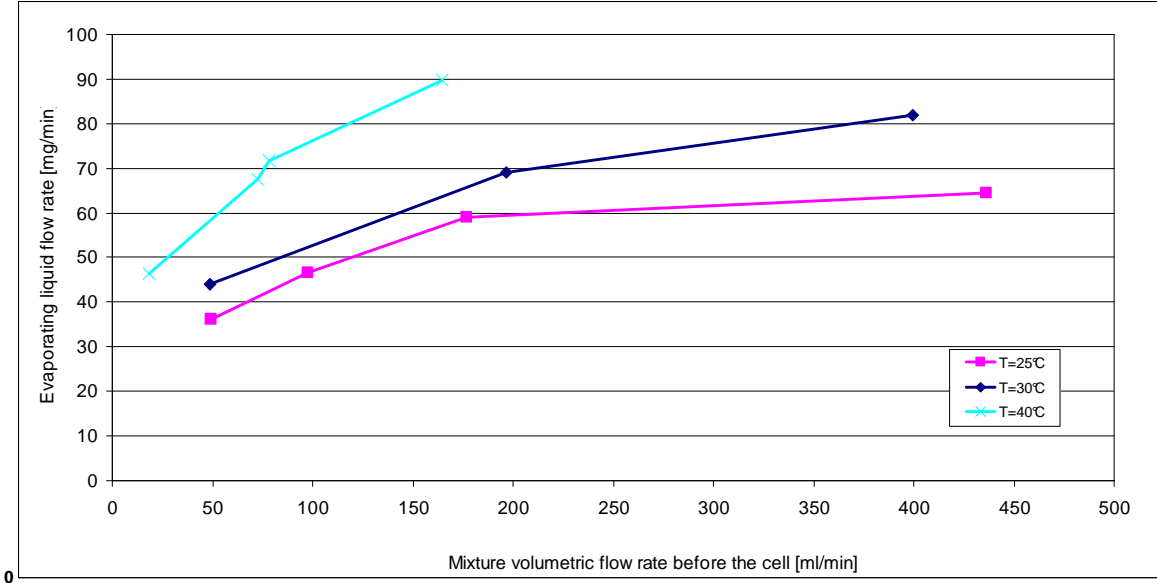
Figure 6-2: Evaporating fluid flow rate vs. mixture volumetric flow rate @ p=1000 mbar

6.4 CSS behavior

The CSS behavior will be assessed using the efficiency defined in section 6.2. Next graph summarizes the results; comments are provided in the next page.
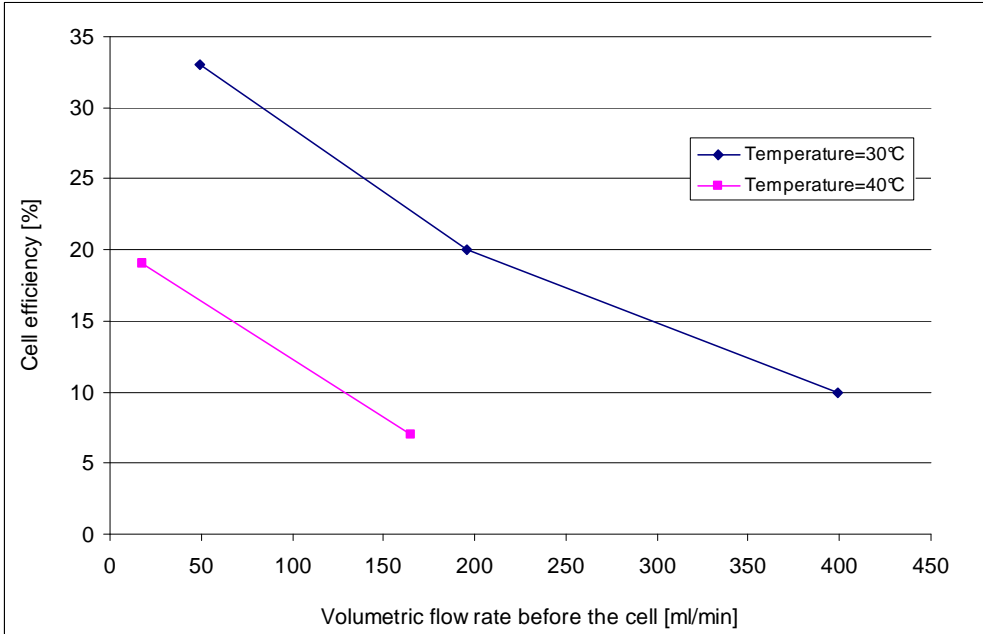
Figure 6-3: CSS efficiency vs. cell temperature @ 1000 mbar

The information contained in the previous graph can be summarized as following:

- The higher the cell temperature, the lower the cell efficiency. This could be explained because of the higher evaporation rate at higher temperatures (see the graphs in section 6.3). With a higher evaporation rate, the cell efficiency decreases.
- The higher the volumetric flow rate, the lower the efficiency. This could be explained because at high volumetric flow rates, the evaporation rate increases (see the graphs in section 6.3) and consequently the CSS efficiency decreases.

Another important result can be easily verified by looking at Table 9 in Annex 3:. The mass concentration after the CSS exceeds the 50% value for about half of the performed tests. This is very important for CIMEX-1, since the requirements state that the concentration should not exceed this value. However, it is important to say that the CSS was designed for Ethanol and not for HFE-7100. For this reason, the requirements are not satisfied. A requirements redefinition or a new CSS design is therefore necessary. Further considerations about the implication of this behavior are reported in chapter 7.

6.5 Comparison with the Ethanol case

In 2008, VERHAERT space [17] tested the CSS with Ethanol. The aim of this section is to compare the results obtained with Ethanol to the ones obtained during the test campaign with HFE-7100.
The graph in Figure 6-4 shows the results obtained with the Ethanol mixture from the VERHAERT test.
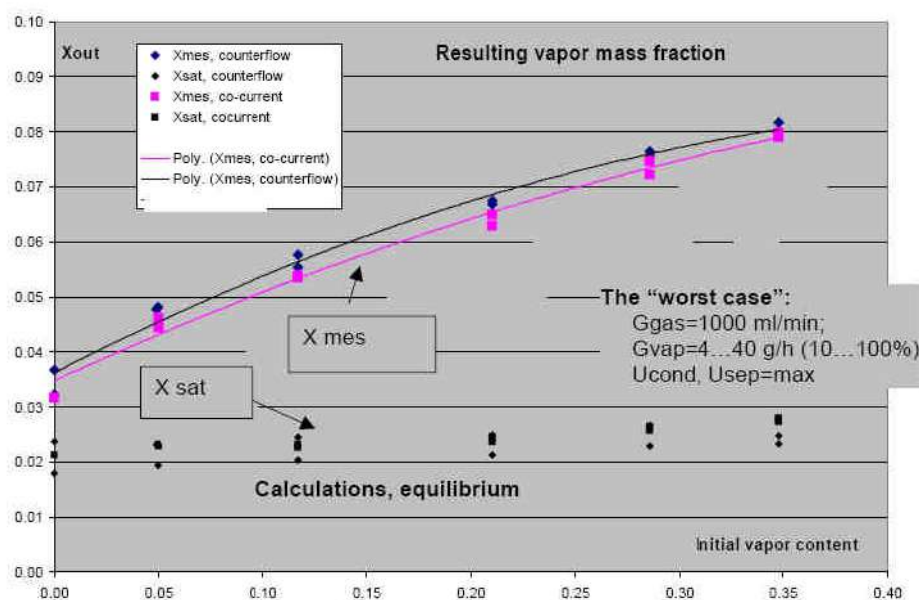
Figure 3: Residual vapour content for the "worst" operating conditions. **X-axis**: inlet mass fraction defined on the base of direct gas and liquid flow rates measurings at the inlet, **Y-axis**: residual mass fraction defined by the means of the technique described in §6.

Figure 6-4: CSS behavior with Ethanol according to reference [4] (from VERHAERT SPACE)

For the values shown in Figure 6-4, the CSS efficiency is calculated according to Eq.35 in section 6.2 and the plot in Figure 6-5 is then obtained. From this plot it is possible to see that the CSS efficiency increases as the concentration of the entering gas increases.
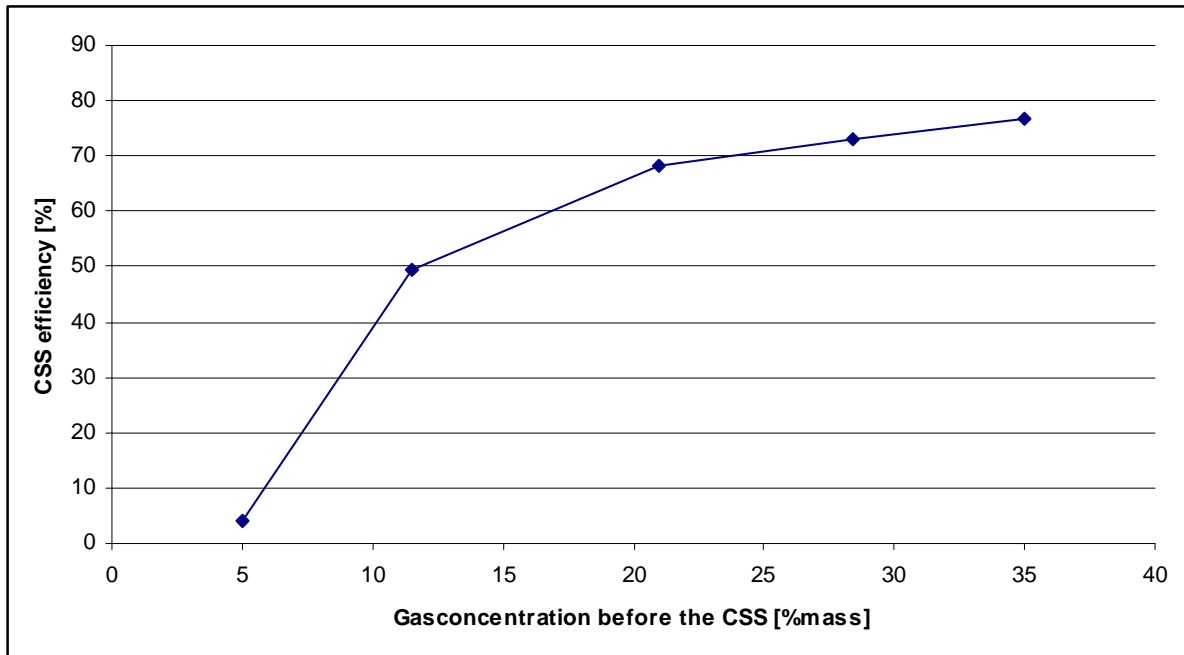
Figure 6-5: CSS efficiency vs. gas concentration entering the CSS using the VERHAERT SPACE test report data. Ethanol case

These results can be compared with the HFE-7100 data which are reported in Figure 6-6

As it is possible to see, the CSS behavior is the same: the efficiency increases as the inlet gas concentration increases.
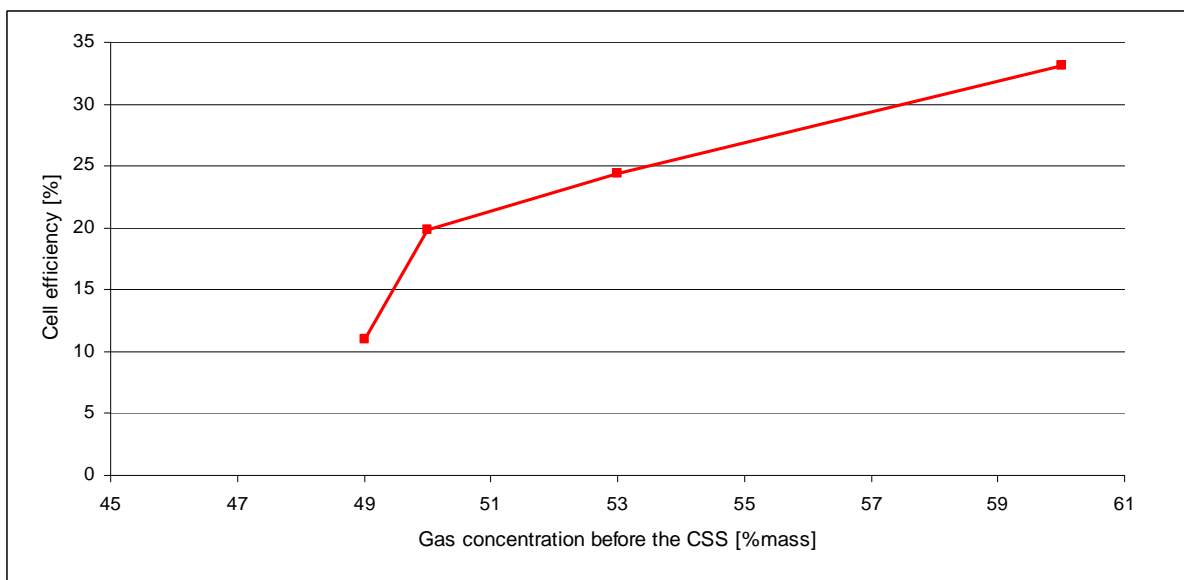
Figure 6-6: CSS efficiency vs. HFE-7100 gas concentration entering the CSS. (1000mbar, condenser @-20°C)

However, the cell efficiency using HFE-7100 mixture is much less than the case with Ethanol mixture.

A possible reason comes from the conversion factor used to obtain the mass concentration from the volumetric concentration. In fact, this transformation is affected by the molar weight ratio between the Nitrogen and the vapor, according to Eq.10 of section 5.2. The graph in Figure 6-7 shows the different relationships between the mass and the volumetric concentration for the Ethanol case and the HFE case. For the same value of volumetric concentration, the corresponding mass concentration would be less in the case of Ethanol because its molar mass is only 46,07g/mol, while the HFE-7100 is 250g/mol. Therefore, the CSS would have more mass to condense in the case with HFE-7100 and the efficiency would consequently decrease.
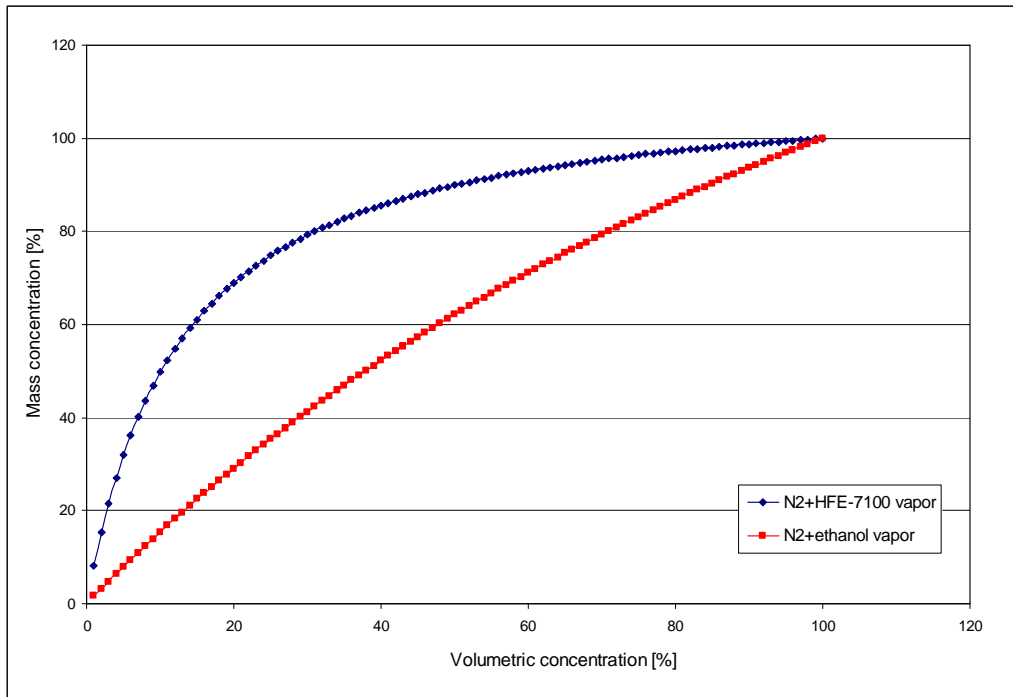
**Figure 6-7: Relationship between the mass and volumetric concentration
HFE-7100 vs. Ethanol**

6.6 Comments

The obtained results make physical sense but they cannot be considered valid for scientific use, since some instruments were not precise enough for scientific purposes. However, they are suitable for engineering purposes like redesigning components or proposing new requirements (as it will be done in the next chapter).

For a correct evaluation of the results, it is important to note that the same conversion factor was used both for the MFM and for the MFC. This assumption caused errors in the performed calculations of this chapter since:

- The same volumetric concentration which was used for the MFC conversion factor was also considered for the MFM conversion factor. Obviously the two concentrations are different due

to the evaporation taking place in the cell. This choice was made, since it is not possible to calculate the exact volumetric concentration after the cell with this test setup, because the respective mass concentration (from which it is possible to calculate the volumetric concentration through Eq.10), depends on the MFM readout, which in turn depends on the volumetric concentration. An extra input parameter is therefore missing. When the flow rate delivered by the liquid pump will be known (by characterizing the pump behavior), the mass concentration can be correctly calculated at the cell outlet. Therefore, after converting the mass concentration to the respective volumetric concentration (by inverting Eq.10 in section 5.2), it will be possible to correctly calibrate the MFM using the formulas presented in section 5.3.

- The MFM and MFC pressures and temperatures were considered equal because of the small influence of these parameters on the conversion.

The CSS was not able to deliver less than 50% of vapor quality for all the conditions. On the contrary the tests performed by VERHAERT Space with Ethanol, instead of HFE-7100, were all within the requirement range. As it was pointed out in section 6.5 the reason for this different behavior is the different molecular weights of the liquids.

The most important remark of this chapter is the discovery that the mass concentration requirement was not satisfied. Therefore, a solution has to be found in order for the project to continue. Since much effort has been made for designing, building and testing the components, it was decided to change the requirements instead of performing a new design (in particular for the CSS). Chapter 7 will present a requirement redefinition which will be proposed and agreed with the European Space Agency and the teams of scientists.

7 System evaluation and requirements redefinition

7.1 Introduction

In this last chapter, the results obtained during the test campaign were summarized and an evaluation of the System Operability/Stability with HFE-7100 was performed. The aim of the following sections is to assess the System behavior and to obtain suitable parameter ranges for the system with HFE-7100.

7.2 System stability and operability evaluation

The start-up of the system was demonstrated to be functional and CIMEX-1 closed loop was stable with the HFE-7100. The surface flatness and the meniscus stability were achieved by manual hand control of the injection rate (the control frequency was estimated to be about 1Hz). At lower pressures and high evaporation rates, the manual control becomes more challenging but it is still achievable. The system stability can be considered achieved. The surface flatness control by PID control loop will be implemented in the future with sampling rates higher than 1Hz. It is assumed to be very feasible to automatically control all required parameter ranges.

The system evaporation across the loop was controlled. It was demonstrated that it is possible to recover the system to the initial operational conditions without opening the loop after chaotic conditions (e.g. boiling of HFE-7100). Moreover, if the spilling of liquid over the micro-groove was enforced, the system recovery was demonstrated to be feasible within 1-3mins as well as a restart of the flatness control.

The operability of the system and the system stability were achieved during the closed loop test campaign. From this point of view, the BB tests were successful.

7.3 Parameters Range

In this section the tested parameter ranges for the HFE-7100 are shown as a result of the test campaign. Table 6 shows the tested parameter ranges.

Orange marked cells are used when the mass concentration exceeds the one imposed by the requirement 3267 reported in Reference [2]. Yellow marked cells are used when the stability of the system is not achievable due to the liquid boiling (see section 4.5). The table highlights that the parameters ranges reported in the requirements (Reference [2]) are partially verified/covered by the performed tests. In particular it is not possible to reach low pressure and high temperature conditions without exceeding the 50% of mass concentration requirement.

| | Pressure [mbar] | Mixture volumetric flow rate [ml/min] converted from the Mass Flow meter Tested values | | Comments |
		Min	Max	
T cell 25℃	400	130	390	Mass concentration > 50%
	500	100	250	Mass concentration > 50%
	600	90	450	Mass concentration > 50%
	800	90	550	
	1000	50	550	
T cell 30℃	400	not tested	not tested	
	500	not tested	not tested	
	600	not tested	not tested	
	800	not tested	not tested	
	1000	50	400	
T cell 40℃	400	BOILING	BOILING	UNSTABLE
	500	BOILING	BOILING	
	600	not tested	324	Mass concentration > 50%
	900	not tested	394	
	1000	98	555	Mass concentration > 50%
T cell 45℃	400	BOILING	BOILING	UNSTABLE
	500	BOILING	BOILING	
	600	BOILING	BOILING	
	800	not tested	367	
	1000	not tested	322	
T cell 50℃	400	BOILING	BOILING	UNSTABLE
	500	BOILING	BOILING	
	800	BOILING	BOILING	
	900	not tested	273	Mass concentration > 50%
	1000	not tested	129	Mass concentration > 50%

Table 6: Tested Parameters and Operating ranges

7.4 New proposed requirements

As a result of the previous findings, the following new requirements are proposed for CIMEX-1 in order to keep the already existing design and, when possible, components.

Spec ID*	Chapter *	Requirement	Current values	New proposed values
3267	4.3.14.1	The CSS shall deliver at outlet a gas phase composed of at least 50% of gas. 95% is considered as a target.	50% of Nitrogen (in Mass)	Up to 20% of Nitrogen (in Mass), target 95%. Or Up to 60% of Nitrogen (in volume) target 95% (*1)
3205	4.3.7.1.1	The temperature setting range shall be 10°C up to 60°C.	10°C to 60°C	10°C to 50°C (*2)
3193	4.3.5.3	The gas flow rate shall be measurable in a range from 10 to max 1000 ml/min.	10-1000 ml/min	10-1000 ml/min (*3)
3197	4.3.6.1	The set pressure shall be adjustable in a pressure range from 400 mbar to 1000 mbar.	400-1000 mbar	Variable from 500 to1000 mbar according to the boiling curve (*4)
*Chapter and ID are intended for Reference [2]				

Table 7: New proposed requirements

Remarks:
- (*1) The molar mass of HFE-7100 is much higher than the Ethanol, therefore the mass concentration while entering the CSS is much higher with the same volumetric concentration (see Figure 6-7) and as a consequence it is better to re-define the requirement to a volumetric concentration. It has been observed that for low evaporation rates, the gas concentration is very low (e.g. 6-7%vol).
- (*2) The hardware is designed to support a temperature up to 60°C. The upper limit of the temperature range is due to the bubbling/degassing of the HFE-7100 at 1bar, which is the maximum experiment pressure (see Figure 4-9).
  Nevertheless, there will be combinations which are not possible due to bubbling as described in the same figure (e.g. high temperature and low pressure).
- (*3) The Bronkhorst devices will be calibrated to pure gas (Nitrogen case), since the real volumetric flow is dependent on the gas concentration (also temp and pressure). This can mean in some cases, a "real" flow (of Nitrogen + HFE-7100), below 500ml/min (even if 1000ml/min where commanded, see Table 9). This occurs in cases when the HFE-7100 concentration is high in the entrance of the cell.
  This means post-processing of the volumetric flow will have to be considered by the scientific team during results evaluation.
- (*4) Pressure ranges are fine, with the remark that it is not possible to have all combinations with the temperatures (see Figure 4-9).

8 Conclusions

This project demonstrated, for the first time, that CIMEX-1 is able to work in a complete closed loop with the new selected HFE-7100 liquid. This is an important step, since it is mandatory for the mission development to be continued. The system worked fine with challenging conditions (i.e. high cell temperatures and low pressures), and manual controlling was possible for all of the tests. The system recovered successfully after chaotic conditions, without the need to open the circuit.

The Bronkhorst meter/controller worked fine during all of the test campaign. Since the instruments were calibrated for another mixture, the measured values were converted using the indications provided by the supplier. It was discovered that this conversion was mostly affected by the mixture quality. Therefore, a conversion would be necessary even in the case that if the meters were calibrated for a mixture of and Nitrogen and HFE-7100 with a certain, but fixed concentration. The conversion formula was affected by an error of 5%. A more precise calculation method should be found in the future for better results. Moreover, for the same reason, the conversion factor variations with the mixture temperature and pressure should be taken into account.

The GCS worked fine, and the jumps problem due to the buffer overflow was solved by implementing the Java program. The program has to be improved since it experienced a wrong behavior when liquid HFE-7100 wetted the instrument. The conversion from volumetric to mass concentration was successfully performed and the theoretical assumptions were validated by performing experimental tests. This conversion also explained why the system behavior with HFE-7100 is different than with Ethanol (i.e. because of the bigger molecular weight). However, a dedicated sensor calibration for mass concentrations is needed for better results.

The metallic foil with the anti-wetting groove worked effectively, demonstrating that is possible to keep the liquid level above the foil surface and to reach the liquid interface stability.

A proposal for new requirements was given in order to maintain wider parameter ranges (regarding pressures and flow rates). Another choice could be a re-design of some components (e.g. the CSS) and the results of this BB could be used for the first design iteration. The science teams, as well as ESA, will verify which of these options is more suitable for the scientific purposes.

It is possible to conclude that CIMEX-1 Closed Loop BB was a success.

Bibliography

[1] M.J. Moran, H.N. Shapiro, Fundamentals of Engineering Thermodynamics, John Wiley & Sons, FIFTH EDITION 2006

[2] CIMEX-1 System Specification, F6-SP-AST-0002 issue 06, EADS Astrium document, 2008

[3] FSL EC B1 CIMEX-1 Design report incl. Functional and Performance analysis report, F6-RP-AST-0380 issue 02, EADS Astrium document, 2008,

[4] CIMEX FCA Bredboard-Test Procedure-Report, F6-RP-VDD-0064 issue C, VERHAERT Space document, 2008

[5] Requirements specifications, CIMEX1-ESA-ERD-001

[6] Instruction manual: Mass Flow/Pressure meters and controllers for gases and liquids, Bronkhorst, doc. N.9.17.001N, 27-06-2011

[7] C. S. Iorio, Experimental and numerical study of the coupling between evaporation and thermocapillarity Preparation of the CIMEX-1 Experiment, PhD thesis, Université Libre de Bruxelles, Septermber 2006.

[8] L.Ganuza, Devolopment Tests for an Evaporation Experiment in Microgravity, Master thesis, October 2010, ISAE University

[9] J. C. Legros, Report on CIMEX-An ESA-Sponsored Reserch Program, September 2007

[10] J.C. Legros, P. Colinet, L.Joannes, P.Stephan, G. Bekaert, G. Lebon, P.Cerisier, A.Delil, M. Bestehorn; Convection and Interfacial Mass Exchange CIMEX

[11] Bronkhorst website, www.bronkhorst.com

[12] ESA website, www.esa.int/esaHS/ESAAYI0VMOC_iss_0.html

[13] CIMEX FCA Bredboard-Test Procedure-Report, F6-RP-VDD-0064 issue C, VERHAERT Space document, 2008

[14] CIMEX-F6 FCA & Optics Design Report, F6-RP-VDD-0018 issue D, VERHAERT Space document, November 21st 2008

[15] FLUIDAT®, program for calculation mixture and fluid properties, Bronkhorst Company

[16] Lab VIEW®, program for data acquisition/conditioning and for automatic controlling http://sine.ni.com/np/app/flex/p/ap/global/lang/en/pg/1/docid/nav-77/

[17] VERHAERT space (now QinetiQ Space nv), company involved in the CIMEX-1 development, http://www2.qinetiq.com/home_qinetiq_space_nv.html

Annex 1: Requirements

Table 8: CIMEX-1 Requirements that were considered for the closed loop test campaign (information taken from [2])

Spec ID	Chapter	Title	Requirement Text
3138	4.2.2.4.1	Gas Flow Control	The gas system including pump shall allow to re-inject a defined gas flow rate at defined constant pressure into the fluid cell throughout the full fluid system pressure range.
3185	4.3.3.3.	Liquid Flow Rate: Pressure Range	The liquid flow rate shall be adjustable and measurable in the presences of at a system-pressure from 400 mbar to 1000 mbar.
3187	4.3.4.1	Range of Depth	The liquid depth shall be adjustable in the range from 1mm to 10 mm for 3D fluid cell with a minimum of 5 steps - 1 mm - 2 mm - 3 mm - 5 mm - 10 mm Note: Fall back option: reduction of liquid layer depth 1 to 5 mm (only 4 depths would be tested).
3191	4.3.5.1	Gas Flow Control: Adjustable Range	The gas flow rate shall be adjustable in a range from 10 to max 1000 ml/min throughout the full pressure range of the gas from 400 to 1000 mbar.
3192	4.3.5.2	Gas Flow Control: Accuracy	The gas flow rate shall be controlled with an accuracy of 2% of the maximum flow rate.
3193	4.3.5.3	Gas Flow Rate: Measurement Range	The gas flow rate shall be measurable in a range from 10 to max 1000 ml/min.
3194	4.3.5.4	Gas Flow Rate: Measurement Accuracy	The gas flow rate shall be measurable with an accuracy of 2% of the maximum measurement range.
3195	4.3.5.5	Gas Flow Rate: Calibration Data	Appropriate calibrations data with the given accuracy shall be supplied for the selected gas and gas mixture (with evaporated liquid).
3196	4.3.6	Pressure Control	The FCA shall provide pressure control of the gas and liquid system in order to maintain a constant pressure in the cell at the pressure set value while other parameters like gas flow rate, liquid depth and separation percentage are adjusted.
3197	4.3.6.1	Pressure Control Range	The set pressure shall be adjustable in a pressure range from 400 mbar to 1000 mbar.
3198	4.3.6.2	Pressure Control Accuracy	The pressure control accuracy shall be better than 2% of the maximum measurement range.
3199	4.3.6.3	Pressure Measurement Range	The pressure shall be measurable in a pressure range from 100 mbar to 1400 mbar.
3200	4.3.6.4	Pressure Measurement Accuracy	The pressure shall be measurable with and accuracy of 2% of the maximum pressure value.
3204	4.3.7.1	Temperature Control of Cell	The fluid cell temperature shall be regulated to a stable level by closed loop control.
3205	4.3.7.1.1	Temperature Range	The temperature setting range shall be 10°C up to 60°C.
3207	4.3.7.1.3	Temperature Absolute Accuracy	The absolute temperature measurement accuracy within the fluid cell shall be better than ± 0.25°C.
3208	4.3.7.1.5	Temperature Stability in Time	The relative temperature control stability in time in the fluid cell shall be better than ± 0.05 K in one hour.
3211	4.3.7.1.8	Condensation Prevention	The cell shall be maintained at a temperature higher than the saturation temperature corresponding to the vapour pressure to prevent condensation on the transparent walls.

Spec ID	Chapter	Title	Requirement Text
3229	4.3.7.4	Injected Liquid Temperature	The liquid reaching the cell shall be at the same temperature as the liquid temperature within the cell within a range of ± 0.05 K, to prevent that the liquid situation within the cell will be perturbed. Note: This can be achieved by controlling the liquid injection path (i.e. reservoir and pipe).
3267	4.3.14.1	Condenser/Separator Performance	The CSS shall deliver at outlet a gas phase composed of at least 50% of gas. 95% is considered as a target.
3268	4.3.14.2	Condenser/Separator Accuracy	The CSS shall allow to control the percentage of residual vapour in the gas phase to a desired value with an accuracy of 2% FS (mass ratio).
3269	4.3.14.3	Temperature Control	The condenser temperature shall be controlled by a feedback from the gas composition sensor (para. 4.3.13). This control shall be completely automatic and telecommanded.
3511	4.3.7.2	Temperature of Gas	The gas temperature shall be regulated to the same temperature as the cell (± 0.5°C).
3512	4.3.7.2.1	Temperature Range	The gas temperature range shall be 10°C up to 60°C.
3514	4.3.7.2.3	Absolute Accuracy	The absolute gas temperature measurement of the gas shall be better than ± 0.25 K.
3784	4.1.8.1.1	Number of Liquid Depths	The FCA shall be capable such that 5 different depths can be adjusted and measured. Note: CIMEX FCA verification by Review only.
3835	4.3.14.6	Worst Operating Conditions	Condenser shall be dimensioned to cope with worst operating conditions, i.e. low pressures (400 mbar) and high flowrates (1000ml/min).
3875	4.2.3.7.3	Material Fluid Compatibility	Surface materials, treatments and coatings shall demonstrate long term stability in material compatibility test against the selected liquids.

Annex 2: Conversion factor variation

In these two graphs it is possible to appreciate the small variations of the conversion factor for the MFC/MFC throughout all the pressure and temperature range. For more information, see the calculations performed in chapter 5.3.
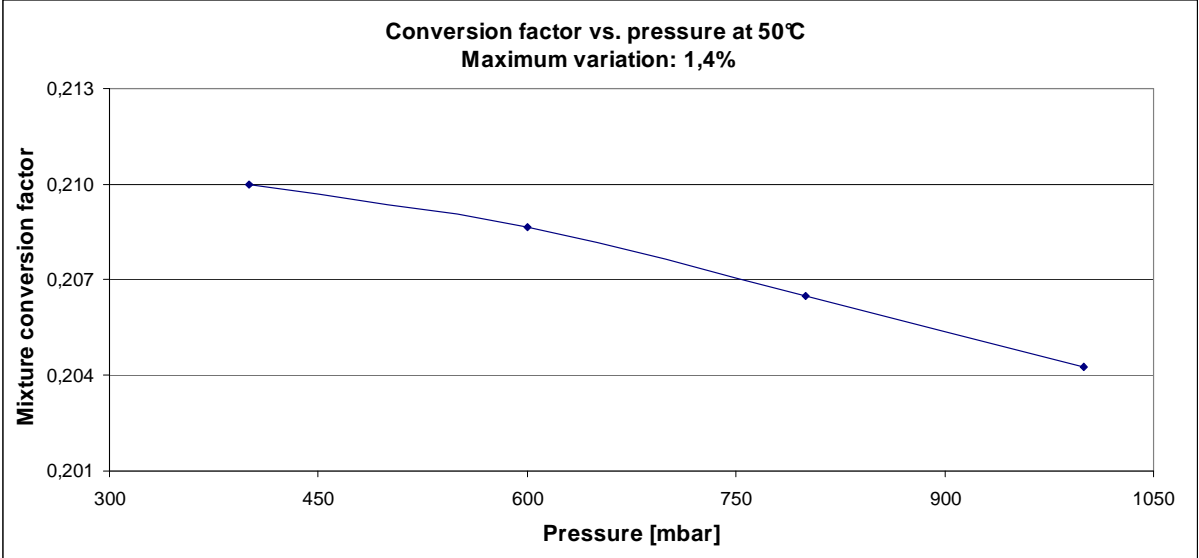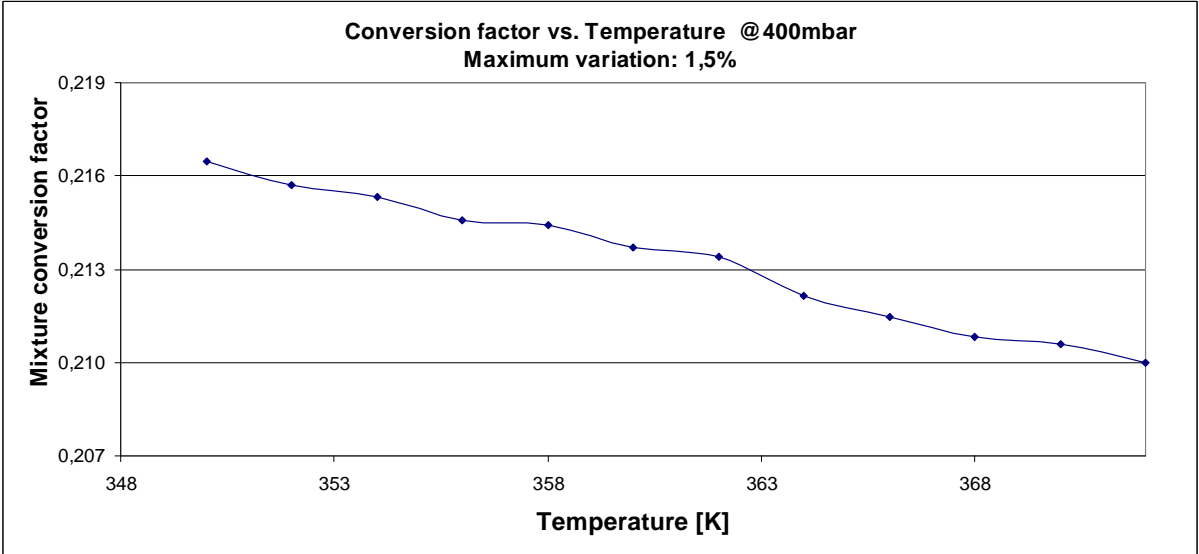
Annex 3: Data elaboration tables

Table 9: Data elaboration table

Test Nr.	Gas pressure	Cell Temp	Gas mass Flow rate (before cell) N2+Ethanol Calibrated	Gas pressure controller	Cell Temp	**Gas properties before the cell**						**Gas properties after the cell**				Evaporating liquid flow rate	Gas Conc before the cell	Gas Conc (%Vol)	Gas Conc after the cell	Percentage of the Gas Concentration reduced by the CSS
						Gas mass Flow rate (before cell) N2+Ethanol Calibrated	Gas Flow rate (before cell) N2 Calibrated	Conversion factor N2->(HFE+N2)$_{mix}$	Gas Flow rate (before cell) HFE-7100 Calibrated	Mixture density (before cell)	Gas Volumetric flow rate (before cell)	Gas mass Flow rate (after cell) N2+Ethanol Calibrated	Gas mass Flow rate (after cell) N2+Ethanol Calibrated	Gas mass Flow rate (after cell) N2 Calibrated	Gas Flow rate (after cell) HFE-7100 Calibrated					
	[mbar]	[°C]	[ml/min] n	[mbar]	[°C]	[mg/min]	[mg/min]	[ ]	[mg/min]	[mg/ml]	[ml/min]	[ml/min]	[mg/min]	[mg/min]	[mg/min]	mg/min	[%Mass]	[%Vol]	[%Mass]	[%]
1	1000	25	100	1	26	125	131	0,658	86	1,8	49	142	178	186	122	36	40,1	7	57,8	30,6
2	1000	25	400	1,06	26	500	524	0,694	364	1,7	218	505	631	662	459	96	36,2	6	49,5	26,8
3	1000	25	800	1,06	26	1000	1048	0,694	728	1,7	437	877	1097	1149	798	70	36,2	6	41,8	13,4
4	1000	25	1000	1,07	26	1250	1310	0,694	910	1,7	546	1078	1348	1413	981	71	36,2	6	40,8	11,3
5	1000	25	900	1,07	26	1125	1179	0,694	819	1,7	491	995	1244	1304	905	86	36,2	6	42,3	14,4
6	1000	25	1000	1,07	26	1250	1310	0,625	819	1,8	444	1075	1344	1409	880	61	43,6	8	47,6	8,3
7	1000	25	400	1,07	26	498	522	0,625	326	1,8	177	470	588	616	385	59	43,6	8	52,3	16,5
9	1000	25	800	1,12	25,9	999	1047	0,694	727	1,7	436	870	1088	1140	791	65	36,2	6	41,4	12,6
10	1000	30	100	1,05	29,9	124	130	0,658	85	1,8	49	150	188	197	129	44	40,1	7	60,5	33,7
11	1000	30	400	1,03	29,9	500	524	0,658	345	1,8	196	480	600	629	414	69	40,1	7	50,1	19,9
12	1000	30	800	1,01	29,9	1002	1050	0,658	691	1,8	393	880	1100	1153	759	68	40,1	7	45,5	11,8
13	1000	30	900	1	29,9	1125	1179	0,625	737	1,8	399	1000	1250	1310	819	82	43,6	8	49,3	11,4
14	1000	40	100	1,08	40,2	125	131	0,394	52	2,8	18	190	238	249	98	46	67,6	19	83,0	18,5
15	1000	40	400	1,04	40,1	501	525	0,408	214	2,7	78	535	669	701	286	72	66,1	18	74,6	11,4
16	1000	40	100	1,06	40,2	125	131	0,394	52	2,8	18	190	238	249	98	46	67,6	19	83,0	18,5
17	1000	40	400	1	40,8	563	590	0,368	217	3,0	72	590	738	773	285	68	70,3	21	77,3	9,1
18	1000	40	900	0,99	40,6	1127	1181	0,394	465	2,8	165	1075	1344	1409	555	90	67,6	19	72,8	7,2
19	1000	50	800	0,97	49,9	1000	1048	0,368	386	3,0	129	983	1229	1288	474	88	70,3	21	75,8	7,3

Test Nr.	Gas pressure	Cell Temp	Gas mass Flow rate (before cell) N2+Ethanol Calibrated	Gas pressure controller	Cell Temp	Gas properties before the cell						Gas properties after the cell				Evaporating liquid flow rate	Gas Conc before the cell	Gas Conc (%Vol)	Gas Conc after the cell	Percentage of the Gas Concentration reduced by the CSS
						Gas mass Flow rate (before cell) N2+Ethanol Calibrated	Gas Flow rate (before cell) N2 Calibrated	Conversion factor N2->(HFE+N2)$_{mix}$	Gas Flow rate (before cell) HFE-7100 Calibrated	Mixture density (before cell)	Gas Volumetric flow rate (before cell)	Gas mass Flow rate (after cell) N2+Ethanol Calibrated	Gas mass Flow rate (after cell) N2+Ethanol Calibrated	Gas mass Flow rate (after cell) N2 Calibrated	Gas Flow rate (after cell) HFE-7100 Calibrated					
	[mbar]	[°C]	[ml/min n]	[mbar]	[°C]	[mg/min]	[mg/min]	[ ]	[mg/min]	[mg/ml]	[ml/min]	[ml/min]	[mg/min]	[mg/min]	[mg/min]	[mg/min]	[%Mass]	[%Vol]	[%Mass]	[%]
20	1000	50	400	0,97	50,5	500	524	0,357	187	3,1	60	590	738	773	276	89	71,5	22	80,7	11,4
21	1000	25	1000	1,03	25,5	1248	1308	0,625	817	1,8	443	1083	1354	1419	886	70	43,6	8	48,0	9,2
21	800	25	800	0,8	26,2	1007	1055	0,694	732	1,3	549	1135	1419	1487	1032	300	36,2	6	54,8	33,9
23	500	25	1000	0,52	26,2	1250	1310	0,625	819	0,9	888	1112	1390	1457	910	92	43,6	8	49,3	11,5
24	600	40	800	0,63	39,6	1003	1051	0,456	479	1,5	324	1020	1275	1337	610	130	61,1	15	69,4	12,0
25	600	45	800	0,65	40,6	1000	1048	0,495	519	1,4	377	1070	1338	1402	694	175	57,1	13	67,9	16,0
26	800	45	800	0,78	45,3	1000	1048	0,517	542	1,8	308	1116	1395	1462	756	214	54,8	12	67,6	18,9
28	900	50	800	0,9	48,5	1000	1048	0,517	542	2,0	273	1002	1253	1313	678	137	54,8	12	63,9	14,2
29	900	25	800	0,95	24,5	1000	1048	0,566	593	1,8	326	877	1097	1149	651	57	49,7	10	54,1	8,2
30	800	25	800	0,8	24,6	1000	1048	0,540	566	1,7	335	892	1115	1169	632	65	52,4	11	57,3	8,6
31	800	25	400	0,8	24,7	500	524	0,540	283	1,7	168	474	593	621	336	52	52,4	11	59,8	12,4
32	800	25	200	0,8	24,7	250	262	0,625	164	1,5	111	265	331	347	217	53	43,6	8	57,4	24,1
33	600	25	800	0,6	24,8	1000	1048	0,540	566	1,3	447	896	1120	1174	634	68	52,4	11	57,5	8,9
34	600	25	400	0,6	25	500	524	0,540	283	1,3	223	480	600	629	340	57	52,4	11	60,3	13,2
35	600	25	200	0,6	25	250	262	0,475	124	1,4	87	260	325	341	162	37	59,2	14	68,6	13,7
36	500	25	400	0,5	25,1	500	52 4	0,517	271	1,1	246	480	600	629	325	54	54,8	12	62,3	12,1
37	1000	25	200	1,02	25,2	249	261	0,658	172	1,8	98	253	316	332	218	47	40,1	7	52,9	24,2
38	800	25	200	0,81	25,3	250	262	0,566	148	1,6	92	250	313	328	185	37	49,7	10	59,8	16,8
39	800	25	800	0,83	25,3	1000	1048	0,625	655	1,5	444	870	1088	1140	712	57	43,6	8	48,2	9,4
40	900	40	800	0,93	39,3	1000	1048	0,625	655	1,7	394	992	1241	1300	812	157	43,6	8	54,5	20,0

						Gas properties before the cell						Gas properties after the cell								
Test Nr.	Gas pressure	Cell Temp	Gas mass Flow rate (before cell) N2+Ethanol Calibrated	Gas pressure controller	Cell Temp	Gas mass Flow rate (before cell) N2+Ethanol Calibrated	Gas Flow rate (before cell) N2 Calibrated	Conversion factor N2->(HFE+N2)$_{mix}$	Gas Flow rate (before cell) HFE-7100 Calibrated	Mixture density (before cell)	Gas Volumetric flow rate (before cell)	Gas mass Flow rate (after cell) N2+Ethanol Calibrated	Gas mass Flow rate (after cell) N2+Ethanol Calibrated	Gas mass Flow rate (after cell) N2 Calibrated	Gas Flow rate (after cell) HFE-7100 Calibrated	Evaporating liquid flow rate	Gas Conc before the cell	Gas Conc (%Vol)	Gas Conc after the cell	Percentage of the Gas Concentration reduced by the CSS
	[mbar]	[°C]	[ml/min]n	[mbar]	[°C]	[mg/min]	[mg/min]	[ ]	[mg/min]	[mg/ml]	[ml/min]	[ml/min]	[mg/min]	[mg/min]	[mg/min]	[mg/min]	[%Mass]	[%Vol]	[%Mass]	[%]
41	800	45	800	0,8	45,4	1000	1048	0,566	593	1,6	367	1050	1313	1376	779	185	49,7	10	61,7	19,4
42	1000	45	800	1,05	45,2	1000	1048	0,594	623	1,9	322	1020	1275	1337	794	171	46,8	9	58,3	19,7
46	500	25	200	0,45	24,9	250	262	0,456	120	1,2	97	285	356	373	170	51	61,1	15	72,7	16,0
47	500	25	400	0,45	25	500	524	0,439	230	1,3	180	520	650	681	299	69	62,9	16	71,5	12,0
48	400	25	200	0,42	25,3	250	262	0,475	124	1,0	131	335	419	439	208	84	59,2	14	75,6	21,8
49	400	25	400	0,44	25,3	500	524	0,408	214	1,1	195	540	675	708	289	75	66,1	18	74,9	11,7
50	400	25	800	0,45	25,4	1000	1048	0,408	427	1,1	390	960	1200	1258	513	85	66,1	18	71,8	7,9

Gas pressure	Cell Temp	Gas Flow rate	Gas Volumetric Flow rate (before the cell)	Condenser temperature	Gas Concentration after the CSS	Gas Concentration after the CSS	Gas Concentration before the CSS	*CSS efficiency*
[mbar]	[°C]	[ml/min]$_n$	[ml/min	[°C]	[%Vol]	[%Mass]	[%Mass]	[%]
400	25	210	131	-10	14	59	94	37
400	25	419	195	-10	18	66	96	31
400	25	838	390	-10	18	66	98	33
500	25	419	180	-10	16	63	71	11
600	40	838	60	-10	13	57	68	16
600	25	838	447	-10	11	52	57	8
600	25	419	223	-10	11	52	60	13
800	25	838	335	-10	11	52	57	8
800	25	419	168	-10	11	52	60	13
800	25	210	111	-10	8	44	57	23
800	45	838	367	-10	10	50	62	20
900	25	838	326	-10	10	50	54	8
1000	30	105	49	-20	7	40	60	33
1000	30	419	196	-20	7	40	50	20
1000	30	943	399	-20	8	44	49	11
1000	40	105	18	-20	19	68	83	19
1000	40	943	165	-20	19	68	73	7
1000	25	210	98	-20	7	40	53	24

Table 10: CSS performance: elaboration table

Annex 4: Conversion factor calculation table for the MFM and MFC

VAPOR TABLE (*)							CONVERSION FACTOR CALCULATIONS					
T(K)		Pressure (bar)					Pressure =0,4bar					
		0.40	0.60	0.80	1.00		Cp(N2)	Cp(HFE)	N2 density	HFE Density	C_N2>HFE	C_MIX
							[KJ/(Kg K]	[KJ/(Kg K]	[Kg/m3]	[Kg/m3]	[]	[]
352	d	3.47	5.25	7.07	8.93		1.0409	0.9500	0.38	3.47	0.1209	0.579
	V	71.78	47.38	35.18	27.86							
	U	57.976	57.914	57.851	57.789							
	H	60.847	60.757	60.666	60.575							
	S	206.23	202.68	200.11	198.07							
354	d	3.45	5.22	7.03	8.87		1.0410	0.9520	0.38	3.45	0.1207	0.578
	V	72.22	47.68	35.41	28.04							
	U	58.433	58.372	58.310	58.248							
	H	61.322	61.233	61.143	61.052							
	S	207.58	204.03	201.46	199.42							
--------	--	---------	---------	---------	---------		-------------	--------------	--------------	-----------------	----------------	---------
366	d	3.33	5.03	6.77	8.53		1.0416	0.9740	0.37	3.33	0.1182	0.573
	V	74.82	49.46	36.77	29.16							
	U	61.214	61.156	61.098	61.039							
	H	64.206	64.123	64.039	63.955							
	S	215.59	212.06	209.51	207.49							
368	d	3.31	5.00	6.73	8.48		1.0417	0.9780	0.37	3.31	0.1178	0.572
	V	75.25	49.75	37.00	29.34							
	U	61.683	61.626	61.568	61.511							
	H	64.693	64.611	64.528	64.445							
	S	216.92	213.39	210.84	208.82							
370	d	3.29	4.97	6.69	8.43		1.0418	0.9800	0.36	3.29	0.1177	0.572
	V	75.69	50.05	37.22	29.52							
	U	62.154	62.098	62.041	61.984							
	H	65.182	65.100	65.019	64.936							
	S	218.24	214.71	212.17	210.15							

LEGEND	
T	Temperature (K)
d	Vapour density (kg/m3)
U	Internal Energy (kJ/Mol)
H	Enthalpy (kJ/Mol)
S	Entropy (J/Mol.K)

Table 11: MFM and MFC Conversion Factor Calculation

(*): *the vapor table of this page is only a part of the one that was used for all the calculations.*

Annex 5: Example of C_p calculation using the pressure-enthalpy chart
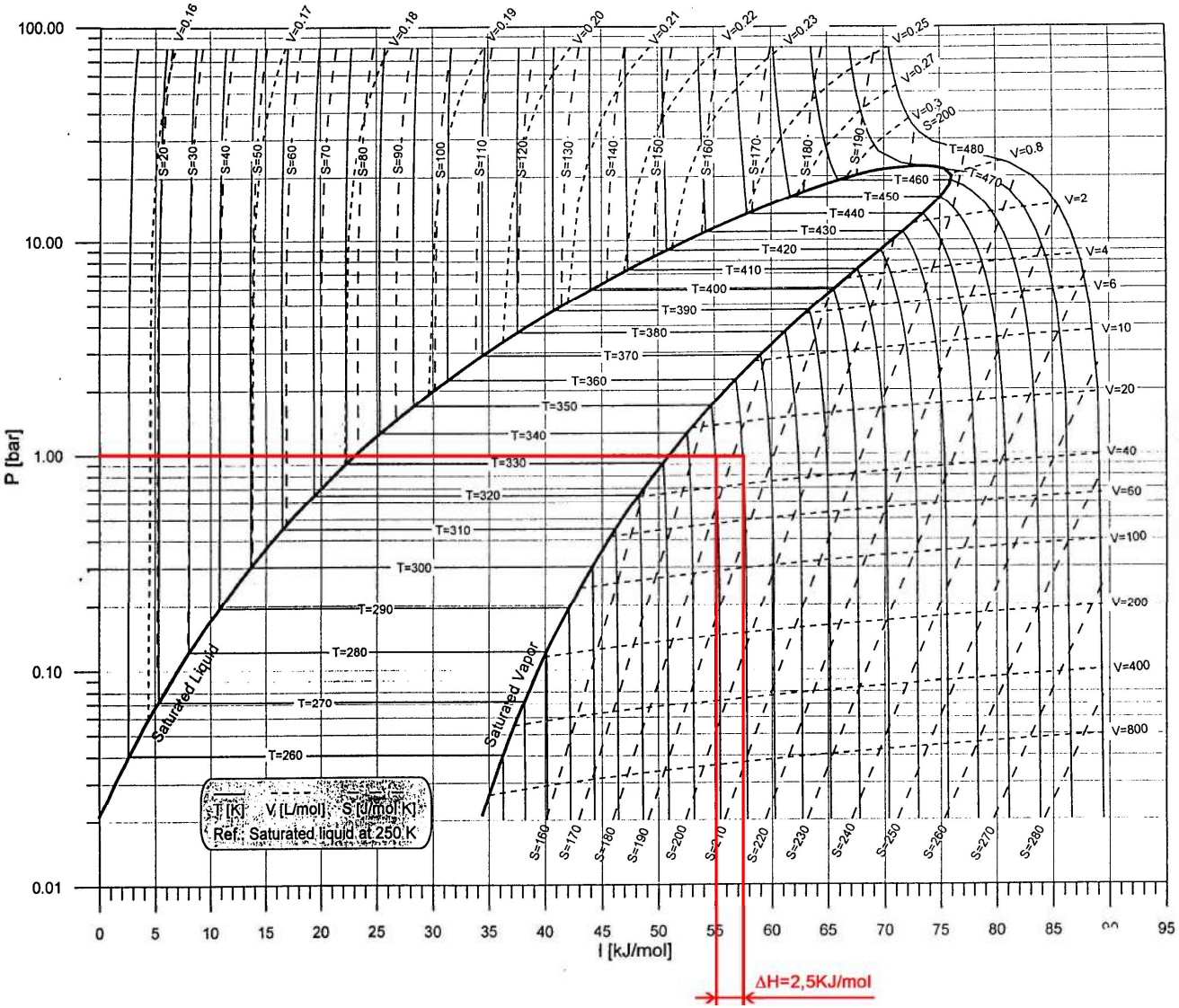
$\Delta T = 10K$
$\Delta H = 2{,}5$ kJ/mol
$M_{HFE} = 250$ kg/kmol

$C_p = \partial h / \partial T \approx (2{,}5*1000)/(250*10)$
≈ 1 kJ/kg*K

Note:

If other combinations of temperature and pressure were considered, the enthalpy difference would remain pretty much constant, and so Cp.

Annex 6: Datasheets

In this appendix the datasheets of the main components are reported following the subsequent order:

- HFE-7100 Operative Liquid from 3M Novec
- Mrz-4661 Liqud Pump from HNP Mikrosysteme GmbH
- Low -ΔP -FLOW Meter/Controller from Bronkhorst
- Pressure controller from Bronkhorst
- ETM-375 Pressure Sensor from Kulite

3M

Novec™
Engineered Fluid
HFE-7100
for Heat Transfer

A New Engineered Fluid
with Unique Heat Transfer Properties

3M™ Novec™ Engineered Fluid HFE-7100
is a clear, colorless, nonflammable and low-odor
dielectric fluid with low toxicity and favorable environmental properties. It is ideal for
use in a variety of heat transfer applications.

Semiconductor
Novec fluid HFE-7100 is the first of a new generation of low-GWP
(Global Warming Potential) dielectric fluids with many of the properties of
perfluorinated liquids. These properties permit its use in many traditional
PFC applications such as thermal management in dry etchers, ion implanters and
thermal shock test equipment.

Industrial/Pharmaceutical
This Novec fluid is an excellent alternative to methylene chloride, trichloroethylene, d-
limonene, silicone oils, chlorofluorocarbons and hydrocarbons. The low temperature
properties are ideal for applications in freeze drying, reaction control, manufacturing
and general process control.

Electronic Cooling
HFE-7100 fluid is compatible with most electronic components. It is being used for
direct contact cooling of computers, transformers and fuel cells.

Food Refrigeration
The unique low temperature properties of HFE-7100 fluid make it ideal for use in
secondary refrigeration systems. Low viscosity translates into high heat transfer
coefficients and low pumping power requirements. Glide matching with this Novec fluid
increases heat transfer efficiency and reduces frost formation.

Material Description

Ingredients	Composition of HFE-7100
Appearance	Clear, colorless
Methoxy-nonafluorobutane[1]	99.5% minimum
Non-volatile residue (NVR)	1.0 ppm maximum

[1] HFE-7100 fluid ($C_4F_9OCH_3$) consists of two inseparable isomers with essentially identical
properties. These are $(CF_3)_2CFCF_2OCH_3$ (CAS No. 163702-08-7) and $CF_3CF_2CF_2CF_2OCH_3$
(CAS No. 163702-07-6).

Properties	HFE-7100
Molecular Weight, g/mol	250.0
Flash Point	None
Freeze Point, °C	-135
Boiling Point, °C	61
Critical Temperature, °C	195.3
Critical Pressure, MPa	2.23
Critical Density, kg/m³ (estimated)	555
Heat of Vaporization @ B.P., kJ/kg	111.6
Surface Tension, dynes/cm	13.6
Solubility of Water in Fluid, ppm by weight	95
Solubility of Air in Fluid, volume air @ 1 atm per volume fluid	53%
Typical Dielectric Strength (0.1 in. gap), kV (RMS)[1]	28
Dielectric Constant, 100 Hz – 10 MHz	7.39
Volume resistivity, ohm-cm	3.29×10^9

[1] The dielectric strength of virgin HFE-7100 fluid is specified as 20 kV minimum. As dielectric properties can be degraded by the presence of dissolved plasticizer, particulate or water, when dielectric properties are critical, careful attention should be paid to material compatibility and moisture content.

Chart 1

HFE-7100 Kinematic Viscosity

Viscosity (cSt) vs. Temperature (°C)
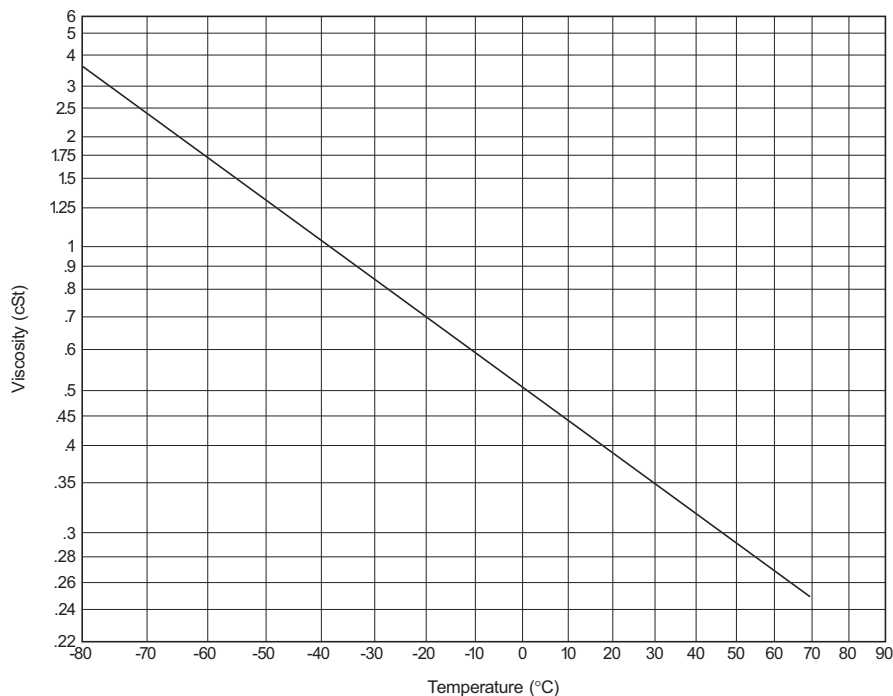
Chart 2

HFE-7100 Liquid Density
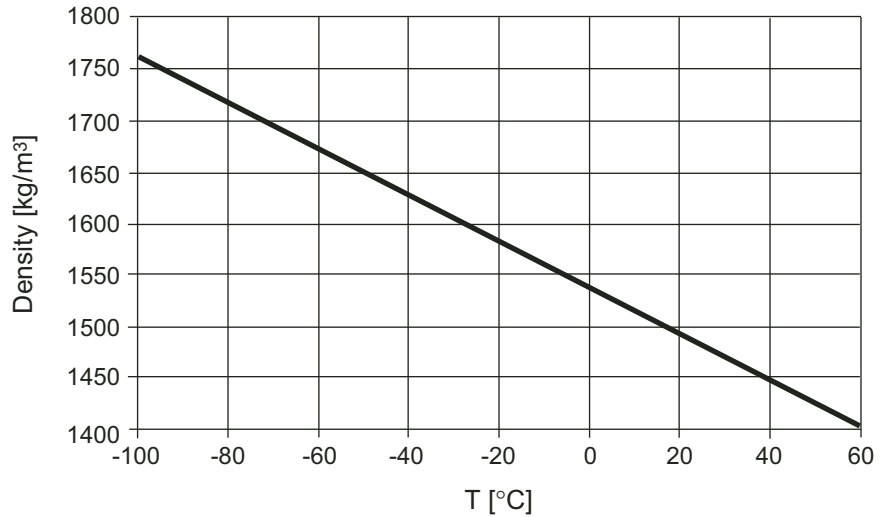
Liquid Density [kg/m³] = -2.2690*T [°C] + 1538.3

Chart 3

HFE-7100 Thermal Conductivity
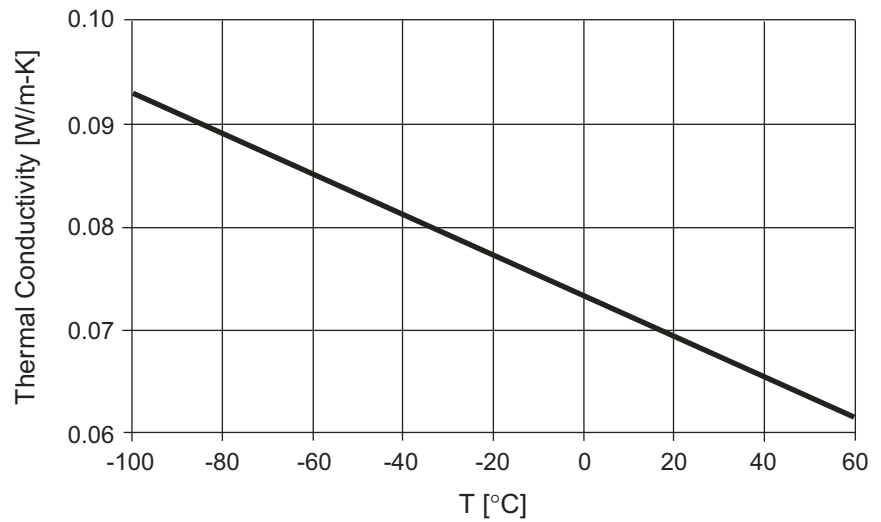
Thermal Conductivity [W/m-K] = -0.00019548*T[°C] + 0.073714

3

Micro Annular Gear Pump mzr®-4661
Magnetic Hermetic Series

Product Launch Hannover Fair H2FC-Fair 2011

- **Hermetic design**
  pump without shaft seal

- **Magnetic drive**
  inner magnet system driven by rotating magnetic field

- **Integrated controller**
  supply voltage 24 V DC,
  speed control by analog input 0-10 V

- **Compact dimensions**
  diameter 22 mm, length 69 mm

- **Long service life**
  wear-resistant, ultra-hard materials

novelty

The magnetic drive of rotary displacement pumps in combination with a liquid separating cup will be used for pump technologies if safety requirements as well as requirements regarding the handling of liquids demand a leak-free pump construction without a shaft seal.

HNP Mikrosysteme implements this functionality in the new magnetic driven, hermetic series (MH) of micro annular gear pumps. The mzr-4661 is equipped with a powerful inner magnet system and an integrated speed control. This first pump of the MH series reaches a precise and pulse less volume flow up to 72 ml/min as well as a pressure of 6 bar. Especially, the compact dimensions have to be outlined. The pump has a diameter of 22 mm and a length of 69 mm.

The compact dimension of the pump is achieved by a completely new product structure (pat. pend.) and an optimal design matching with the integrated drive system. The materials in contact with liquid of the current style available are stainless steel, ceramics and coated NdFeB-magnets. A pump featuring biocompatible materials for use in medical applications is under development.

Applications for this magnetic hermetic pump are typically crystallizing, oxygen sensitive or outgassing liquids as well as fuel cells, AdBlue delivery or dialysis. All areas, where avoidance of leakage is an important criterion this new pump can be used and prove its superiority regarding to long service life.

06/11

Applications

– Fuel cells
– AdBlue
– Dialysis

Technical data

Flow rate	4.8 – 72 ml/min
Displacement volume	12 µl
Max. system pressure	6 bar (inlet pressure+differential pressure)
Differential pressure range	0 – 5 bar (73 psi)
Pulsation	6 %
Operating temperature range	-15 … +60 °C (-40 … +60 °C *)
Viscosity range	0.3 – 100 mPas
Speed range	400 – 6000 rpm
Fluid connection	slip fittings with outside diameter 2 mm
Wetted parts	stainless steel: 1.4305, 1.4404, ceramics, tungsten carbide Ni-based, epoxy resin, nickel; static seals: FPM
Motor	canned BLDC-motor, 24 V DC, 8.9 W
Control	integrated speed controller
Interface	0–10 V
Electrical connection	6-pole connector
Measurements	diameter 22 mm, length 68.5 mm
Weight	approx. 100 g

* Customized solution on request.

Measurements
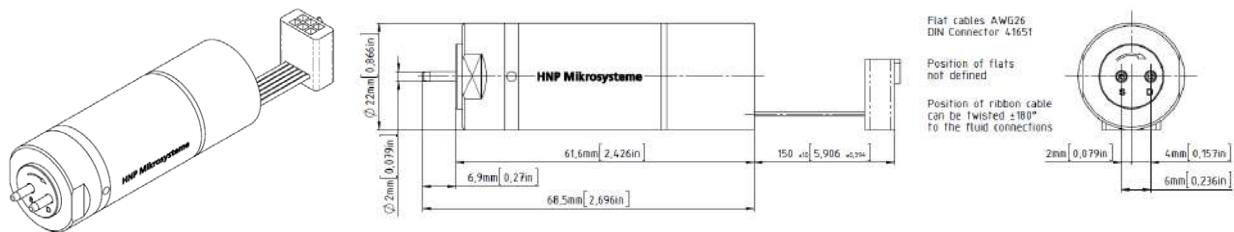
Subject to technical changes.

Flow charts

Liquid water

Liquid oil
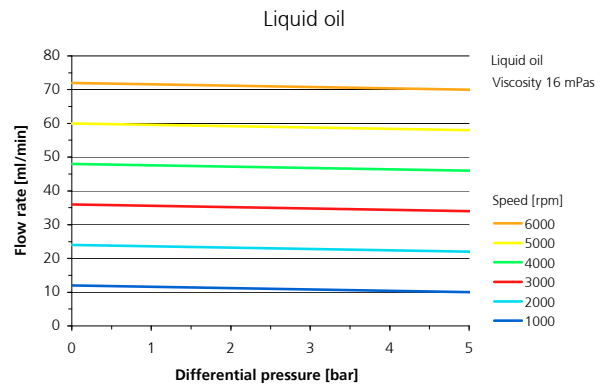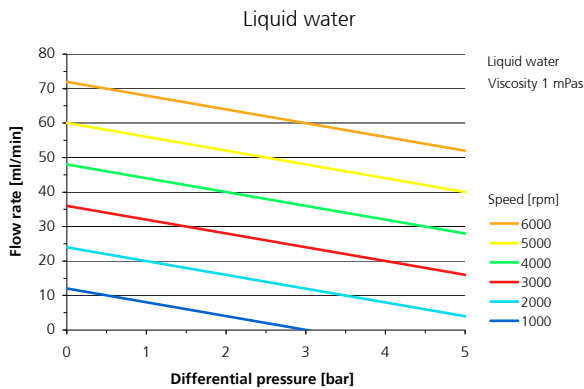
Item number

14 01 20 01   low pressure series pump mzr-4661 with canned BLDC-motor

Accessories

Liquid supply accessories   tubes, filters etc.

LOW-ΔP-FLOW

Mass Flow Meters/Controllers for low pressure drop or corrosive gas service

> Introduction

Bronkhorst High-Tech B.V., the European market leader in thermal Mass Flow Meters/Controllers and Electronic Pressure Controllers, has more than 25 years experience in designing and manufacturing precise and reliable measurement and control devices. With a wide range of instruments, Bronkhorst High-Tech offers innovative solutions for many different applications in many different markets. The instruments are made to customers' specification, in various styles, suitable for use in laboratory, industrial and hazardous areas, in such diverse applications as semiconductor and analytical installations, to name but two.

> LOW-ΔP-FLOW series for low pressure drop or corrosive gases

In a number of applications for measuring and controlling gas flows there is only little differential pressure available and/or allow-able. These are the applications for which Bronkhorst High-Tech developed the LOW-ΔP-FLOW series, in which the flow resistance is minimised by using a large bore capillary (thermal bypass sensor) in combination with a cylindrical flow splitter (laminar flow element). Based on this concept, mass flow capacities between $0…10$ ml_n/min and $0…1000$ m^3_n/h can be measured. At a flow up to 2 l_n/min a pressure drop of less than 1 mbar is required.

Furthermore the larger flow channels minimise the risk of clogging and facilitate the cleaning and purging of these LOW-ΔP-FLOW instruments, which will contribute to a significantly longer lifetime when the instruments are used on corrosive gas service. All fluid wetted parts are of electro-polished stainless steel. Optionally the flow meter body, sensor and flow element can be supplied in Hastelloy or Monel.

> For laboratory or industrial conditions

The LOW-ΔP-FLOW series are derived from the laboratory style EL-FLOW series, however they can also be supplied with a rugged IP65 (dust and waterproof) IN-FLOW housing, suitable for industrial environments. The latter are also ATEX Category 3, approved for use in Zone 2 hazardous areas. In addition to the standard analog I/O-signals and the RS232 connection, there is the possibility of integrating an interface board with DeviceNet™, Profibus-DP®, Modbus-RTU or FLOW-BUS protocol.

> Mass flow control with low differential pressure

The control of mass flow with small pressure difference comprises the LOW-ΔP-FLOW Mass Flow Controllers in compact construction (model series F-200/201/202). The integrated proportional, electromagnetic control valves of these MFC's have extremely fast and smooth control characteristics. Depending on the operating properties, the maximum flow in these models is $1…50$ l_n/min air-equivalent.

For the control of higher flow rates at very low differential pressures Bronkhorst High-Tech have devised special control valves with pressure compensation bellows (series F-004). These control valves are close-coupled to the flow meter while the electric PI-control function is an integral part of the flow meter. This F-004 valve has proven to be an excellent alternative to large, slow and expensive servo driven valves.

> LOW-ΔP-FLOW features

- very low pressure drop
- suitable for corrosive gases
- wetted parts: electro-polished stainless steel; other on request
- also available with IP65 housing, ATEX approval Cat.3, Zone 2
- analog and digital (fieldbus) communication
- alarm and counter functions

Bronkhorst®
HIGH-TECH

> Technical specifications

Measurement / control system

Accuracy (incl. linearity)	: ± 1% FS (of Full Scale)
Turndown	: 1 : 50 (2 … 100%)
Repeatability	: < 0,2% Rd (of Reading)
Settling time (controller)	: standard: 2…3 seconds
Control stability	: < ±0,1% FS (typical for 1 l_n/min N2)
Operating temperature	: -10…+70°C
Max. operating pressure	: 10 bar
Temperature sensitivity	: 0,1% FS/°C;
	for ATEX Cat.3 max. 50°C
Pressure sensitivity	: 0,1%/bar typical N2
Leak integrity	: tested < 2 x 10^{-9} mbar l/s He
Mounting position	: horizontal
Warm-up time	: 30 min. for optimum accuracy;
	2 min for accuracy ± 2% FS

Mechanical parts

Material (wetted parts)	: stainless steel, other on request
Process connections	: compression type or face seal
	couplings; wafer type on series F-106;
	DIN or ANSI flanges on series F-107
Seals	: standard: Viton
	options: EPDM, Kalrez (FFKM)
Ingress protection (housing)	: IP40 or IP65

Electrical properties

Power supply	: +15…24 Vdc
Power consumption	: meter: 70 mA;
	controller: max. 320 mA;
	add 50 mA for Profibus, if applicable
Analog output/command	: 0…5 (10) Vdc or 0 (4)…20 mA
	(sourcing output)
Digital communication	: standard: RS232
	options: Profibus-DP®, DeviceNet™,
	Modbus-RTU, FLOW-BUS
Electrical connection **IP40 configuration**	
Analog/RS232	: 9-pin D-connector (male);
Profibus-DP	: bus: 9-pin D-connector (female);
	power: 9-pin D-connector (male);
DeviceNet™	: 5-pin M12-connector (male);
Modbus-RTU/FLOW-BUS	: RJ45 modular jack
Electrical connection **IP65 configuration**	
Analog/RS232	: 8 DIN (male);
Profibus-DP®	: bus: 5-pin M12 (female);
	power: 8 DIN (male)
DeviceNet™	: 5-pin M12 (male)
Modbus-RTU/FLOW-BUS	: 5-pin M12 (male)

Technical specifications subject to change without notice.

> Models and flow ranges (based on Air)

Mass Flow Meters (MFM)

Model	min. flow	max. flow
F-100D/F-100DI	0,2…10 ml$_n$/min	0,44…22 ml$_n$/min
F-101D/F-101DI	0,42…21 ml$_n$/min	0,042…2,1 l$_n$/min
F-101E/F-101EI	0,028…1,4 l$_n$/min	0,24…12 l$_n$/min
F-102E/F-102EI	0,17…8,5 l$_n$/min	1…50 l$_n$/min
F-103E/F-103EI	0,9…45 l$_n$/min	4…200 l$_n$/min
F-106Z/F-107Z	0,2…10 m³$_n$/h	20…1000 m³$_n$/h

Mass Flow Controllers (MFC)

Model	min. flow	max. flow
F-200DV/F-200DI [1]	0,2…10 ml$_n$/min	0,44…22 ml$_n$/min
F-201DV/F-201DI [1]	0,42…21 ml$_n$/min	0,042…2,1 l$_n$/min
F-201EV/F-201EI [1]	0,028…1,4 l$_n$/min	0,24…12 l$_n$/min
F-202EV/F-202EI [1]	0,17…8,5 l$_n$/min	1…50 l$_n$/min

[1] Kv-max = 6,6 x 10^{-2}

Control Valve series F-004

	F-004AC/F-004AI	F-004BI
Kv-value	0,3	1,0
Max. operating press ure	10 bara	10 bara
Min. P (approx.)	1 mbard	1 mbard
Max. P	5 bard	5 bard
Max. power (at 15 Vdc)	3,5 Watt	3,5 Watt
Protection class	F-004AC: IP40	IP65
	F-004AI: IP65	

Models F-004BI and F-004AC bellows operated control valves

EL-PRESS

Digital Electronic Pressure Meters and Controllers

> Introduction

Bronkhorst High-Tech B.V. the European market leader in thermal Mass Flow Meters/Controllers and Electronic Pressure Controllers, has 30 years experience in designing and manufacturing precise and reliable measurement and control devices. With a wide range of instruments, Bronkhorst High-Tech offers innovative solutions for many different applications in many different markets. The instruments are made to customers' specification, in various styles, suitable for use in laboratory, industrial and hazardous areas, in such diverse applications as semiconductor and analytical installations, to name but two.

> EL-PRESS series Pressure Meters and Controllers

The EL-PRESS series electronic Pressure Meters and Controllers have a well-proven compact thru-flow design and are available in pressure ranges from 2…100 mbar up to 8…400 bar, both in absolute and relative (gauge) pressure. A differential pressure transducer can also be supplied in the ranges of 2…100 mbar up to 0,3…15 bar. The pressure controller performs with high accuracy and repeatability and should be specified for forward or backward pressure control.

> State of the art digital design

Todays EL-PRESS series are equipped with a diaphragm type piezoresistive pressure sensor and a digital pc-board as standard and offer high accuracy, stability and reliability. The basic digital pc-board contains all of the general functions needed for measurement and control. In addition to the standard RS232 output, the instruments also offer analog I/O. As an option, an integrated interface board provides DeviceNet™, PROFIBUS-DP®, Modbus-RTU or FLOW-BUS protocols. The latter is a fieldbus based RS485, specifically designed by Bronkhorst High-Tech for their mass flow and pressure metering and control solutions, and with which the company already has over ten years of experience with digital communication.

> Pressure Controllers for every application

The control valve can be furnished as integral part of an EL-PRESS Pressure Controller (EPC), or as a separate component. It is a proportional, electromagnetic control valve with extremely fast and smooth control characteristics. With reference to the specific field of application there are different series of control valves. There is a standard direct acting valve for common applications, a pilot operated valve for high flow rates, the so-called Vary-P valve that can cope with up to 400 bar ΔP and a bellows valve for applications with very low differential pressure.

> EL-PRESS features

◆ High accuracy and repeatability
◆ High pressure capability up to 400 bar
◆ Stable control even at varying process volumes
◆ Optional metal sealed and downported constructions
◆ Analog I/O signals: 0…5(10) V / 0(4)…20 mA
◆ Digital communication: RS232, DeviceNet™, PROFIBUS-DP®, Modbus-RTU or FLOW-BUS

> Fields of application

◆ Semiconductor processing
◆ Gas and liquid chromatography
◆ Vapour pressure control in MOCVD processes
◆ Protective gas pressure control in extrusion moulding processes
◆ Autoclave / reactor pressure control

Bronkhorst®
HIGH-TECH

> Technical specifications

Measurement / control system

Accuracy	: ±0,5% of full scale (FS)
(incl. linearity and hysteresis)	
Pressure rangeability	: Measurement: 1 : 50 (2 …100%)
	Control (with flow range 1 : 50)
	P-602CV/P-602CM/P-612CV 1 : 20
	P-702CV/P-702CM/P-712CV 1 : 5
Repeatability	: ≤ 0,1% RD
Response time sensor	: 2 msec
Control stability	: ≤ ±0,05% FS (typical for 1 l_n/min N_2
	at specified process volume)
Operating temperature	: -10…+70°C
Temperature sensitivity	: 0,1% FS/°C
Leak integrity	: tested $< 2 \times 10^{-9}$ mbar l/s He
Attitude sensitivity	: $<$ 0,3 mbar (abs./rel. sensors);
(at 90° change)	$<$ 6 mbar (dif. sensors)
Warm-up time	: negligible

Mechanical parts

Material (wetted parts)	: stainless steel 316L or comparable
Surface quality (wetted parts)	: Ra = 0,8 μm typical
Process connections	: compression type or face seal
	couplings
Seals	: standard: Viton
	options: EPDM, FFKM (Kalrez)
Ingress protection (housing)	: IP40

Electrical properties

Power supply	: +15…24 Vdc
Power consumption	: meter: max 115 mA;
	controller: max. 385 mA;
	add 50 mA for Profibus, if applicable
Analog output/command	: 0…5 (10) Vdc,
	min. load impedance $>$ 2 kOhm;
	0 (4)…20 mA (sourcing output),
	max. load impedance $<$ 375 Ohm
Digital communication	
Standard (9-pin D-conn. male)	: RS232
By optional interface board	: Profibus-DP®, DeviceNet™,
	Modbus-RTU, FLOW-BUS
Electrical connection	
Analog/RS232	: 9-pin D-connector (male);
Profibus-DP®	: bus: 9-pin D-connector (female);
	power: 9-pin D-connector (male);
DeviceNet™	: 5-pin M12-connector (male);
Modbus-RTU/FLOW-BUS	: RJ45 modular jack

Calibration

References verified by an ISO 17025 calibration laboratory, directly traceable to Dutch and international standards.

Technical specifications and dimensions subject to change without notice.

> Models and pressure ranges

Electronic Pressure Transducers (EPT)

Models, elast. sealed		Pressure ranges	
P-502C	(absolute/relative)	min. 2…100 mbar	max. 1,28…64 bar
P-512C	(absolute/relative)		max. 2…100 bar
P-522C	(absolute/relative)		max. 4…200 bar
P-532C	(absolute/relative)		max. 8…400 bar
P-506C	(differential)	min. 2…100 mbar	max. 0,3…15 bar

Model, metal sealed		Pressure ranges	
P-502CM	(absolute/relative)	min. 7…350 mbar	max. 1,28…64 bar

Electronic Pressure Controllers (EPC)

Models, elast. sealed		Pressure ranges (abs/rel)	
P-602CV[1]	(forward pressure control)	min. 5…100 mbar	max. 3,2…64 bar
P-612CV[1]	(forward pressure control)		max. 5…100 bar
P-702CV[1]	(back pressure control)	min. 20…100 mbar	max. 12,8…64 bar
P-712CV[1]	(back pressure control)		max. 20…100 bar

Models, metal sealed		Pressure ranges (abs/rel)	
P-602CM[1]	(forward pressure control)	min. 17,5…350 mbar	max. 3,2…64 bar
P-702CM[1]	(back pressure control)	min. 70…350 mbar	max. 12,8…64 bar

1) Kv-max = 6,6 x 10^{-2}

For ranges of 200 or 400 bar rated pressure controllers and for low-ΔP control applications with Kv-values up to 1.0 please contact factory.

> Model number identification
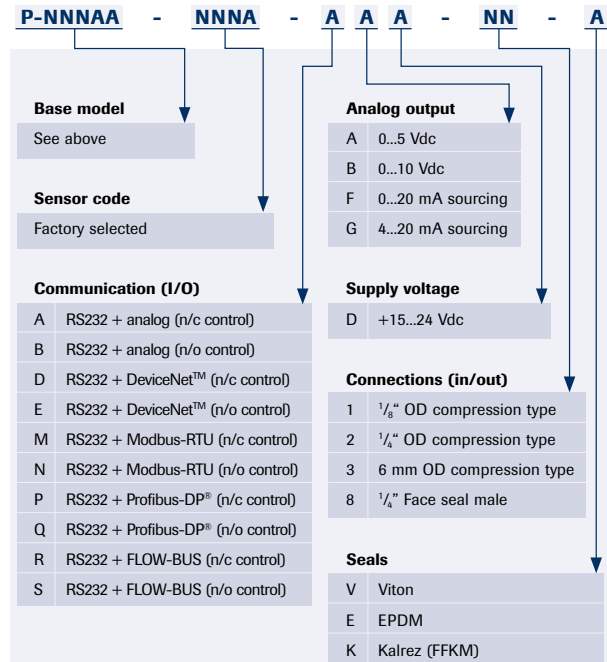
P-NNNAA - NNNA - A A A - NN - A

Base model

See above	

Sensor code

Factory selected	

Communication (I/O)

A	RS232 + analog (n/c control)
B	RS232 + analog (n/o control)
D	RS232 + DeviceNet™ (n/c control)
E	RS232 + DeviceNet™ (n/o control)
M	RS232 + Modbus-RTU (n/c control)
N	RS232 + Modbus-RTU (n/o control)
P	RS232 + Profibus-DP® (n/c control)
Q	RS232 + Profibus-DP® (n/o control)
R	RS232 + FLOW-BUS (n/c control)
S	RS232 + FLOW-BUS (n/o control)

Analog output

A	0...5 Vdc
B	0...10 Vdc
F	0...20 mA sourcing
G	4...20 mA sourcing

Supply voltage

D	+15...24 Vdc

Connections (in/out)

1	$^1/_8$" OD compression type
2	$^1/_4$" OD compression type
3	6 mm OD compression type
8	$^1/_4$" Face seal male

Seals

V	Viton
E	EPDM
K	Kalrez (FFKM)

5 VDC OUTPUT IS® PRESSURE TRANSDUCER
ETM-375 (M) SERIES

- 5 VDC Output
- Hybrid Microelectronic Regulator-Amplifier
- Silicon on Silicon Integrated Sensor **VIS**®
- Flush Diaphragm
- All Welded Construction
- Secondary Containment On Absolute And Sealed Gage Units
- Aerospace Quality Components
- 3/8-24 UNJF or M10 X 1 Thread
- 4 Wire (ETM-375)   3 Wire (ETM-300-375)
- Intrinsically Safe Applications Available (i.e. IS-ETM-375)

ETM-375 series transducers are miniature, threaded flush diaphragm instruments. They utilize a flush metal diaphragm as a force collector. Force is transferred to a solid state piezoresistive sensing element via a thin intervening film of non-compressible silicone oil. This sensing sub-assembly is protected from mechanical damage by a solid screen which has been shown to have minimal influence of the frequency response of the sensor. For applications where a true flush diaphragm is needed, Kulite will supply these transducers without 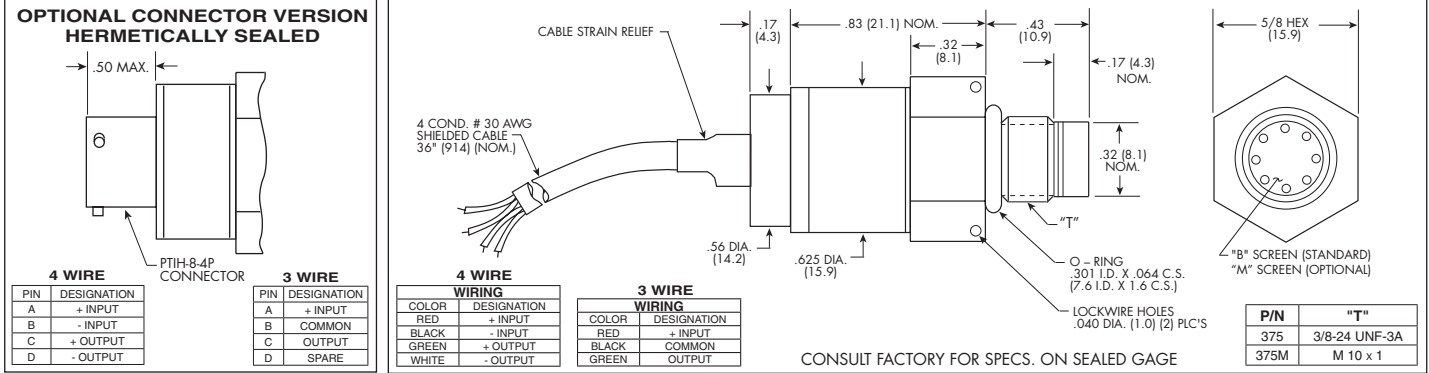the screen. Incorporation of a Kulite proprietary electronics module within the main body of this product allows for operation from an unregulated power supply of 12 ± 4 VDC or 28 ± 4 VDC. Standard output is a stable, low noise 0 to 5 VDC signal.

OPTIONAL CONNECTOR VERSION HERMETICALLY SEALED

PTIH-8-4P CONNECTOR

4 WIRE

PIN	DESIGNATION
A	+ INPUT
B	- INPUT
C	+ OUTPUT
D	- OUTPUT

3 WIRE

PIN	DESIGNATION
A	+ INPUT
B	COMMON
C	OUTPUT
D	SPARE

CABLE STRAIN RELIEF

4 COND. # 30 AWG SHIELDED CABLE 36" (914) (NOM.)

.17 (4.3) · .83 (21.1) NOM. · .43 (10.9)
.32 (8.1)
.17 (4.3) NOM.
.32 (8.1) NOM.
.56 DIA. (14.2)
.625 DIA. (15.9)
"T"
O – RING .301 I.D. X .064 C.S. (7.6 I.D. X 1.6 C.S.)
LOCKWIRE HOLES .040 DIA. (1.0) (2) PLC'S
5/8 HEX (15.9)
"B" SCREEN (STANDARD) "M" SCREEN (OPTIONAL)

4 WIRE WIRING

COLOR	DESIGNATION
RED	+ INPUT
BLACK	- INPUT
GREEN	+ OUTPUT
WHITE	- OUTPUT

3 WIRE WIRING

COLOR	DESIGNATION
RED	+ INPUT
BLACK	COMMON
GREEN	OUTPUT

P/N	"T"
375	3/8-24 UNF-3A
375M	M 10 x 1

CONSULT FACTORY FOR SPECS. ON SEALED GAGE

INPUT Pressure Range	17 250	35 500	70 1000	170 2500	350 5000	700 10000	1400 BAR 20000 PSI
Operational Mode	Absolute, Gage, Sealed Gage						
Over Pressure	2 Times Rated Pressure to 1000 PSI (70 BAR) 1.5 Times Rated Pressure Above 1000 PSI to a Max. of 30000 PSI (2100 BAR)						
Burst Pressure	3 Times Rated Pressure to a Max. of 35000 PSI (2400 BAR)						
Pressure Media	Any Liquid or Gas Compatible With 15-5 PH or 316 Stainlesss Steel						
Maximum Electrical Current	25 mA						
Rated Electrical Excitation	8 - 16 VDC			13 - 32 VDC			
OUTPUT Full Scale Reading	5 VDC ± 150 mV			5 VDC ± 150 mV or 10 VDC ± 300 mV			
Output Impedance	200 Ohms (Max.)						
Bandwidth (-3dB)	DC to 5 KHz						
Residual Unbalance	0 to 100 mV (ETM-375)			200 mV ± 50 mV (ETM-300-375)			
Combined Non-Linearity, Hysteresis and Repeatability	± 0.1% FSO BFSL (Typ.), ± 0.5% FSO (Max.)						
Resolution	Infinitesimal						
Natural Frequency (KHz) (Typ.)	Greater Than 400 KHz						
Acceleration Sensitivity % FS/g Perpendicular Transverse	2.2×10^{-4} 1.0×10^{-5}	1.1×10^{-4} 7.0×10^{-6}	6.2×10^{-5} 4.3×10^{-6}	2.6×10^{-5} 2.3×10^{-6}	1.5×10^{-5} 1.5×10^{-6}	1.3×10^{-5} 1.3×10^{-6}	8.0×10^{-6} 1.0×10^{-6}
Insulation Resistance	100 Megohm Min. @ 50 VDC						
ENVIRONMENTAL Operating Temperature Range	-65°F to +250°F (-55°C to +120°C)						
Compensated Temperature Range	0°F to +212°F (-18°C to +100°C) Other Ranges Quoted on Request						
Thermal Zero Shift	± 1% FS/100° F (Typ.)						
Thermal Sensitivity Shift	± 1% /100° F (Typ.)						
Linear Vibration	100g Peak, Sine up to 5000 Hz						
Altitude	-150 ft. to +70,000 ft. Will Not Damage Sensor						
Humidity	100% Relative Humidity						
Mechanical Shock	100g half Sine Wave 11 msec. Duration						
PHYSICAL Electrical Connection	4 Conductor 30 AWG Shielded Cable 36" Long						
Weight	24.5 Grams (Max.) Excluding Cable						
Pressure Sensing Principle	Fully Active Four Arm Wheatstone Bridge Dielectrically Isolated Silicon on Silicon						
Mounting Torque	80 Inch-Pounds (Max.)						

Note: Custom pressure ranges, accuracies and mechanical configurations available.   Dimensions are in inches. Dimensions in parenthesis are in millimeters.
Continuous development and refinement of our products may result in specification changes without notice - all dimensions nominal. (J)